SAPIENZA
UNIVERSITÀ DI ROMA

FACOLTÁ DI SCIENZE MATEMATICHE FISICHE E NATURALI

DOTTORATO DI RICERCA IN SCIENZE BOTANICHE

XXVI ciclo

A non-targeted metabolomics approach to evaluate the effects of biomass growth and chitosan elicitation on primary and secondary metabolism of *Hypericum perforatum in vitro* roots

PhD Thesis

Elisa Brasili

Tutors

Prof.ssa Gabriella Pasqua

Prof.re Alfredo Miccheli

Tables of contents

CHAPTER I

INTRODUCTION

1.1 A brief history of Metabolomics

The term metabolomics made its debut in the scientific literature barely fifteen years ago. Stephen Oliver was the first to suggest the word "metabolome" to describe the metabolite complement of living tissues (Oliver et al. 1998) but metabolomics application goes back to ancient times, just think of the Middle Ages, when the medical doctor recognized urine as an important source of health-related information and used "urine charts" to diagnose diseases by the colour and smell of the patient's urine. These charts linked supposedly metabolic features to various medical conditions such as diabetes (Nicholson et al. 2008).

In the late 1970s, the development of chromatographic techniques that allowed the quantitative determination of various substances in complex mixture marked the beginning of the modern-day metabolomics. The first publication on metabolomics, though not called metabolomics at the time, was by Pauling in 1971 and concerned the quantitative analysis of urine vapor and breath by gas-liquid partition chromatography (Pauling et al. 1971). Subsequently, the application of ^{1}H-NMR spectroscopy to study the metabolic composition of biofluids, cells and tissues, led to define the concept of "metabonomics" as the "quantitative measurement of the dynamic multiparametric metabolic response of living systems to pathophysiological stimuli or genetic modification" (Nicholson et al. 1999). In a short time, metabolomics has gone from being just an ambitious concept to being a rapidly growing, powerful tool to gain a more global picture of the molecular organization of all multicellular organisms. Finally, in 2002 Oliver Fiehn (Max Plank Institute, Golm, Germany) introduced the word "metabolomics" to designate a comprehensive analysis in which all the metabolites of an organism were supposed to be identified and quantified (Fiehn 2002). Currently, metabolomics is generally defined as the comprehensive, qualitative and quantitative study of all the small molecules, the metabolites, present within a biological system under specific conditions (Verpoorte et al. 2007, Nicholson et al. 2008, Allwood et al. 2008).

As a member of the '-omics' family in the systems biology, metabolomics aims at system-level understanding of biological systems, at the study of the interactions between the components of

biological systems and how these interactions give rise to the function and behaviour of that system (Kitano 2002).

The organism's metabolome, that is the whole set of its metabolites, varies in response to perturbations and/or environmental conditions. This is in contrast to its genome, representing the organism's set of genes and its transcriptome, which is the changing range of mRNA molecules expressed by those genes in each cell type. Both, genome and transcriptome are fixed for life, except when mutations occur, and can be seen as medium in the flow of gene expression, while the metabolome represents the final omic level in a biological system and reflects changes in phenotype and function (Hunter 2009). In this sense, whereas gene and protein expression represent the potential of an organism to respond to adverse conditions, metabolites represent the outcome of gene expression and define the biochemical phenotype of a cell, tissue, organ and organism.

Achieving the ability to visualize the metabolome of any organism, is currently still a difficult task because the metabolome is vastly complex. Just imagine all the metabolic pathways that need to be mapped, every intermediate and chemical compounds that to be determined, and the mechanisms by which they flow through various cycles into a cell. The whole picture is enormous and it is difficult to envision in its entirety. Moreover, the complexity of the metabolome increases particularly when the different levels of the biological organization (tissues, organs, whole organisms) and the effect of the environment on the metabolism of an organism, have been considered.

Despite its relative youth (in comparison to genomics, transcriptomic and proteomics), metabolomics is a key technology for understanding the molecular complexity of life and its integrated application with genomics, transcriptomics, and proteomics provides greater understanding of global system biology (Weckwerth 2003).

1.2 Modern-day Metabolomics

Over the last decade, the field of metabolomics continues to grow rapidly and a wide range of biological systems have benefited from metabolomics studies, from microbes to plants and complex multi-organism systems such as mammals; metabolomics is also widely applied to diagnose human diseases, biomarker discovery, pharmacology, toxicology, nutrition and food technology.

Microbes are important biological systems in the field of metabolomics since they have been initially used for development of experimental procedures, especially the optimization of sample preparation and metabolite measurements. Recently, interesting metabolomics studies have been carry out to describe the metabolic pathways in *S. cerevisiae* (Clasquin et al. 2011), to analyse the interactions between two organisms in co-culture system (Nakanishi et al. 2011), to develop metabolic engineering strategies aimed to finding of target genes to optimize fermentation processes (Hasunuma et al. 2011). All examples demonstrating that the metabolomics analysis of microorganisms will remain invaluable for the development of methods used in the study of higher organisms.

In the field of plant biochemistry/biotechnology, the extensive use of metabolomics tools is due the benefit produced on human health of various products of plant origin, including food, pharmaceuticals, and industrial raw materials, as well as its use in plant breeding and nutrition assessment. In addition, the vast chemical diversity of plants also contributes to the prominence of metabolomics in plant research. Plant tissues consist of heterogeneous cell populations and multiple cell compartments. Consequently, multiple metabolite concentration gradients and duplicate pathways are present in tissue samples. Moreover, the plants exhibit constantly changing, transient behaviour in response to diurnal, circadian, and seasonal cycles. These plant-specific properties of highly compartmentalized metabolic networks and the resulting complexity of metabolite connectivity present great challenges for metabolomics (Gomez-Casati et al. 2013).

In the field of food science, metabolomics is emerged as an important tool to evaluate food quality and safety (Cevallos-Cevallos et al. 2012). The quality of food products is greatly affected by pre-

harvest (genetic origin, cultivation area and growing environment) and post-harvest (milling, modified/controlled and atmosphere storage) processes. Changes in metabolite composition that occur during these processes are important for safety, acceptability and nutritional value of foods. Recently, metabolomics has been employed to identify the relationship between metabolite profiles of food and quality. For example, it has been applied for the analysis of major crops potato, tomato, cereals and fruits and popular beverages as wine and beer (Carreno-Quintero et al. 2012, Kusano et al. 2013, Rasmussen et al. 2012, Mannina et al. 2012, Inui et. al 2013, Schmidtke et al. 2013) but also for the manufacturing, formulation and optimization of food processing or authentication of cheese, meat, fish and oils (Ochi et al 2013, Liu et al. 2013, Wagner et al. 2014, Dais et al. 2013), for the monitoring of the different fermentation phases of milk (Bouteille et al. 2013) and for the quantitative evaluation of preservatives in complex matrices such as margarine, syrup, avocado paste, sausages (Simmler et al. 2014).

With the recent breakthrough in metabolomics technologies, application of metabolomics is increasing in the medical field mainly to acquire knowledge on the mechanisms of the drug action or of the diseases and to explore biomarkers used as indicators for early diagnosis of diseases, or for toxicity and therapeutic effects. Recently, several researches have conducted to identify biomarkers and to clarify the detailed pathogenic mechanisms of diabetes, obesity and cancer (Zhang AH et al. 2013, Zhang A et al. 2013, Kinross et al. 2013). Metabolomics tools are applied in nutrition research to understanding the interactions that can occur between the variety of chemical components of food and the biochemical networks of complex organisms, to evaluate their bioavailability and metabolism, the role of gut microbiota and the physiological response to a particular diet regimen, food or nutraceuticals (Astarita et al. 2013). It is reasonable to think that in the foreseeable future, the integration of metabolomics with other omics sciences, as genomics, transcriptomics and proteomics will lead to a better understanding of the link between changes that occur in body and pathological conditions. On the other hand, the discovery of novel disease-related biomarkers will allow to diagnose diseases as cancer in its early stages thus contributing to improve prognosis.

1.3 Strategies for metabolomic analysis

The general goal of most metabolomics studies is to generate a snapshot of the metabolic state of a biological system (cells, tissues, organs or whole organism) and to characterize the changes in the measured metabolites at a given time point and arising from specific physiological conditions such as natural fluctuations or external, experimental biotic or abiotic perturbations (Schuhmacher et al. 2013). Different metabolomics strategies have thus been developed for different applications and depending on the goal of each experiment, the approach used will differ.

The principal approaches for the metabolome analysis are the untargeted metabolomics, the targeted metabolomics, metabolite fingerprinting, metabolite footprinting, metabolic profiling and metabonomics (Putri et al. 2013).

The **untargeted metabolomics** is the measurement of the levels of all detected metabolites in a biological sample, including substances which are currently unknown (or at least unidentified) at the time of measurement without the need of previous sample knowledge. It is usually considered a hypothesis-free approach since reveals the behaviour of known and unknown metabolites allowing to detect the synergic effects between metabolites which cannot be observed at an individual level and to potentially probing the entire metabolic space.

The **targeted analysis** is the qualitative and quantitative analysis of one, or several metabolites related to a specific metabolic reaction but for practical reasons this is generally feasible for a limited set of predefined known substances, which are generally chosen on the basis of metabolites available as authentic reference standards. Such approach relies on optimised metabolite extraction, separation and detection.

Metabolite fingerprinting is the global and rapid analysis of the metabolic composition of an organism or tissue aims to provide sample comparison and classification. It is also utilized as a screening tool to discriminate between samples from different biological status or origin (i.e., treated/control, disease/healthy). In general, metabolites are neither quantified nor identified.

Metabolite footprinting is the measurement of metabolites secreted from the intracellular

complement of an organism (or biological system) into its extracellular medium or matrix. This approach is commonly used in microbial metabolomics.

Metabolic profiling is the identification and quantification of a selective number of predefined metabolites, which are generally related to a specific metabolic pathway.

Finally, **metabonomics** is a term coined by Jeremy Nicholson and is normally used in non-plant systems. Generally it refers to the quantitative detection of endogenous metabolites that are dynamically altered within a living system in response to pathophysiological stimuli or genetic modification. More specifically, the overall aim is to measure the small molecules in biological samples, be they urine, blood samples, tissue from a patient or a small cluster of yeast cells (Nicholson et al. 2008).

1.4 Analytical technologies employed in metabolomics: Nuclear Magnetic Resonance Spectroscopy (NMR)

A wide range of analytical technologies may be used in metabolomics, including gas chromatography-mass spectrometry (GC-MS), capillary electrophoresis-mass spectrometry (CE-MS), liquid chromatography-mass spectrometry (LC-MS), liquid chromatography-electrochemistry-mass spectrometry (LC-EC-MS), nuclear magnetic resonance (NMR) spectroscopy, and Fourier-transform infrared (FT-IR)- and Raman spectroscopies. Among these, NMR has been widely used for metabolomics research since the last decade (Kim et al. 2010).

The use of NMR-based metabolomics marked the beginning of metabolomics as a tool in biochemistry and phytochemical analysis. NMR spectroscopy is an unbiased, rapid, non-destructive technique that requires little sample preparation and none analyte separation process (as is the case in chromatographic analyses). It is a qualitative and quantitative method that detects the specific resonance absorption profiles of metabolites in a magnetic field (which is dependent on chemical structure). When samples in a deuterated solvent are placed in a strong magnetic field and irradiated with a radio frequency, the absorption of energy allows the nuclei to be promoted from low-energy to high-energy. Only atomic nuclei with odd numbers of protons are perturbed by the magnetic field, including hydrogen, which is fortunately present in almost every metabolite. The spectral signal intensity is directly proportional to the number of nuclei that give rise to a specific resonance. Despite its lower sensitivity (limit of detection, in the low μM range) when compared to other techniques as mass spectrometry (limit of detection in the low pM range), improvement in NMR instrumentation and technology such as solvent suppression technique, versatile pulse sequences, cryoprobes and the use of labeled compounds (e.g., using ^{13}C or ^{15}N NMR) have led significant improvements in sensitivity. Although NMR spectroscopy can yield detailed information on the quantity and identity of metabolites present in the extracts, the chemical elucidation of NMR-detected compounds is highly complex as a result of overlapping signals and shielding effects by neighbouring electrons. However, the development of multidimensional techniques such as Total

Correlation Spectroscopy (TOCSY), Correlation Spectroscopy (COSY), Heteronuclear multiple-bond correlation spectroscopy (HMBC) and Heteronuclear Single Quantum Coherence (HSQC), allowed to spread the spectral content over a two-dimensional plane, therefore the identification of compounds is facilitated and minor compounds can be better observed, even allowing for structural elucidation in extracts. Moreover, NMR spectroscopy offers an unbiased view of the sample composition and the possibility to simultaneously quantify multiple compounds, as well as to elucidate the structure of unknown and natural compounds. One major advantage of NMR analysis is its non-invasiveness and thus the samples can be recovered for further analyses. Another advantage of NMR is that the chemical shift scale is reasonably constant, there can be some small changes between samples, but nothing of the magnitude of the elution time shift in chromatography, allowing to a method that is relatively reproducible. Spectra are fast to acquire and for interesting spectra it is possible to perform many further experiments such as pulse sequences to further probe the structure of compounds in a mixture.

Given its characteristics, NMR has become the method of choice for metabolomics studies, but also for quality control of complex mixture such as foods, plants or herbal remedies, and biofluids.

1.5 The workflow for metabolomic analysis

Regardless of used approach, the metabolomics analysis comprises three main experimental stages: sample preparation, acquisition of the data using analytical methods and data mining using chemometric methods followed by compound identification. The resulting analysed data from the various experimental phases form the basis for meaningful biochemical interpretation.

Sample preparation is a critical step in transforming the sample into a solution that can be analysed. This step involves a series of different experimental stages: selection and harvesting of samples, drying or enzyme quenching procedures, extraction of metabolites and preparation of the samples for analysis. The selection and harvesting of samples depend mainly on the biological question that seeks to investigate. Quenching is the process of stopping biological reactions in a cell necessary to measure the true quantity of metabolites at a given time, it should be rapid to limit the leakage of metabolites. The extraction method is the process to obtain metabolites from the cells and must be chosen considering the biochemical composition of the system under investigation, the physicochemical properties of the target metabolites and the properties of the solvent used. Data acquisition or sample analysis requires advanced analytical platforms each with its own advantages and limitations, either in selectivity or sensitivity.

In order to provide a holistic picture of the examined system a large number of metabolites should be quantified and all the obtained variables should be considered simultaneously, making univariate and other classical statistical methods unfeasible. In order to take into account also the correlations between the measured variables, multivariate statistical methods must be applied. Mathematical and statistical methods that allow to extract important information from multivariate data set belong to chemometrics discipline. In chemometrics, the most important task is to construct an organized data matrix containing the several samples and their measurements. In NMR spectroscopy, it is possible record a spectrum at hundreds of measurements (concentrations of metabolites) on a single sample. Since the resulting data matrix is usually extremely large, it is useful highlight significant differences and the main relationships between samples using multivariate analysis.

1.6 Plant Metabolomics

Metabolomics is a key technology for understanding plant metabolism. It is well known that plants, being sessile obligate autotrophs, have been forced to evolve complex multicellular structures such as leaves, roots, stems and tubers each of which comprise multiple specialized cell types (epidermis, guard cells, parenchyma, glandular hairs, etc.) with a dedicated metabolism in order to perform its desired function and survive environmental changes (Hall 2006). In effect, plants are continually affected by abiotic (light, UV, water) and biotic (herbivory, parasitism and pathogen attack) stress factors and for this reason have developed complex defence responses based predominantly on metabolic changes. Speculative estimations of the total number of metabolites which are produced within the plant kingdom, including the 'secondary' metabolites which play specific roles in allowing adaptation to specific environmental changes, vary considerably but the real number is likely be more than 250 000. When a metabolic pathway is activated, precursors and intermediates are channelled to produce a metabolite. The production of these compounds can be regulated in turn by other compounds (signalling molecules, such as plant hormones) not related to the regulated pathway or intermediates that can feedback activate or inactivate different metabolic steps. This high complexity due to the enormous chemical diversity of the compounds, represents the main hindrance when characterizing the plant metabolome. Much of plant biochemistry can, unfortunately, still be defined in terms of unidentified compounds derived from undefined pathways and with unknown function. It is also for this reason that, owing to our restricted knowledge of plant biochemistry, the untargeted metabolomics is a particularly suitable approach. Having a more complete insight into the metabolic composition of plant, it will be possible to apply this knowledge both in fundamental research in order to provide a better understanding of plant metabolism and applicative research in order to discover plant compounds that could be important in improving human health.

The application of metabolomics to plant science was pioneered by research groups at the Max Planck Institute. In 2004, Weckwerth and coworkers obtained a series of metabolomic data from

potato tubers using GC/MS (Weckwerth et al. 2004). They presented an approach to study of silent plant phenotypes and demonstrated that the structure of the correlation network could be changed in a mutant with a silent phenotype, in which metabolic changes were observed despite a lack of visible changes. In recent years, metabolomics have drawn attention of researchers in different areas of plant science such as phytopathology, botany and systematics, stress and environmental physiology and phytochemistry.

In particular, metabolomic research is utilized in studies relating to evaluation of the impact of biotic and abiotic stresses, of wounding, herbivory and infections on plant metabolism, to the characterization or classification of different species/cultivars, to determine genetic origin and cultivation conditions, to discriminate wild/transgenic plants, to discover new metabolites and to identify potential biochemical markers for contamination detection and product adulteration, but also to perform quality control of medicinal plants or of plant food, as previously described. Furthermore, metabolomics studies have been carried out to monitor metabolic changes during plant developmental, biomass accumulation and secondary metabolite production (Hall 2006).

By way of example, Sardans and collaborators studied the metabolic changes of leaves of mediterranean sclerophyllous tree *Quercus ilex* after wounding treatment, simulating herbivore attack (Sardans et al. 2013). They observed a rapid increase in glucose, a shift in N-storing amino acids, from leucine and isoleucine to asparagine and choline and an increase in C-rich secondary metabolites content such as quinic acid and quercitol, both related to the shikimic acid pathway and linked to defence against biotic stress. ^{1}H-NMR and multivariate data analysis were used to demonstrate the correlation between the specific metabolic profile of leaves, stems, roots and flowers of *Catharanthus roseus* and the expression of different flower colours suggesting an interesting application in the plant breeding industry (Pan et al. 2014). Metabolomics approach based on ^{1}H-NMR spectroscopy and multivariate data analysis was also used to detecting both primary and secondary metabolites in *Salvia miltiorrhiza* and screening potential geographical biomarkers (Jiang et al. 2014), to monitor the metabolite response of plants to jasmonic acid (Kim et al. 2013), to

investigate samples of Greek grape marc spirits according to their provenance, variety, vintage year and production process (Fotakis et al. 2013), to quality assessment and authentication of virgin olive oil (Dais et al. 2013). NMR metabolic profiling were also applied to rice subjected to different stresses such as drought, extreme temperatures, and flooding to understanding the complex biochemical and molecular response of rice plants to submergence and provides insights into biological response mechanisms that can influence survival (Barding et al. 2013).

Interestingly, NMR-based metabolomics was applied to the study of medicinal plants. In the field of herbal medicines or natural products, metabolomics is actually focus on the authentication and identification of herbal medicines and biomarker discovery required for both pharmaceutical and industrial purposes. Herbal medicines and their preparations have been widely used for hundreds of years all over the world. Among the characteristics of herbal medicine preparations, is that they are all presented either as single herbs or as a combination of several herbs in composite formulae. The incomparable molecular diversity and biological functionality that characterize the metabolites present in plant extracts are the major features that distinguish them as a potential drug source. However, the natural products-based drug discovery, poses some challenges, mostly connected with their inclusion in a complex matrix composed of mostly uncharacterized compounds with a large dynamic range (i.e. the difference in the levels of major compounds as compared to that of minor compounds, differences in polarity, in boiling points, or in melting points, etc.). On the other hand, one or two markers or pharmacologically active components in herbs and/or herbal mixtures have been used for evaluating the quality and authenticity of herbal medicines, both in the identification and quantitation of single herbs and in multicomponent preparations (Gad et al. 2013). However, in any medicinal plant and its extract, there are hundreds of unknown components, many of them present only in trace amounts. These multiple constituents, difficult if not impossible to separate into active parts, may work 'synergistically' and be responsible for its therapeutic effects. Moreover, the chemical constituents in medicinal plant may vary depending on harvest season, habitat, drying processes and many other factors. Consequently, to obtain a complete picture of the herbal

preparations that represent pharmacologically active and chemically characteristic components is not an easy task, but it seems necessary in order to ensure the reliability and repeatability of pharmacological and clinical research, to understand their bioactivities and possible side effects and to enhance product quality control.

In herbal medicine researches, metabolomics approach based on ^{1}H-NMR spectroscopy has become one of the most suitable technique to carry out comprehensive plant qualitative and quantitative analysis. It offers an integral view of the extract composition allowing the detection and quantitation of all metabolites contributing to the pharmacological activity. Metabolomics approach was used to screening bioactive metabolites responsible for antitussive and expectorant activities of *Tussilago farfara* L. For this purpose, different parts (roots, flower buds, and leaves) of the title plant were analyzed systematically (Li ZY et al. 2013). Untargeted metabolic profiling coupled to transcriptome analysis has been applied in *Ophiorrhiza pumila* hairy roots to understand the biosynthesis of the anti-cancer alkaloid camptothecin, a potent inhibitor of DNA topoisomerase I activity, and of the anthraquinones, derived from the combination of the isochorismate and hemiterpenoid pathways (Yamazaki et al. 2013). A metabolic fingerprinting has been used to quantitative analysis of monoterpenoids, sesquiterpenoids, and cannabinoids in *Cannabis sativa L.*,. an important medicinal plant, and to clear chemotaxonomic discrimination between different *C. sativa* varieties for drug standardization purposes (Flores-Sanchez et al. 2012). A metabolomic profiling of *Catharanthus roseus L.* infected by phytoplasmas has been carried out using ^{1}H- NMR spectroscopy and principal component analysis to identify those metabolites that were present at different levels in phytoplasma-infected *C. roseus* leaves than in healthy ones, indicating that the biosynthetic pathway of terpenoid indole alkaloids, together with that of phenylpropanoids, were stimulated by the infection of phytoplasma (Choi et al. 2004). Another popular and widely used herbal medicinal is *Echinacea purpurea*. Studies of its interactions with conventional drugs are of particular importance. Modarai et al. showed that Echinacea preparations and some common alkylamides, an important class of active constituents, weakly inhibited several cytochrome P450 (CYP) isoforms, with

considerable variation in potency. They used ^{1}H-NMR and multivariate data analysis to investigate the nature of the compounds responsible for CYP3A4 inhibition, discovering extensive differences in the composition of the commercially available preparations, with an inevitably impact on the product efficacy, safety and pharmacological effects (Modarai et al. 2010). Metabolomics analysis has also been applied in *Echinacea angustifolia* cell suspension cultures under light controlled revealing accumulation of specific secondary metabolites, mainly caffeic acid derivatives never previously described (Guarnerio et al. 2012). Agnolet et al. (2010) used ^{1}H NMR-based metabolomics and other metabolomics technologies to investigate different commercially available preparations of *Ginkgo biloba*, identifying unexpected and extract constituents. Commercial preparations of *Ginkgo biloba* are prepared from raw leaf extracts and pharmacological activity is attributed to a number of flavonoid glycosides and unique terpene trilactones (TTLs), but the composition of the entire preparation remains largely uncharacterized. Among medicinal plants, *Panax ginseng* is certainly the more studied example. Considering that the age of the ginseng plant is considered an important criterion to determine the quality of this species, metabolite profiling has been applied to discriminate the age of *P. ginseng* samples confirming a potential tool to standardize quality control in the *P. ginseng* industry (Kim et al. 2011). Moreover, non-targeted metabolomics approach has been applied in hairy roots of *P. ginseng* to identify key metabolites that can be used as biomarker candidates for quality assurance in ginseng (Kim et al. 2012). Among medicinal plants, *Hypericum perforatum* is one of the most prominent and best investigated medical plants.

1.7 *Hypericum perforatum*

1.7.1 Taxonomy and morphological characters

In earlier classifications, *Hypericum perforatum L.* was included in the family Clusiaceae (Guttiferae), under the subfamily Hypericoideae. Recent molecular phylogenetic analyses suggested that Hypericoideae do not form a monophyletic group with other Clusiaceae but is a distinct family, Hypericaceae (Stevens et al. 2007).

The plant is a glabrous perennial, erect and usually woody at the base. The leaves are opposite, simple and characterized by the presence of different types of secretory structure including translucent glands, black nodules and secretory canals that accumulate pharmacologically active compounds (Ciccarelli et al. 2001). In particular the glands translucent, distributed over the entire surface of the leaf blade, mainly contain essential oils, while black nodules are generally localized on the stem, leaves, flowers and contain hypericin and pseudohypericin. The flower has five short, subequal, entire, imbricate, basally connate sepals, and five persistently withering yellow petals. The ovary is superior, capsicular, and three-styled whereas the stamens are many, arranged in bundles of threes. The flowers are profuse, arranged in branched cymes which bloom from June until September (Crockett et al. 2011).

1.7.2 *Hypericum perforatum* in history

Hypericum perforatum, also known as St John' s wort, is a herbaceous plant native to Europe and Asia but naturalized in many parts of the world, notably North America and Australia (Nurk et al. 2013). There are several explanations as to the origins of the names hypericum and St John's wort. Commonly, the name υπερεικον was given just by the ancient Greek who attributed to the plant also the ability to protect from the devil or evil spirits (υπέρ – above, εικών – image) and used it to decorate religious images. In the Middle Ages, the name for this plant was fuga daemonum (flight of the demons) and was originally used against melancholy, mood swings, nervous agitation, and some forms of hysteria, which were once attributed to evil influences. The first Christians gave the name "St John's wort" because it flourished around the June 24St (Baptish John's Day) (Barnes et al. 2001, Saddique et al. 2010).

Long before drugs were invented, herbs were proved to have strong therapeutic properties and *H. perforatum* is one of the oldest and best investigated medicinal herbs, since antiquity.

The first to describe the therapeutic properties of the plant as a healing, diuretic, analgesic, and a drug antimalaria, was Pedanius Dioscorides, the most popular pharmacologist of antiquity (1st century a.c.). In his work, "About Medical Material", a synopsis regarding plants, he describes *Hypericum* as follows: "It is a big, tufted, red bush; its flower resembles the leucoia and, if rubbed between the fingers, it produces a juice that resembles human blood". For this reason the plant has been named "Androhaimon" (human blood) (Istikoglou et al. 2010). His contemporary Greek and Roman physicians, Galen and Plenius respectively, found it extremely effective for the healing of snake bites, when mixed with wine. For many centuries, *Hypericum* has been associated with pharmacy and folklore and among the first most effective and widely spread pharmaceutical uses of *H. perforatum* in Europe after the 16th century was the use of the distilled oil of the herb as a therapy for wounds and bruises. It was so effective that surgeons not only used it to clean wounds but also included it in the first official pharmacopoeia of London as Oleum Hyperici (Urdang 1944). Other popular folk-uses recorded for St. John's Wort included as a decoction for gravel and ulcerations of

the ureter (Hill 1808), for ulcerations of the kidneys, as a febrifuge or vermifuge, and for jaundice, gout, and rheumatism (Greene 1824). In the last century, Duke et al. (1985) recounted its use in folk medicine in the treatment of ovarian carcinoma, uterine cancers, stomach cancers, and tumors of the lymph. Duke cites a Russian application in bronchial asthma and numerous others: diarrhea, dysentery, neurasthenia, nervous depression, hysteria, chronic catarrh, rabies, worms, hemorrhages, and bladder problems, to name a few.

For a long time, St. John's wort was used extensively in herbal products as well as in homoeopathic preparations, in order to treat a vast number of disease, like neuralgia, sciatica, menopausal neurosis, anxiety, as a nerve tonic, skin infections and wounds (Newall et al. 1996). In reality today, *H. perforatum* is best known for its use in the treatment of mild-to-moderately severe depression (Butterweck 2003, Crockett and Robson 2011, Nahrstedt et al. 2010).

1.7.3 Bioactive compounds and pharmacological effects of *Hypericum perforatum* preparations

The term "bioactive compound" is defined as the specialized metabolite presents in particular plants for which there is either direct evidence of a biological effect on other biological systems or a structural similarity to known other bioactive compounds. In many cases specific bioactive compounds or their combinations, useful in human health are not completely known. Since it was found that the effectiveness of medical preparations of *Hypericum* is based on the entire mixture of the metabolites, through a synergistic action of the different components, rather than on the single constituent, finding suitable methods that enable the analysis of the entire extract has become the current challenge (Tatsis et al. 2007).

Hypericum perforatum contains a wide spectrum of chemical compounds, among which flavonoids, biflavones, naphtodianthrones, phloroglucinols, phenylpropanes, procyanidines. Additionally, lesser amounts of tannins, xanthones, essential oils, and amino acids are present (Butterweck et al. 2007, Saddique et al. 2010). Flavonol glycosides represent with an amount of up to 4% the largest group of secondary metabolites. The major components, rutin, hyperoside, isoquercitrin, quercitrin, miquelianin, and quercetin, in smaller amount, are found in the aboveground portions of the plant, including the leaves, stalk, flowers, and buds. The biflavonoids such as I3, II8-biapigenin and amentoflavone exclusively occur in the flowering part of plant. The naphtodianthrones hypericin, pseudohypericin, protohypericin and protopseudohypericin occur in the flowers and leaves of the crude drug material in concentrations of 0.03 to 0.3%. The amount of pseudohypericin is approximately 2 to 4 times higher than that of hypericin. The main representative of the phloroglucinol group of constituents is hyperforin. Together with adhyperforin it occurs in the "pale glands" of the leaves (Crockett and Robson 2011). Hyperforin occurs in amounts up to 2–5% in the crude drug material and can reach about 6% in some extracts. The phenylpropanes mainly occur as esters of hydroxycinnamic acids, such as p-coumaric acid and caffeic acid. Besides, ferulic, isoferulic, and gentisic have also been observed. The proanthocyanidins are represented by tannins. The

essential oil of *H. perforatum* contains aliphatic compounds (2-methyl octane, n-nonane, n-decane, n-undecane, n-tetradecanol, 2-methyl-decane, and 2-methyl-dodecane) along with terpenoids (α-pinene, β-pinene, geraniol, β-caryophyllene, β-farnesene, humulene, and germacrene D) (Saddique et al. 2010). Differences in the biosynthesis of sesquiterpene and aliphatic hydrocarbons, and in oxygenated aliphatics, in flowers and leaves have been indicated. The data have shown that concentrations of β-caryophyllene and caryophyllene oxide in essential oils from the leaves are higher than those from the flowers, whereas dodecanol, spathulenol, viridiflorol, carotol and tetradecanol are present in higher quantities in the flowers (Radusiene et al. 2005). Other chemical constituents are xanthones and kielcorin C, acids (isovalerianic, nicotinic, myristic, palmitic, and stearic), carotenoids, choline, nicotinamide, pectin, β -sitosterol, pectin, fatty acids, amino acids, and vitamin C. Xanthones, in particular kielcorin, 1,3,6,7- tetrahydroxyxanthone and mangiferin, are present at higher concentrations in the roots, whereas the upper parts contain 1,3,6,7-tetrahydroxyxanthone at 0.0004% and traces of mangiferin in the dried material (Jürgenliemk et al. 2002). The concentrations of all these constituents in medical preparations depend on many factors: geographic origin of the plant, harvest of wild cultivated plants, harvest time (there is a decrease in naphthodianthrones and an increase in phloroglucinols from flowering to fructification), processing of fresh or dried plant material, lipophilicity and temperature of the extraction solvent and final formulation, exposure to sunlight, time and conditions of storing (Isacchi et al. 2007). Therefore, information on the specific preparation used in experiments or clinical trials is crucial for interpretation and reproducibility of data.

Although >150 constituents that exhibit many synergistic and partly antagonistic effects have thus far been identified in *H. perforatum*, most intensively studied constituents are naphthodianthrones (hypericin and pseudohypericin) and phloroglucinols (hyperforin and adhyperforin) (Butterweck et al. 2007), for their antidepressive activity.

Depression is a mental illness characterized by symptoms such as anxiety, hopelessness, loss of energy and appetite, insomnia, and thoughts of death. It is one of the leading causes of disability

worldwide, with approximately 120 million persons affected in industrial countries. In recent years, the consumption of *H. perforatum* derived products has increased dramatically, and *H. perforatum* is presently one of the most consumed medicinal plants in the world for the treatment of mild to moderate forms of depression More than 50 controlled clinical studies in depressed patients have been performed with a dosage of 600-900 mg of extract per day (equivalent to approximately 3 to 5 g of crude drug material), showing efficacy equal to standard antidepressants including the modern selective serotonin reuptake inhibitors (SSRIs) in the treatment of mild to moderate depressive episodes and for the short-term treatment of symptoms in mild depressive disorders (Nahrstedt et al. 2010, Chen et al. 2011, Kasper et al. 2010). Studies on chronic stress and antidepressant animal models (e.g. forced-swimming test) have shown that the treatment with *H. perforatum* extracts caused downregulation of β-adrenergic receptors (De Marchis et al. 2006), and altered animal behaviour, consistent with the effects of conventional antidepressants (i.e. fluoxetine; De Marchis et al. 2006, Butterweck 2003, Crupi et al. 2011, Bukhari et al. 2013).

Although *H. perforatum* is most widely used for either the treatment of depressive syndromes, the literature reveals uses of this plant for other pharmacological and medical purposes.

Recently, it has been proposed the use of *H. perforatum* preparations for the prevention of Alzheimer's disease because hypericin may interfere with the processes of polymerization of beta-amyloid peptide responsible for the onset of Alzheimer's disease (Griffith et al. 2010). Moreover, it is also has been hypothesized a protective effect of *H. perforatum* on gastritis and gastric ulcer (Zdunić et al. 2009). Lately, it has been also demonstrated that *H.perforatum* compounds protect rat and human pancreatic islets against cytokine effects by counteracting key mechanisms of cytokine-mediated β-cell injury and represent promising pharmacological tools for prevention or limitation of β-cell dysfunction and loss in type 1 diabetes (Novelli et al. 2013).

Increasing evidence also suggested that *H. perforatum* possess anti-inflammatory activity which could be potentially be used to alleviate conditions like inflammatory bowel disease, diarrhea, and respiratory infection (Birt et al. 2009, Zdunic et al. 2009). Huang et al. (2011) have shown that *H.*

perforatum ethanol extract inhibited LPS-induced prostaglandin E2 (PGE2) and nitric oxide (NO) production, tumor necrosis factor-α (TNF-α), and interleukin-1β (IL-1β) in RAW 264.7 mouse macrophages, attributing part of the activity of the extract to a group of four compounds including pseudohypericin, amentoflavone, quercetin and chlorogenic acid.

Pharmacological research has revealed two different fields in anticancer effects of *H.perforatum*: light-dependent mechanisms related to photoactivation of the hypericins and light-indipendent mechanisms attributable to hyperforin. Huntosova et al. (2012) investigated cell death response of U87 glioma cells on hypericin photoactivation and observed that was strongly influenced by the dynamics of hypericin subcellular redistribution processes and its aggregation in cellular organelles. Sharma et al. (2012) treated human squamous cell carcinoma cells *in vitro* with hypericin (1-7 μM) photoactivated resulting in greatly increased rates of cell death: the authors postulated a caspase-independent apoptotic mechanism of cell death. Menichini et al. (2013) reported significant phototoxicity with 50% cell destruction in A375 human melanoma keratinocyte cells at a concentration of 78 μg/mL of a hydroalcoholic *H. perforatum* extract and UV light. Light – independent anticancer mechanisms of hyperforin were reported by Schempp et al. (2002). A novel activity of hyperforin, namely its ability to inhibit the growth of tumour cells by induction of apoptosis, has been described. Hyperforin was able to inhibite the growth of various human and rat tumour cell lines in vivo, generating dose-dependent apoptotic oligonucleosomes, typical DNA-laddering and apoptosis-specific morphological changes. Moreover, hyperforin was capable of releasing cytochrome c from isolated mitochondria, suggesting that hyperforin activates a mitochondria-mediated apoptosis pathways as confirmed in acute myeloid leukemia (AML) cell lines by Merhi et al. (2011). Additionally, numerous studies have supported wound-healing effects, antimicrobial properties (one of the oldest historical uses of HP, predominantly as St John's wort oil) against a number of bacterial and fungal strains and antiviral activity of *H. perforatum*.

Dermatological applications of St. John's wort have a long tradition. As previously said, topical St. John's wort preparations are used for the treatment of minor wounds and burns, sunburns,

abrasions, bruises, contusions, ulcers, psoriasis, rheumatism and myalgia (Wolfle et al. 2013). Pharmacological research supports the use in these fields suggesting interesting pharmacological effects that include antioxidant, anti-inflammatory, anticancer and antimicrobial activities. The antibacterial activity of an ethanolic extract of *H. perforatum* was investigated against several Gram-negative bacteria such as *Pseudomonas*, *Erwinia*, *Enterobacter*, *Klebsiella*, *Agrobacterium*, *Azotobacte*r and Gram-positive bacteria such as *Bacillus subtilis*. These species (except *Klebsiella pneumonia*) showed extreme sensitivity to the extract of *H. perforatum* (Saddiqe et al. 2010). Recently, it has been demonstrated the antifungal activity of root extract of *H. perforatum* against plant (Crockett et al. 2011) and human pathogens (Tocci et al. 2010, 2011, 2012, 2013). Antifungal activity has been attributed to xanthones, secondary metabolites belonging to the class of polyphenols. Antiviral activity of several *Hypericum* constituents against many forms of viruses *in vitro* has been demonstrated over the last years, including herpes simplex virus type 1 and 2 and anti-hepatitis B virus (HBV). In particular, it has been observed that ethanol extracts of *H. perforatum* L. are able to inhibit HBV transcription in HepG2 2.2.15 cells, a stable HBV-producing cell line, suppressing the secretion of HBsAg and HBeAg in a dose-dependent manner, as well as the extracellular HBV DNA (Pang et al. 2010). However, clinical research in these fields is still scarce. Furthermore, considering that 30-40% of the compounds present in *H. perforatum* extracts are as yet not structurally assigned, and among these could be further constituents directly or indirectly contributing to the overall clinical efficacy, identification of the active constituents is highly important in order to ensure pharmaceutical and thereby therapeutic quality of the crude drug and its extracts. On the other hand, to a lesser extent the identified active compounds may be used as leads for the development of highly active synthetic drugs. The knowledge of active compounds also helps to optimize the crude drug material by selection and breeding. Once the active constituents are known, further investigations on the mechanism(s) of action can be performed. Finally, not only active constituents of an herbal preparation should be known but also its entire phytochemistry, because interactions between constituents are possible in a positive and a negative manner.

CHAPTER 2

MATERIALS AND METHODS

2.1 Plant material and organ culture

Seeds of *H. perforatum* were surface sterilized in accordance with Zobayed et al. (2004) and transferred on Murashige and Skoog (MS) medium (Duchefa Biochemie, Haarlem, The Netherlands) supplemented with 3% (w/v) sucrose and solidified with agar. Seed cultures were grown under a photoperiod of 16/8 h (light/dark) at 26°C (photon lux density, 70 μmol m−2 s−1). To induce the formation of callus, leaf and stem explants were excised from 2-month-old seedlings and placed on solid MS medium supplemented with 5 mg l−1, 2,4-dichlorophenoxyacetic acid (Duchefa Biochemie, Haarlem, The Netherlands), 1 mg l−1 kinetin (Duchefa Biochemie, Haarlem, The Netherlands), and 3% (w/v) sucrose; the cultures were maintained under continuous darkness. After 28 days of culture, the callus were transferred to hormone-free (HF) agarized MS medium to induce the formation of roots. Regenerated roots, 2–3 cm in length, were isolated from the callus (after 30 days) and subcultured in the same medium. To induce branching (lateral root formation) and to increase biomass, the roots (after 30 days) were cultured in MS medium supplemented with glucose (2,2 g l-1) and indole-3-butyric acid (IBA) (1 mg l−1).

Liquid cultures were established after 30 days, by inoculating 1 g fresh weight (FW) of roots in magenta vessels containing 80 ml liquid MS medium supplemented with glucose (2,2 g l-1) and IBA (1 mg l-1). The magenta vessels were shaken at 100 rpm at 25±1°C and maintained in the continuous darkness. Since optimum nutrient concentration is a critical point in controlling growth of regenerated roots and accumulation of secondary metabolites (Lian et al 2002), the medium was renewed every 4 days, time necessary for biomass duplication. The roots were elicited using chitosan (medium molecular weight; Sigma-Aldrich, Milan, Italy), dissolved in acidified water with HCl (1M), at a final concentration of 200 mg l−1 which was added using 0,22 μm sterile filter. An adequate amount of water was added to the control samples.

2.2 NMR sample preparation

The metabolic quenching of the root samples was performed by a rapid freezing in liquid N_2. Frozen biomass (1.5 g) was powdered by steel pestle in liquid N_2 and extracted by a solvent mixture of methanol, chloroform and distilled water at 2: 2: 1.2 (v/v ratio), according to the modified Bligh-Dyer procedure for plant samples (Miccheli et al. 1988, Manetti et al. 2004). 4.5 ml CH_3OH: $CHCl_3$ (2:1 v/v ratio) mixture was added to frozen powder and after mixing 1.5 ml $CHCl_3$ and 1.8 ml H_2O were added. The samples were mixed by vortex for 1 min and kept overnight at 4°C then centrifuged for 30 min at 11,000 × g at 4°C. The resulting upper hydro-alcoholic and lower organic phases were carefully separated and dried under N_2 flow. The dried phases were stored at -80°C until the NMR analysis.

2.3 NMR spectroscopy

The dried residue of the hydro-alcoholic phase was dissolved in 0,6 ml $CD_3OD/D2O$ (1:2 v/v ratio) containing 3-(trimethylsilyl)- propionic-2,2,3,3,-d4 acid sodium salt (TSP, 2mM) as internal standard (chemical shift reference). The dried residue of the chloroformic phase was dissolved in 0,6 ml $CDCl_3$, (Cambridge Isotope Laboratories, Inc.), (99,8%), containing 1,1,3,3,5,5-hexamethyl-cyclo-tri-siloxane (HMS) (Sigma-Aldrich, Usa), as internal standard (2mM). NMR spectra were carried out using a Bruker Avance 400 spectrometer operating at a frequency of 400,13 MHz for the proton. Monodimensional proton spectra were acquired at a temperature of 298 K with a spectral width of 15 ppm, 64k data points, 128 scans with an acquisition time of 5.45 s and a relaxation delay of 5.05 s for a total repetition time of 10.5 s complying with the full relaxation condition after a 90 degree pulse.

The univocal assignation of proton resonances was achieved by means of bidimensional ^{1}H homonuclear Total Correlation Spectrosopy (TOCSY) experiments and by bidimensional ^{1}H-^{13}C heteronuclear Single Quantum Coherence (HSQC) experiments.

Homonuclear experiments were recorded at 298 K with a spectral width of 15 ppm in both dimensions employing a matrix of 2k x 512 data points, a repetition time of 2 s and 64 scans. The mixing time for the ^{1}H–^{1}H TOCSY was 110ms. HSQC experiments were acquired with a spectral width of 15 ppm in proton dimension and 220 ppm in the carbon one employing a matrix of 2k x 256 data points for the proton and the carbon dimensions respectively, a repetition delay of 2 s and 128 scans. The water signal was suppressed using solvent pre-saturation, with the irradiation time following the relaxation delay. In order to minimize the variability of the signals intensity due to water suppression, a careful calibration of the soft pulse for water suppression was always performed.

1D-NMR spectra were processed with 1D-NMR Manager ver. 12.0 software (Advanced Chemistry Development, Inc., Toronto, Ontario, Canada), whereas 2D-NMR spectra were processed by using Bruker Top Spin (Bruker, Germany).

The quantification of the signals of extracts was based on the respective reference used as internal standard at a known concentration (2mM). The integral of each signal was normalized by the number of protons and the value obtained was reported in concentration through the relationship:

$$C_m = \frac{I_m \times C_r}{I_r}$$

where C_m and C_r represent the concentration of the single metabolite and the reference respectively, while I represent the area of the corresponding integral. The concentration obtained was normalized to the weight of the sample compared to the volume of 600 µl and then expressed in mmol/g.

2.4 Multivariate data analysis

Multivariate data were analysed by Principal Component Analysis (PCA), ANOVA simultaneous component analysis (ASCA) and Partial Least Square 2 (PLS2).

2.4.1 Principal Component Analysis (PCA)

The most widely-used multivariate techniques in metabolomics study are those based on projection methods which combine the measured variables into so-called latent variables.

Principal components analysis (PCA) is the most widespread multivariate chemometric technique performed to explore samples in a data set (Brereton 2003). Multivariate datasets can be represented as a matrix **X**. Each row of this matrix contains the measurements of one sample *n* and each column contains the measurement of one variable *j*. Given a dataset, described by *j* variables, each variable could be regarded as constituting a different dimension, in a p-dimensional hyperspace. Multi-dimensional hyperspace is often difficult to visualize and thus the main objectives of PCA are to simplify and reduce dimensionality of original data set extracting the smallest number components that account for most of the variation in the original multivariate data and to summarize the data with little loss of information. The new obtained set of variables is formed by linear combinations of the original variables which maximize the variance in the data set and are called principal components (PCs). These PCs are extracted in decreasing order of importance so that the first PC accounts for as much of the variability in the data as possible and each successive component accounts for as much of the remaining variability as possible. To reproduce the total system variability of the original n variables, we need all PCs. However, if the first few PCs account for a large proportion of the variability (80-90%), we have achieved our objective of dimension reduction.

From a mathematical point of view, PCA results in an abstract transformation of the original data matrix, which takes the form $\mathbf{X} = \mathbf{T}.\mathbf{P} + \mathbf{E}$, where **T** is a matrix containing the component scores of the model, **P** is a matrix containing the component loadings and **E** is a matrix containing the residuals of the model. Hence, each PC is characterized by two types of information, the score and

the loading. The scores or coordinates of the samples along a component describe the structure of the data in terms of similarities and differences between the samples. The loadings are correlation coefficients between the PC scores and the original variables and measure the importance of each variable in accounting for the variability in the PC. On the other hand, the loading represent the weight for each original variable when calculating the principal component. Samples with similar scores along a component will be similar for variables with a high loading for that component.

There are two way to interpret the obtained results: the score plot that summarize the relationship among the observations (or samples) and the loading plot that summarize the relationship among the variables.

Although PCs are abstract mathematical entities they are represented as vectors in an imaginary multidimensional space, in which each vector represents an axis. The first principal component is the direction in multidimensional space along which projections have the largest variance. The second principal component is the direction which maximizes variance among all directions orthogonal to the first.

In practice, PCA acts as a form of variable reduction, reducing the large original dataset to a much smaller more manageable dataset which can be interpreted more easily.

2.4.2 Partial Least Square (PLS)

PCA does not always extract hidden information that explains system behaviour because this may not correspond to the information summarized in the latent variables. In these cases, latent variable regression methods as Partial Least Square (PLS) may be preferred. PLS is a supervised pattern recognition method to identify interesting metabolites through orthogonal score vectors, also called latent variables (LV) or components, maximizing the covariance between different blocks of variables (Brereton 2003), called X and Y. It is particularly useful when we need to predict a set of dependent variables from a (very) large set of independent variables (i.e., predictors). In PLS modelling we assume that the investigated system is influenced by a few underlying LVs. The number of these LVs is usually not known, and one aim with the PLS analysis is to estimate this number.

Although there are several algorithms to describe PLS, it is often presented in the form of two equations:

$$\mathbf{X = T.\ P + E}$$

$$\mathbf{c = T.\ q + f}$$

where **X** represents the experimental measurements (metabolites) and **c** the concentrations. The vector **q** has some analogy to a loadings vector, although is not normalized. **E** is an error matrix for the x block and **f** an error vector for the c block.

It is important to emphasize that **T** and **P** for PLS are different to **T** and **P** obtained in PCA, and unique sets of scores and loadings are obtained for each compound in the dataset. Moreover, scores and loadings are dependent both on experimental measurements (i.e. spectra) and the concentrations. The optimum number of significant PLS components can be estimated using cross-validation. Unlike applications in PCA for pattern recognition, in PLS most prefer to use the c block performance as a criterion. Typically cross-validation errors level off and then increase after the true number of components has been calculated. In contrast, auto-prediction errors always decrease with increasing number of components. The reason for this is that the later components model noise,

and so samples left out of the original calibration set are predicted worse when using more components. Hence the shapes of graphs for auto-prediction and cross-validation will diverge at a certain point. This information is important because, to be effective, calibration models will be used to determine the concentration of unknowns, so the user must understand at which point he or she is 'over-fitting' the data.

Two variants of PLS are the most frequently used as PLS regression methods: the most common PLS1 is used when one of the block of data consists of a single variable) and PLS2 is used when both blocks are multidimensional.

In particular PLS2, is an extension to PLS1. Considering that the concentration (or **c**) block consists of more than one variable, PLS2 is helpful especially since it would predict all the concentrations simultaneously. Instead of obtaining several independent models, we can analyse all the data in one go. In PLS1 one variable is modelled at a time, whereas in PLS2 all known variables can be included in the model simultaneously. If there are interactions between variables this method can have advantages. A second advantage is that only one PLS2 model is required however many **c** variables are measured, whereas separate PLS1 models (often with different numbers of significant components) are required for each c variable. In PLS2, the regression is carried out by projecting both blocks onto a reduced space of latent variables (LVs), selected as the ones into which the covariance between X and Y is maximal. Hence, the corresponding X- and Y-scores possess the property of explaining as much as possible of the variation in the respective block under the constraint of being linearly correlated. Therefore, together with the overall regression relation linking the two blocks, PLS2 provides a wealth of tools to interpret the correlation structure. The inspection of the distribution of the samples into the space spanned by the significant LVs (scores plot) allows defining similarities and differences between the analysed samples. On the other hand, the examination of the contribution of the experimental variables to the definition of the latent vectors (X- and Y-loadings) allows interpreting the correlation structure within each block and, when the two sets of loadings are plotted together in what can be called a biplot, to unravel the relations

between variables in the different blocks. Operationally, when analysing a loadings biplot, useful information can be obtained; first of all, the variables lying farthest from the origin are those contributing the most to the model. Moreover, variables falling close to one another on the plot are highly positively correlated, and negatively correlated to the variables lying on the opposite side of the plot with respect to the origin. Lastly, when comparing the scores and the loadings plot (which refer to the same set of latent vectors), one can state that samples occupying a position of the scores plot where one or a group of variables lies in the corresponding loadings plot, have the highest value of this(ese) variable(s).

2.4.3 ANOVA-Simoultaneous component analysis (ASCA)

A novel approach for the analysis of multivariate data is ANOVA-simultaneous component analysis (ASCA). In this method the parameter estimation aspect of ANOVA is merged with PCA or Simultaneous Component Analysis (SCA), such that the drawbacks of both methods are removed (Jansen et al. 2005). As a matter of fact, ANOVA is a univariate method used to determine the effect of different experimental factors on the variation in a dataset but cannot take the covariance between different variables into account. SCA can be seen as PCA for multiple matrices and is a widely used method that models the relationships between the different variables in a multivariate dataset by analyzing its covariance or correlation matrix. However, PCA or SCA, does not take the experimental design into account, which means that the different contributions to the variation caused by the experimental design are confounded in the model. Indeed, ASCA takes both the covariance between the multiple variables and the design of the experiment into account and is particularly useful when the significance of the effect of one or more factors on the experimental data can be evaluated. In particular, it operates by partitioning the variation of the experimental signal collected on different samples into the contributions induced by the effect of controlled factors, usually a treatment or an experimental condition, or of their interactions, and by analyzing the resulting matrices by SCA (Smilde et al. 2005). Simultaneous component analysis is then performed on the individual matrices to model the variability corresponding to each effect. From a purely mathematical standpoint, SCA is identical to PCA: the difference is only philosophical in nature. Indeed, in SCA different samples are modelled at the same time. Accordingly, each of the matrices resulting from the ANOVA partitioning is decomposed as:

$$\mathbf{X}_i = \mathbf{T}_i \mathbf{P}_i^T + \mathbf{E}_i \qquad (1)$$

where $\mathbf{T}_i$ and $\mathbf{P}_i$ are the scores and loadings for the i^{th} partition, respectively, and $\mathbf{E}_i$ is the corresponding residual matrix.

It must be stressed that for mean centred two level balanced design like the one in this study, all the partitions corresponding to main effects and interactions are rank one, resulting in zero errors.

As previously described, ASCA partitions the variation of the original matrix into the contribution of the main effects of the controlled factors, of their interactions and residuals. The extent of each contribution is expressed in the form of the sum of squares of the elements of the matrix corresponding to the effect:

$$SSQ_k = \|\mathbf{X}_k\| = \sum_i \sum_j \left(x_{ij}^k\right)^2 \quad (2)$$

where x^k_{ij} is the i[th] row, j[th] column entry of the matrix $\mathbf{X}_k$. In order to assess whether an effect is significant or not, the experimental sum of squares has to be compared with the distribution of values corresponding to the null hypothesis. In this study, for each factor and interaction, the distribution of the values of the sum of squares corresponding to the null hypothesis (no significance of the considered effect) was estimated non parametrically by means of a permutation (randomization) test. The permutation test works by uncoupling the group labels from the data and randomly reassigning them: it does not change the metabolite value for a sample, but just reassigns the sample randomly to one of the treatment groups. Partitioning the permuted data according to the ANOVA scheme and computing the corresponding sum of squares

$$SSQ_k^{perm} = \left\|\mathbf{X}_k^{perm}\right\| = \sum_i \sum_j \left(x_{ij}^{k,perm}\right)^2 \quad (3)$$

allows it to be checked whether the results with randomized data are as different from zero as those obtained from the experimental data. Repeating the randomization procedure for an appropriate number of times, each time calculating the corresponding sum of squares, provides an empirical distribution of the SSQ_k values for the null hypothesis. Validation of the significance of the effect is then carried out by comparison of the SSQ_k obtained from the experimental data with this distribution (Vis et al. 2007).

The total variation of the experimental matrix was then partitioned according to equation 1 and the significance of the main effects (time and/or elicitation) and of their interaction was evaluated by permutation test (Vis et al. 2007).

SCA (after Pareto scaling) was used to model the variation in the two corresponding matrices $\mathbf{X}_{treatment}$ and $\mathbf{X}_{time}$. As only two levels were considered for each factor, single component models explained 100% of the variance of the individual matrices, i.e. each matrix $\mathbf{X}_i$ was decomposed into the product of one score and one loading vector.

In order to use SCA results for the interpretation of the metabolic effect of the considered factors, the significance of the contribution of the experimental variables to the definition of the models (i.e. the significance of the loadings) had to be assessed: if the loading of a variable is statistically different from zero, then the factor has an effect on the concentration of that metabolite. In particular, a bootstrap procedure was used to calculate the empirical distribution of the loadings, so as to be able to check their significance. Operationally, at each bootstrap cycle, a new partition $\mathbf{X}_i^{bstp}$ was constructed from the mean centered matrix by including, for each level, a random subset of the original samples with repetitions, taking care that the numerosity of each treatment group was preserved. For instance, if the effect considered has two levels and, in the original matrix, samples 1-10 correspond to level 1 and samples 11-20 correspond to level 2, one bootstrap cycle could produce a matrix made up of samples [1 2 2 2 5 5 6 7 9 10 12 13 13 14 16 16 16 18 19 19]. ASCA analysis on this matrix will result in an estimate of the loading vector for the effect so that repetition of the procedure for a significant number of times (in our study 100000) will produce an empirical distribution of the values of the loadings for each variable. A metabolite is then considered to contribute significantly to the model if, based on this distribution, its loading is statistically different from zero.

2.5 Histological analysis

To investigate the effect of culture time and chitosan elicitation on root anatomy, sections of fresh samples and fixed samples embedded in resin were analysed.

To obtain fresh sections, *in vitro* regenerated roots were embedded in agar (4%), longitudinally and transversely sectioned at 30 μm thikness with a vibratome (T.P.I. series 1000), stained with 0.1% toluidine blue, and directly observed under a light microscope (Zeiss Axioscop 2 Plus) equipped with a digital camera (Zeiss AxioCam MRc5).

To obtain resin sections, root samples were fixed for 24 h in 70% ethanol and dehydrated for 12 h trough two soak in absolute ethanol series. Pre-infiltration phase was carried out by transferring root samples in a mixture (basic solution) composed by equal parts of absolute ethanol and base liquid Technovit 7100 (1:1 v/v) at 4 °C, for 2-3 h. Samples were infiltrated for 24 h in a working solution constituted by 1 g hardener I (=1 bag) dissolved in 100 ml base liquid Technovit 7100 and mixed for 10 minutes. Polymerization phase was carried out in a mixture composed by 1 ml hardener II added to 15 ml of working solution. Root samples were embedded into 1-3 ml of polymerization solution and poured in histoforms, at room temperature (23 °C) for 24 h. To mount samples, a mixture of Technovit 3040 in a volume ratio of 2 parts powder to 1 part liquid was used. The mixture was poured into the recess at the back of the histoblocs to a level of about 2 mm above the base of the histoblocs. After about 10 min, the histoblocs together with the fixed roots was removed from the histoforms. Fixed roots were longitudinally and transversely sectioned at 7 μm with a microtome (Microm HM 350 SV microtome, Microm, Germany), stained with 0.1 % toluidine blue and observed under a light microscope.

To investigate the effect of culture time and chitosan elicitation on roots morphology, whole roots samples were analyzed by a Zeiss stereomicroscope equipped with reflected and transmitted light.

2.6 Histochemical analysis

Regenerated *in vitro* roots were analyzed through histochemical essay for the terpenes detection.

Roots samples were embedded in agar (4%), longitudinally and transversely sectioned at 30 μm thikness with a vibratome (T.P.I. series 1000), stained with Nadi reagent and observed under a light microscope. Nadi solution was prepared at the time of use, mixing 0.5 ml of a 1% α-naphthol solution in 40% alcohol with 0.5 ml of 1% dimethyl-*p*-phenylenediamine chloride in water and with 49 ml of 0.05 M phosphate buffer [pH 7.2]) (David et al. 1964). Some roots were directly treated with the reagent Nadi, fixed on slides and examined with a Zeiss optical microscope. The analyses were also performed on roots of seedlings obtained by *in vitro* seed germination.

CHAPTER 3

STUDY I

A non-targeted metabolomics approach to evaluate the effects of biomass growth and chitosan elicitation on primary and secondary metabolism of *Hypericum perforatum in vitro roots* after 24 and 72 hours

3.1 Introduction

Hypericum perforatum (common St. John's wort) is a perennial herb which is distributed globally (except Antarctica) (Nürk et al. 2013) and is commonly used worldwide for the treatment of mild and moderate depression (Butterweck 2003, Crockett and Robson 2011, Nahrstedt et al. 2010). Research on St. John's wort has been focused primarily on hypericins and hyperforins as the major constituents of the aerial parts of the plant and responsible for the antidepressant activity (Walker et al. 2002). *H. perforatum* plant extracts also show a broad range of other pharmacological activities, including anti-cancer, anti-inflammatory, antiviral, antioxidant, and antibacterial properties (Birt et al. 2009, Saddiqe et al. 2010, Caraci et al. 2011) that may be correlated to other bioactive compounds.

Although much is known about the medicinal properties of the aerial parts, little is known about the chemical composition or the potential applications of the *H. perforatum* root extracts (Tocci et al. 2013, Crockett et al. 2011). Roots of many species have been studied because of the presence of high value bioactive molecules (Baque et al. 2012, Paek et al. 2009) but the composition of products obtained from wild-grown plants can be greatly affected by several environmental biotic and abiotic factors and the content of bioactive secondary metabolites can be variable and not always satisfactory for application purposes. Since the production of biomass and metabolites is significantly affected by various parameters that need to be optimized, plant cell, tissue and organ cultures are considered effective systems to produce natural products for bioprocessing applications (Rao et al. 2002, Pasqua et al. 2003, Ferrari et al. 2005, Zhang DW et al. 2013). It has been demonstrated that *H. perforatum* root cultures, because of their high rate of proliferation and high genetic and metabolic stability, are an efficacious alternative system for controlling the factors that affect metabolic pathways and for biosynthesizing phytochemical compounds (Cui et al. 2010, 2011, Zobayed et al. 2004).

Chitosan is frequently used as an elicitor to stimulate the production of pharmaceutically useful compounds both in *in planta* and in *in vitro* systems (Yin et al. 2012). Chitosan elicitation has been also adopted as an effective strategy to enhance secondary metabolite production, such as xanthones

and other polyphenols, in *H. perforatum in vitro* roots (Tocci et al. 2012, 2013) but up to date how the chitosan affects the root metabolome has not been studied.

Metabolomic analysis is a powerful tool by which to gain a comprehensive view of how metabolic networks are regulated and has indeed been applied in many researches in recent years (Nicholson et al. 1999).

An analytical technique employed to study the metabolome and to obtain a large quantity of data is nuclear magnetic resonance (NMR) spectroscopy. In non-targeted metabolomic analysis, NMR spectroscopy has afforded some important advantages that can be summarized as ease of quantification, reproducibility, straightforward metabolite identification and its ability to determine unexpected metabolites (Kim et al. 2011). NMR based metabolomic has been applied in quality controls for medicinal plants (Rasmussen et al. 2006, Agnolet et al. 2010, Yang et al. 2006, Falasca et al. 2013), in chemotaxonomy studies (Kim et al. 2010, Matsuda et al. 2010), in the study of the biological activity of plant preparations (Modarai et al. 2010) of plant interactions with other organisms (Jahangir et al. 2008) of the fruit ripening process (Capitani et al. 2010) and of genetically transformed plants (Manetti et al. 2006). Finally, NMR-based metabolomic analysis has been applied to investigate the interplay between primary and secondary metabolism in *Opium poppy* cells treated with a fungal elicitor (Zulak et al. 2008). Recently, NMR fingerprinting was used to investigate the natural product diversity within the genus *Hypericum* and its correlation to bioactivity, exemplified by cytotoxic properties (Porzel et al. 2013).

Applying multivariate analysis to NMR spectroscopy data it is possible to obtain comprehensive information about the biochemical constituents of a biological system and to achieve the quantitative assessment of time-related multiparametric metabolic responses to patho-physiological stimuli (Nicholson et al. 1999, Lindon et al. 2001).

3.2 Objective

The aim of the present study was to characterize the changes in the primary and secondary metabolism of *in vitro* regenerated roots of *H. perforatum* during growth in a confined culture environment and in response to chitosan after 24 and 72 hours after elicitation in order to obtain baseline information to be used in the design of optimal bioprocesses employing this biotechnological system.

A metabolomic platform integrating non-targeted NMR-based metabolic profiling and multivariate analysis such as ANOVA-simultaneous component analysis (ASCA) was used.

An histological analysis was carried out to investigate the effect of chitosan elicitation on the morphology and anatomy of *Hypericum perforatum in vitro* roots after 24 and 72 hours of treatments.

3.3 Material and Methods

Liquid cultures were established inoculating 1 g fresh weight (FW) of roots in magenta vessels containing 80 ml liquid MS medium supplemented with glucose (2,2 g l-1) and IBA (1 mg l-1). The medium was renewed every 4 days, time necessary for biomass duplication. The roots were elicited using chitosan (medium molecular weight; Sigma-Aldrich, Milan, Italy), dissolved in acidified water with HCl (1M), at a final concentration of 200 mg l−1, which was added on the twelfth day of culture using 0,22 μm sterile filter. An adequate amount of water was added to the control samples.

In vitro regenerated roots were harvested at twelfth day (time 0), at thirteenth day (24 h, time 1) and at fifteenth day (72 h, time 2) and divided into five groups: basal (time 0), control and treated at 24 hours after elicitation (time 1) and control and treated to 72 hours after elicitation (time 2). The samples were subjected to metabolic quenching and prepared for the NMR acquisition (as explained in the paragraph 2.1). NMR spectra were acquired and analysed (as explained in the paragraph 2.2).

Multivariate data analysis was carried out using Unscrambler 10 Software (CAMO, Oslo, Norway) and routines operating in a Matlab R2012a environment (The MathWorks, Inc., Natick, MA).

Spectral data were mean-centered and scaled before analysis. To explore the whole data set and highlight significant differences among sample, inherent clustering and potential outliers, thus obtaining a simple visual idea as to the main relationships between these samples, principal component analysis (PCA) was used. PCA was applied to the data matrix containing data relative to root samples (control and treated) consisting of 24 rows and 49 columns, each row contains the measurements (concentrations) for a given sample and each column the measurement for a given variable (metabolites).

In order to assess whether treatment, time (corresponding to biomass density) and their interaction could have an effect on the metabolic profile of the samples as determined by NMR spectroscopy, ANOVA-Simultaneous component analysis (ASCA) was used (Smilde et al. 2005, Jansen et al. 2005). In order to have a balanced design, only the data collected at time 24 h and 72 h were considered for the analysis, which was then carried out on a data matrix made of 20 observations,

i.e. 5 replicates for each of the 4 time/treatment combinations (control 24 h; control 72 h; treated 24 h; treated 72 h). Accordingly, the mean-centered matrix $\mathbf{X}_c$ of the experimental data was partitioned into the individual matrices accounting for the effects of time, treatment, time-treatment interaction, and for the residual variation (associated to the experimental error):

$$\mathbf{X}_c = \mathbf{X} - \mathbf{X}_{mean} = \mathbf{X}_{treatment} + \mathbf{X}_{time} + \mathbf{X}_{time^{*}treatment} + \mathbf{X}_{residual}$$

where $\mathbf{X}_{mean}$ is a matrix whose rows are all identical to the overall mean profile. Operationally the computation of each of the matrices corresponding to the main effects was carried out as follows. For each of the considered factors, the rows of the centered matrix $\mathbf{X}_c$ corresponding to the different levels of the design were found and averaged, and these calculated mean values were used to build the matrix associated with the effect: if the i^{th} sample corresponds to the 1^{st} level of factor A, the i^{th} row of the matrix $\mathbf{X}_A$ will contain the average vector calculated on all samples for which factor A is at level 1, and so on. Computation of the interaction matrix was made analogously, after deflation (=subtraction) of the matrices corresponding to the main effects (Figure 1).

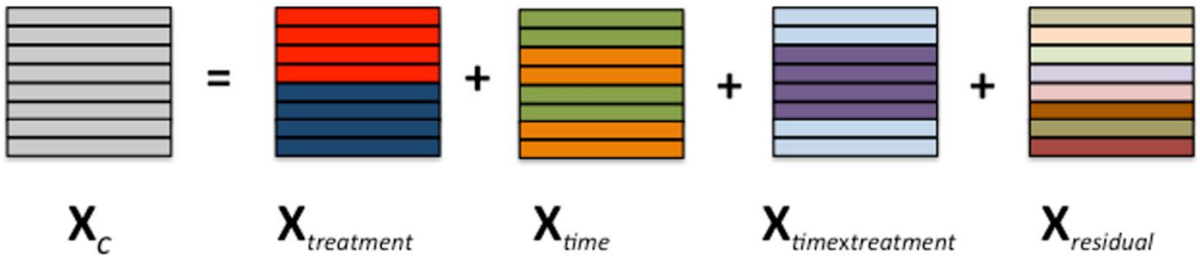

Figure 1. Simultaneous component analysis was then performed on the individual matrices to model the variability corresponding to each effect. The total variation of the experimental matrix was then partitioned according to equation (1) and the significance of the main effects and of the interaction was tested by permutation tests, as described in the Materials and Methods section.

Having verified that treatment and time had a significant effect on the metabolic profiles of samples, SCA (after Pareto scaling) was used to model the variation in the two corresponding matrices $X_{treatment}$ and X_{time}. As two levels only were considered for each factor, single component models

explained 100% of the variance of the individual matrices, i.e. each matrix Xi was decomposed into the product of one score and one loading vector.

In order to use SCA results for the interpretation of the metabolic effect of treatment and time, the significance of the contribution of the experimental variables to the definition of the models (i.e. the significance of the loadings) had to be assessed: if the loading of a variable was statistically different than zero, then the factor had an effect on the concentration of that metabolite. In particular, a bootstrap procedure was used to calculate the empirical distribution of the loadings, so to be able to check their significance. Operationally, at each bootstrap cycle a new partition Xibstp was built from the mean centered matrix by including, for each level, a random subset of the original samples with repetitions, having care that the numerosity of each treatment group was preserved. A metabolite was then considered to contribute significantly to the model if, based on this distribution, its loading was statistically different than zero.

To assess the statistical significance of the metabolic changes among experimental groups and compare with the results obtained by multivariate analysis, Student's t test was applied. To evaluate the time effect compared to elicitation effect, Student's t test for paired data was used. To evaluate the variations between experimental groups, Student's t test for unpaired data was applied. Differences showing P-values less than 0.05 were considered statistically significant.

To investigate the effect of culture time and chitosan elicitation on root anatomy, sections of fresh samples and fixed samples embedded in resin were analysed. To investigate the effect of culture time and chitosan elicitation on roots morphology, whole roots samples were analysed by a Zeiss stereomicroscope equipped with reflected and transmitted light.

Histochemical assay for the detection of terpenic compounds was conducted both on in vitro regenerated roots (control and elicited) and on roots of seedlings obtained by *in vitro* seed germination. Root samples were directly treated with the Nadi reagent, mounted on glass slides and observed under an optical microscope. Some root samples, before being treated and observed, were

included in 4 % agar and sectioned with a thickness of approximately 30 μm using a vibrating microtome.

3.4 Results

The growth curve of both elicited and non-elicited *H. perforatum in vitro* roots was measured during the course of fifteen days and is plotted in Figure 2.

In control roots, it is possible observe an exponential phase of growth curve from day 0 to day 13, whereas the stationary phase can be observed from day 13 to day 15.

In elicited roots, the chitosan addition at day 12 caused a sudden slowdown of growth, whereas the growth of the control roots continued.

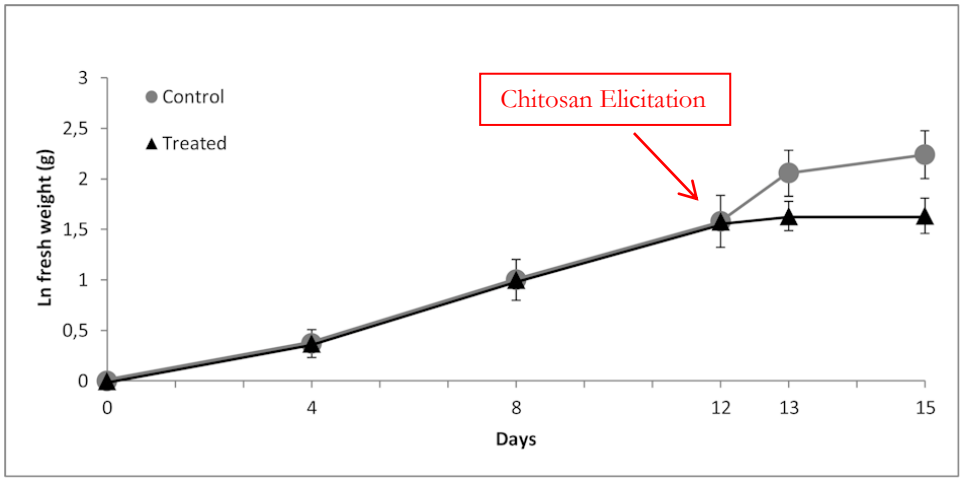

Figure 2. The growth curve of *H. perforatum in vitro* roots over a period of 15 days. Growth is expressed as a natural logarithm of fresh weight biomass. Data are presented as the mean ± standard deviation (SD) of five samples in five independent experiments.

The hydroalcoholic and chloroformic total extracts obtained from chitosan elicited and control roots were investigated by ^{1}H-NMR spectroscopy. Typical ^{1}H-NMR spectra of control and treated roots obtained are shown in Figure 3.

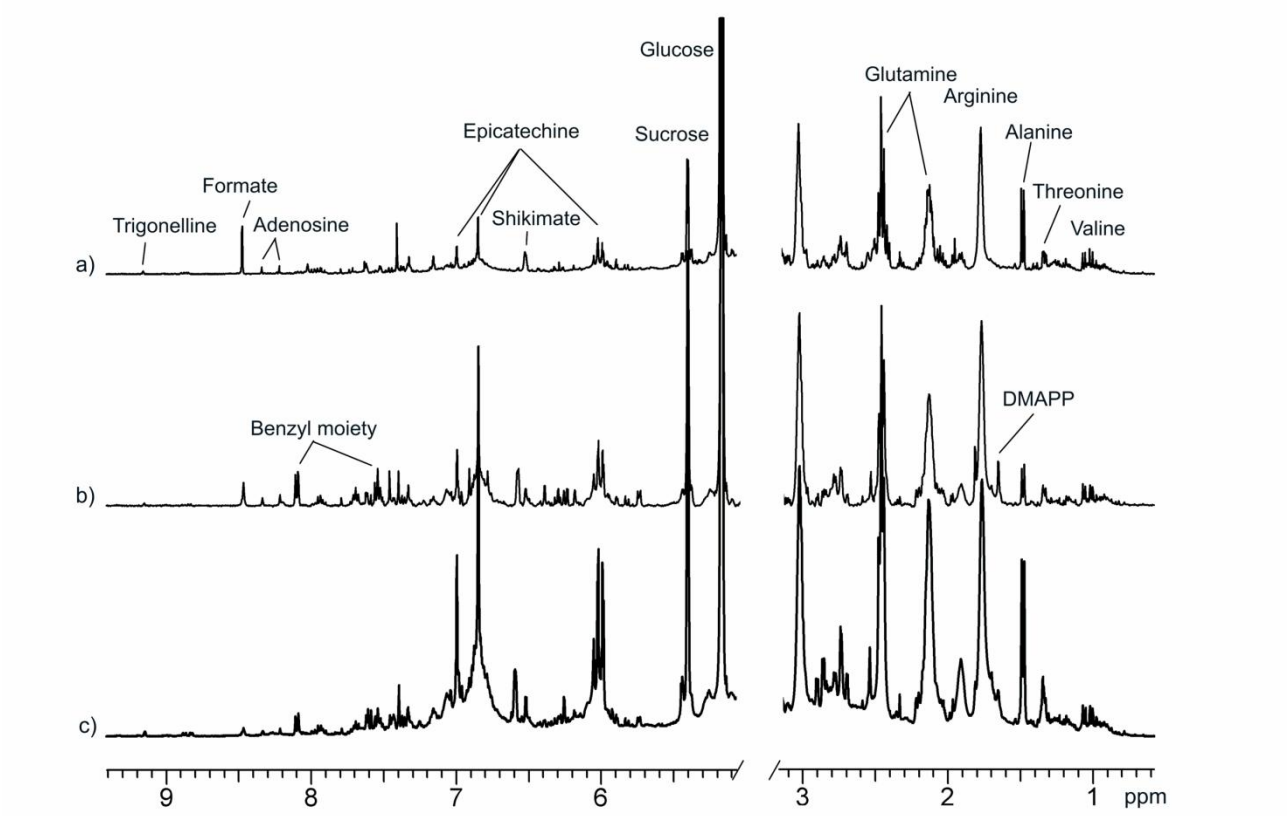

Figure 3. Typical ^{1}H-NMR spectra of hydroalcoholic phase of control and treated roots. a) Control sample at time 0; b) elicited sample at time 24 h; c) elicited sample at time 72 h.

The hydroalcoholic and chloroformic spectra were analysed and sixty-four metabolites were assigned (Table 1).

Table 1. ^{1}H chemical shifts of metabolite signals in hydroalcoholic and chloroformic root extracts.

Hydroalcoholic extract

Class	No	Compound	Chemical shifts and coupling constants
Amino Acids			
	1	Alanine	δ 3.70 (α-CH,q), **δ 1.48** (β-CH_3,d)
	2	Arginine	δ 3.69 (α-CH), δ 3.25 (δ-CH_2, t), δ 1.9 (β -CH_2), δ 1.72 (γ-CH_2)
	3	Glutamic Acid	δ 3.67 (α-CH), δ 2.42 (γ-CH_2), δ 2.14 (β-CH), δ 2.04 (β'-CH)
	4	Glutamine	δ 3.70 (α-CH,t), **δ 2.46** (γ-CH_2, m), δ 2.13 (β -CH_2, m)
	5	Histidine	**δ 8.03** (CH-$_2$ ring), δ 7.16 (CH-4 ring), δ 3.93 (α-CH), δ 3.27 (β-CH), δ 3.16 (β'-CH)
	6	Isoleucine	δ 3.68 (α-CH), δ 1.96 (β-CH), δ 1.54(γ'-CH_2),δ 1.26 (γ-CH_2), **δ 1.02** (β-CH_3),δ 0.97 (δ-CH_3)
	7	Leucine	δ 3.62 (α-CH), δ 1.77 (β-CH_2), δ 1.67 (γ-CH), **δ 0.97** (δ-CH_3), δ 0.92 (δ'-CH_3)
	8	Threonine + Lactate	δ 4.22 (β-CH), δ 3.49 (α-CH, d), **δ 1.34** (γ-CH_3)
	9	Tryptophan	**δ 7.73** (CH-4 ring, d), δ 7.54 (CH-7 ring, d), δ 7.40 (CH-2 ring, s), δ 7.32 (CH-6 ring), δ 7.19 (CH-5 ring)
	10	Valine	δ 3.53 (α-CH), δ 2.28 (β-CH), **δ 1.06** (γ-CH_3), δ 1.01 (γ'-CH_3)
Organic Acids			
	11	α-Hydroxy-n-valeric Acid	δ 1.60 (β-CH_2), δ 1.38 (γ-CH_2), δ 0.92 ($CH_{3,t}$)
	12	γ-Aminobutyric Acid	δ 3.01 (γ-CH_2), **δ 2.33** (α-CH_2) δ 1.90 (β-CH_2)
	13	Acetic Acid	δ 1.95 (β-CH_3, s)
	14	Citric Acid	δ 2.73 (α,γ-CH, dd), δ 2.50 (α',γ'-CH, dd)
	15	Formic Acid	**δ 8.48** ($HCOO^-$, s)
	16	Lactic Acid	δ 4.03 (α-CH), **δ 1.33** (β-CH_3,d)
	17	Malate (conjugated)	δ 5.33 (α-CH, dd, J=3.30 Hz, 10.08 Hz), δ 2.87 (β-CH, dd), δ 2.77 (β'-CH, dd)
	18	Pyruvic Acid	**δ 2.33** (β-CH_3, s)
	19	Shikimic Acid	**δ 6.52** (H-3, m), δ 4.36 (H-4), δ 3.96 (H-6), δ 3.64 (H-5), δ 2.77 (H-7'), δ 2.18 (H-7)
Phenols and Polyphenols			
	20	Benzoyl moiety	**δ 8.10** (H-2, H-6, d, J=7.34 Hz), δ 7.69 (H-4, pt), δ 7.54 (H-3, H-5, pt)
	21	Epicatechin	δ 7.00 (CH-2' ring B), δ 6.85 (CH-5',CH-6' ring B),δ 6.02 (CH-8 ring A, d), **δ 5.99** (CH-6 ring A, d), δ 4.87 (CH-2 ring C), δ 4.25 (CH-3 ring C), δ 2.89 (CH-4 ring C), δ 2.75 (CH-4' ring C)
	22	Gallic acid	**δ 7.02** (s)

Carbohydrates			
	23	Fructose	**δ 4.13** (H-3, d, J=8.99 Hz), δ 4.00 (H-5), δ 3.79 (H-6'), δ 3.63 (H-6'')
	24	α-Glucose	**δ 5.17** (H-1, d, J=3.67 Hz), δ 3.80 (H-6), δ 3.70 (H-3), δ 3.45 (H-5), δ 3.35 (H-2)
	25	β-Glucose	**δ 4.56** (H-1,d, J=7.89 Hz), δ 3.87 (H-5), δ 3.69 (H-3), δ 3.36 (H-4), δ 3.18 (H-2)
	26	Sucrose	**δ 5.41** (CH-1, Glc), δ 3.82 (CH-5, Glc), δ 3.75 (CH-3, Glc), δ 3.49 (CH-2, Glc), δ 3.41 (CH-4, Glc), δ 4.15 (CH-3, Fru, d, J=8.62 Hz), δ 4.03 (CH-4, Fru), δ 3.81 (CH-6, Fru)
Miscellaneous Compounds			
	27	Acetoacetate	**δ 2.59** (α-CH_2, s)
	28	DMAPP	δ 5.20 (γ-CH=), δ 4.06 (α-CH), δ 1.81 (δ-CH_3), **δ 1.65** (δ-CH_3)
	29	Ethanol	δ 3.61 (α-CH), δ 1.19 (β-CH_3)
	30	Ethanolamine	δ 3.80 (CH2-OH), δ 3.11 (CH2-NH)
	31	Trigonelline	**δ 9.16** (CH-1, s), δ 8.87 (CH-5, CH-3, m), δ 8.10 (CH-4, m), δ 4.45 (CH_3-N, s)
	32	UXP	δ 7.99 (CH-6, d), **δ 5.94** (CH-5, d), δ 5.94 (CH-1'), δ 5.10 (CH-2'), δ 3.82 (CH-5')
	33	Adenosine	δ 8.35 (CH-8, s), **δ 8.22** (CH-2, s)
Unknown Compounds			
	34	U0	**δ 0.65** (s)
	35	U1	**δ 0.78**, δ 1.31
	36	U2	**δ 0.82**, δ 1.28
	37	U3	**δ 1.31** (s)
	38	U4	**δ 5.14** (s)
	39	U5	**δ 5.38** (d, J=3.85 Hz), δ 3.96
	40	U6	**δ 5.44** (d, J=3.85), δ 4.03, δ 3.84, δ 3.72, δ 3.49
	41	U7	**δ 5.79** (s)
	42	U8	**δ 6.19** (s)
	43	U9	δ 6.56 (d, J= 2.02 Hz), **δ 6.27** (d, J=2.0 Hz)
	44	U10	**δ 6.29** (s)
	45	U11	**δ 7. 40** (s)
	46	U12	**δ 7.46** (CH-8, s)
	47	U13	**δ 7.90** (s)
	48	U14	**δ 5.74** (d, J=7.52 Hz), δ 3.57

49	U15	**δ 6.23** (CH-2, d, J=2.02 Hz), δ 6.39 (CH-4, d, J=2.02 Hz)
50	U16	**δ 6.32** (s)
51	U17	**δ 6.96** (s)
52	U18	**δ 7.61** (s)
53	U19	**δ 7.59** (s)
54	U34	**δ 5.45** (s)
55	UY	**δ 6.19** (s)
56	UX	**δ 6.29** (s)
57	U21	**δ 7.27** (s)
58	U22	**δ 7.33** (s)
59	U23	**δ 7.52** (s)

Chloroformic extract

Class	No	Compound	Chemical shifts and coupling constants
Fatty Acids			
	1	Polyunsatured Fatty Acids (linolenic)	δ 5.35 (CH=CH), **δ 2.82** (CH=CH-*CH_2-CH=CH), δ 2.33 (*CH_2COO^-), δ 2.04 (*CH_2CH=CH), δ 1.30 ((*$CH_2)_n CH_2CH_2COO^-$), δ 0.98 (CH_3)
	2	Polyunsatured Fatty Acids (linoleic)	δ 5.35 (CH=CH), **δ 2.77** (CH=CH-*CH_2-CH=CH), δ 2.33 (*CH_2COO^-), δ 2.04 (*CH2CH=CH), δ 1.30 ((*CH_2)n$CH_2CH_2COO^-$), δ 0.88 (CH_3)
	3	Satured Fatty Acids	δ 2.33 (*CH_2COO^-), δ 1.61 (*CH_2*$CH_2CH_2COO^-$), δ 1.28 ((*CH_2)n$CH_2CH_2COO^-$), δ 0.88 (CH_3)
	4	Omega-6	**δ 2.72** (1/2 t)
	5	Omega-3	**δ 2.78** (1/2 t)
Glycerols			
	6	Triacylglycerols	δ 5.27 (*(sn_2)CHOCOR, pd, J=6.14), δ 4.30 (*(sn_3)CH_2OCOR, dd, J=4.22), δ 4.15 (*(sn_1)CH_2OCOR, dd, J=6.14)
	5	Diacylglycerols (Phospholipids)	δ 5.09 (*(sn_2)CHOCOR), δ 4.28 (*(sn3)CH_2OCOR, d), δ 3.72 (*(sn_1)CH_2OP)
Sterols			
	7	β-Sitosterol	δ 3.54 (CH-4, ring A), δ 2.26 (CH-3, ring A), δ 1.86 (CH-2, ring A), δ 1.51 (CH-1, ring A), δ 1.09 (CH-1', ring A), δ 0.81 (CH_3-21, s), **δ 0.69** (CH_3-18, s)
	8	Stigmasterol	**δ 0.71** (CH_3-18, s)
	9	Other Sterols	δ 0.68 (CH_3-18, s)

	10		δ 0.66 (CH_3-18, s)
	11		δ 0.60 (CH_3-18, s)
	12		δ 0.55 (CH_3-18, s)
Xanthones			
	13	Xanthone (Furanic ring)*	**δ 8.04** (CH-2', d, J= 10.09 Hz), δ 5.83 (CH-1', d, J= 10.09 Hz)
	14	Other xanthone (Furanic ring)* *	**δ 8.02** (CH-2', d, J= 10.09 Hz), δ 5.83 (CH-1', d, J= 10.09 Hz), **δ 1.50** (CH_3-6'6",s)
	15	Brasilixanthone B	**δ 8.05** (CH-2', d, J= 10.12 Hz), δ 5.83 (CH-1', d, J= 10.12 Hz), **δ 1.50** (CH_3-6'6",s)
	16	Rheediaxanthone	**δ 4.55** (CH-q), 1.43 (CH3-d)
	17	Xanthone X	**δ 5.55** (1/2 d)
	18	Xanthone Y	**δ 5.56** (1/2 d)
Unknown Compounds	19	U35	**δ 1.14** (d), 3.48, 4.01
	20	U36	**δ 1.15** (d), 3.48, 4.24
	21	U37	**δ 6.92** (1/2 d)
	22	U38	**δ 7.13** (1/2 d)
	23	U39	**δ 7.44** (1/2 d)
	24	U40	**δ 7.63** (1/2 d)

Signals used for quantitative analysis by integration are highlighted in bold.

Abbreviations: d, doublet; dd, double

doublet; dt, double triplet; m, multiplet; q, quartet; s, singlet; t, triplet; U0-U40, unassigned signals.

*Xanthone (STUDY I) corresponds to Brasilixanthone like in STUDY II; **Other xanthones (STUDY I) correspond to Total brasilixanthones in STUDY II

The concentrations of forty-three metabolites measured at basal time, 24 and 72 h both in the control and the chitosan-elicited roots are reported in Figures 4-7.

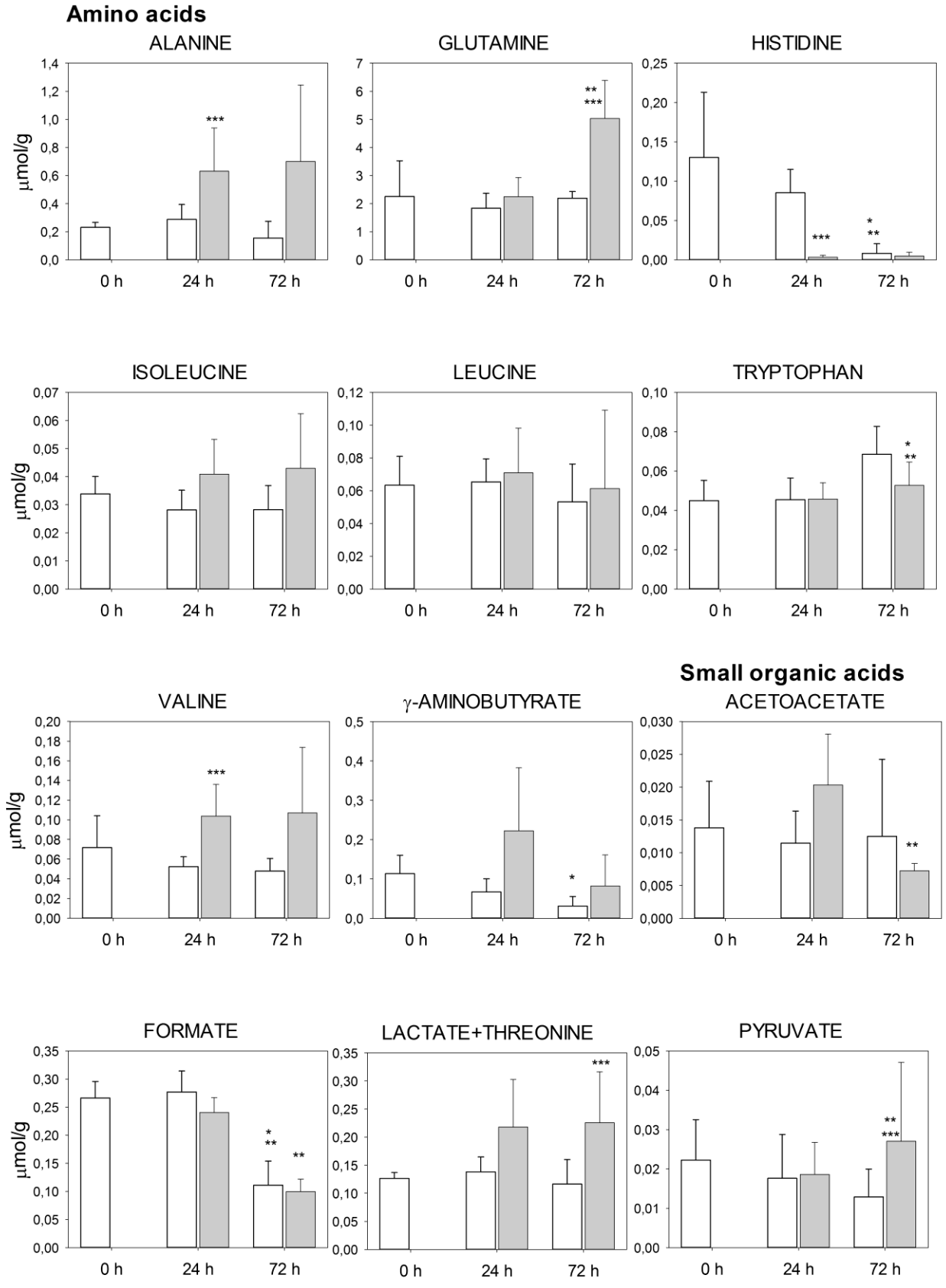
Amino acids
ALANINE
GLUTAMINE
HISTIDINE
ISOLEUCINE
LEUCINE
TRYPTOPHAN
Small organic acids
VALINE
γ-AMINOBUTYRATE
ACETOACETATE
FORMATE
LACTATE+THREONINE
PYRUVATE
µmol/g
0 h
24 h
72 h

Figure 4.

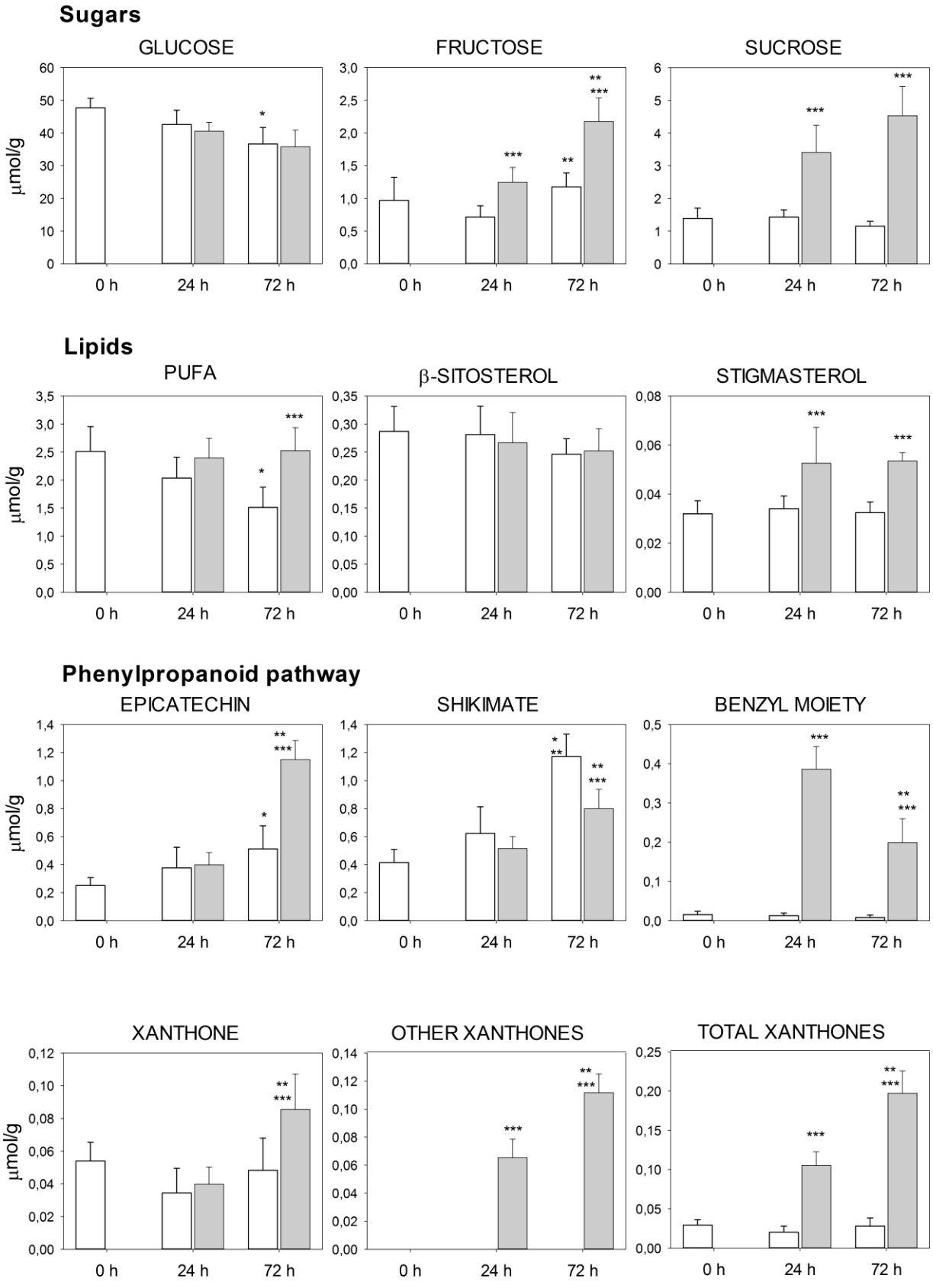
Sugars
GLUCOSE
FRUCTOSE
SUCROSE
µmol/g
0 h
24 h
72 h
Lipids
PUFA
β-SITOSTEROL
STIGMASTEROL
Phenylpropanoid pathway
EPICATECHIN
SHIKIMATE
BENZYL MOIETY
XANTHONE
OTHER XANTHONES
TOTAL XANTHONES

Figure 5.

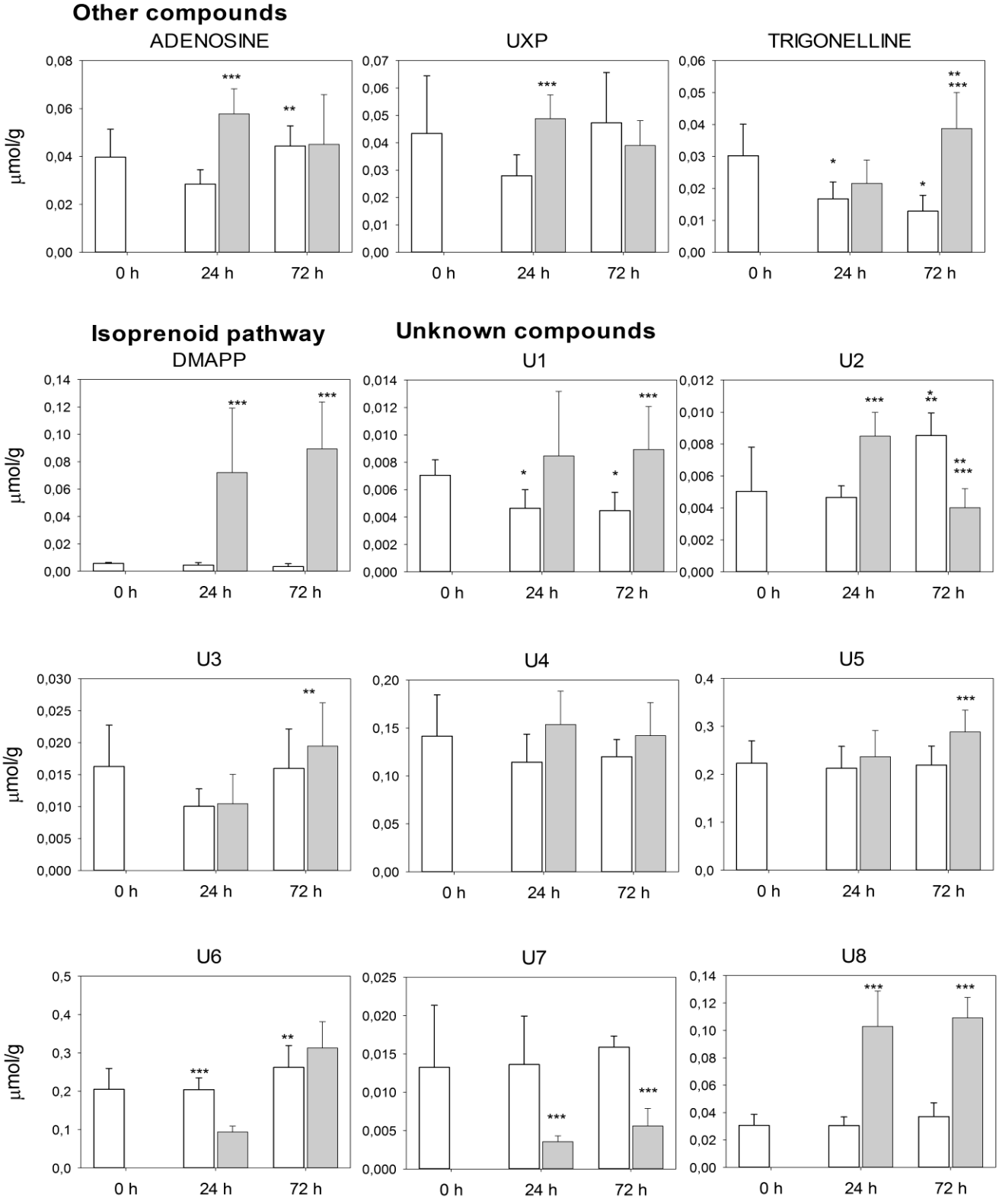
Other compounds
ADENOSINE
UXP
TRIGONELLINE
Isoprenoid pathway
DMAPP
Unknown compounds
U1
U2
U3
U4
U5
U6
U7
U8
µmol/g
0 h
24 h
72 h

Figure 6.

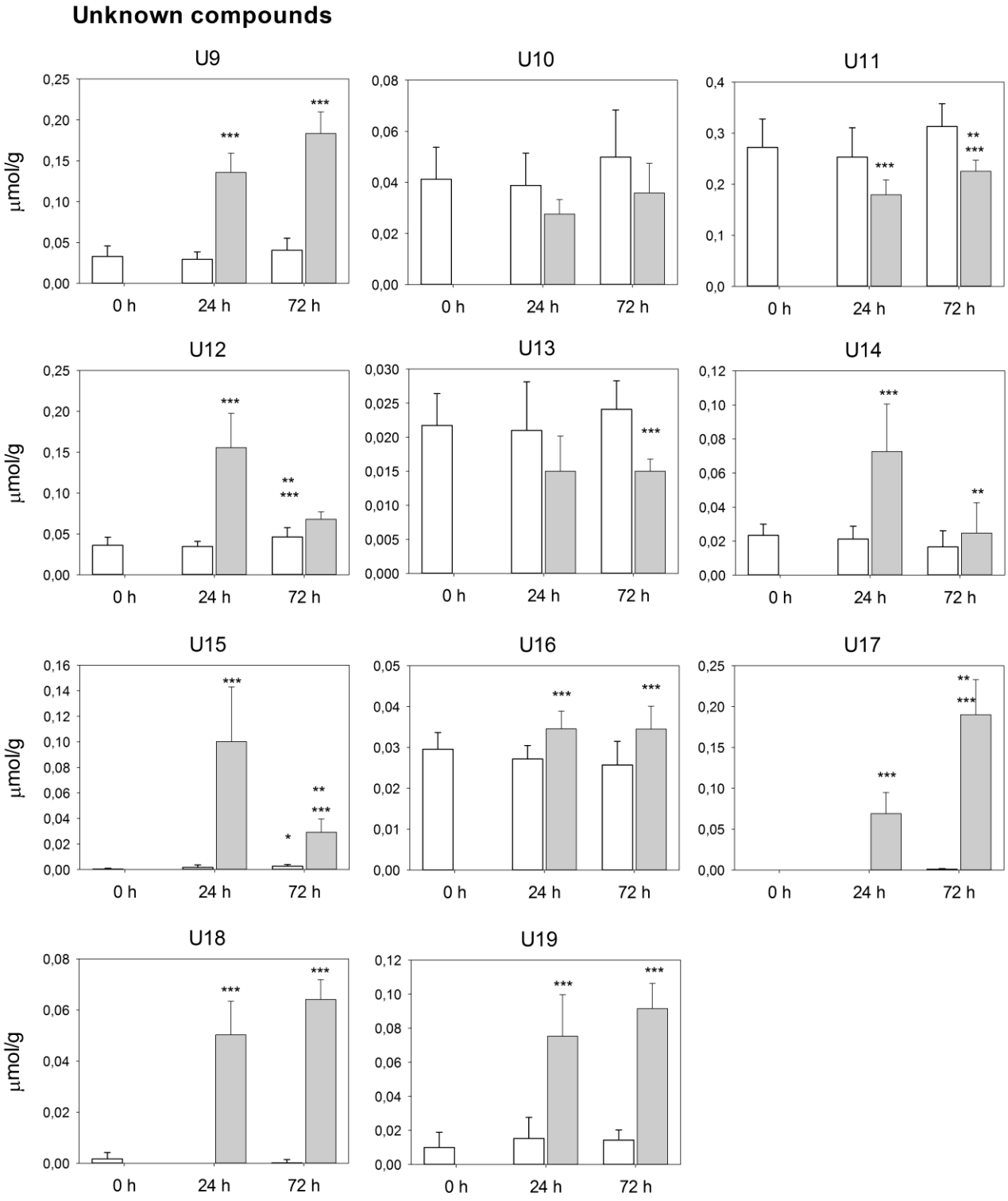
Unknown compounds
U9
U10
U11
U12
U13
U14
U15
U16
U17
U18
U19
µmol/g
0 h
24 h
72 h

Figure 7.

Figure 4-7. Metabolic composition of the root extracts. Histograms representing the quantitative composition of the assigned metabolites grouped into distinct classes. Data are expressed in μmol/g of fresh weight and are presented as the mean ± standard deviation (SD) of five samples in five independent experiments. White and grey bars represent control and chitosan elicited samples, respectively, at various experimental times. * Different from control at time 0; ** Different from corresponding treatment at 24 hours; *** Different from control at the same experimental time as assessed by univariate unpaired Student's t-test. $P < 0.05$.

Several changes of primary and secondary metabolites, including levels of amino acids, carbohydrates, small organic acids, lipids, phenolic, isoprenoid, and other compounds related to plant metabolism were observed.

An initial exploration of the whole data set to identify a possible clustering of samples and possible outliers was performed by Principal Component Analysis (PCA). PCA was performed on the concentration of metabolites measured at time 0 (day 0), 24 and 72 h after elicitation, and the resulting score plot is shown in Figure 8.

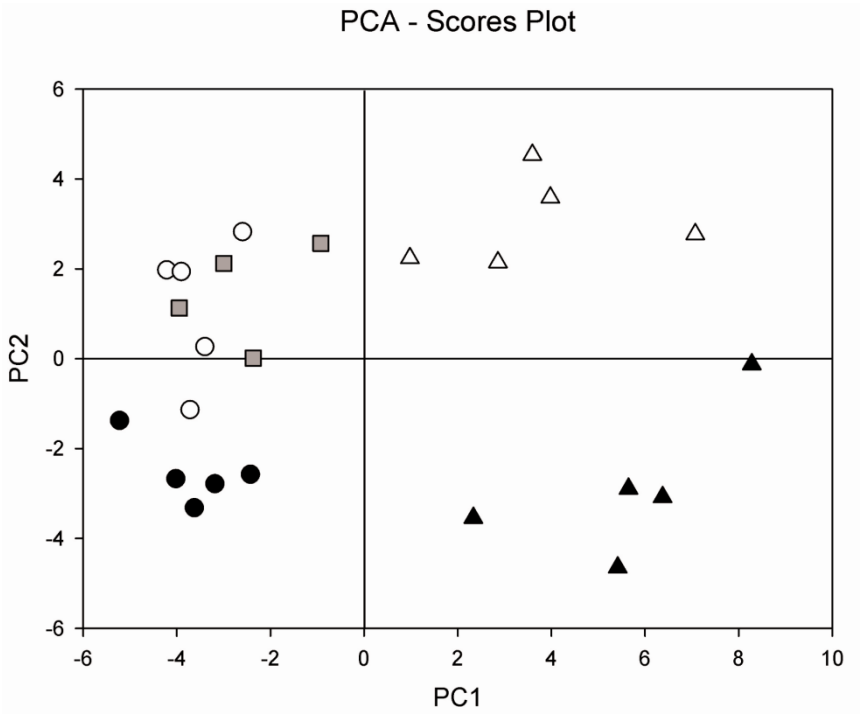

Figure 8. The PC scores plot relative to whole set of *H. perforatum* root data.

■ Control sample at time 0 (day 0); ○ control samples at 24 h; △ control samples at 72 h; ● chitosan-elicited samples at 24 h; ▲ chitosan-elicited samples at 72 h.

Total variance explained by PCs was 40% and 15.4 % for PC1 and PC2, respectively.

PCA score plot showed that root samples were clustered on the basis of PC1 and PC2 scores corresponding to chitosan elicitation and to biomass growth-related changes, respectively. Total variance explained by PCs was 40% and 15.4 % for PC1 and PC2, respectively.

However, the PC2 scores did not allow a separation between basal and 24 h root samples. Furthermore, the PCA model does not allow to obtain an easy interpretation of the metabolic variations induced by the different factors (treatment and time) distinguishing 'between' and 'within' of factors identified.

For this reason, in order to discriminate the metabolic variations related to root biomass growth and to chitosan treatment, and to their interaction, ASCA modelling was applied. A balanced experimental design has been built considering only the data at time 24 h and 72 h, excluding the basal samples.

ASCA modelling showed that chitosan treatment and biomass growth accounted for 24.1% and 23.5% of the variation in the original matrix, while their interaction explained 3.7% of the variance. The randomization test with 100,000 permutations showed that only the effects of chitosan treatment and biomass increase were significant (the *p*-values for elicitation and biomass increase were 0.0048 and 0.0053, respectively), while the effect of the their interaction was not statistically different from zero (p=0.2493). Having verified that elicitation and biomass growth had a significant effect on the metabolic profiles of *H. perforatum* roots, simultaneous component analysis (SCA) was used (after Pareto scaling) to model the variation in the two corresponding matrices $\mathbf{X}_{elicitation}$ and $\mathbf{X}_{biomass\ growth}$. The distribution of the loadings for the SCA models of the two main effects is reported in Figure 9.

A

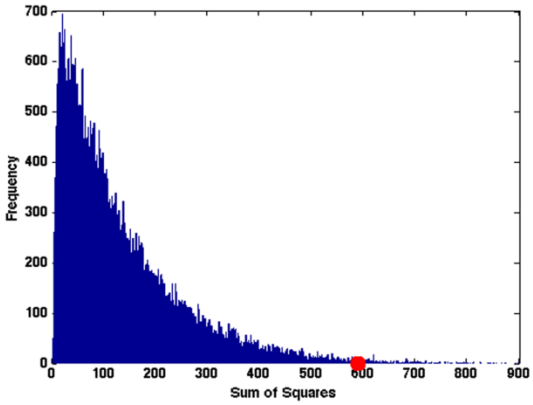

B

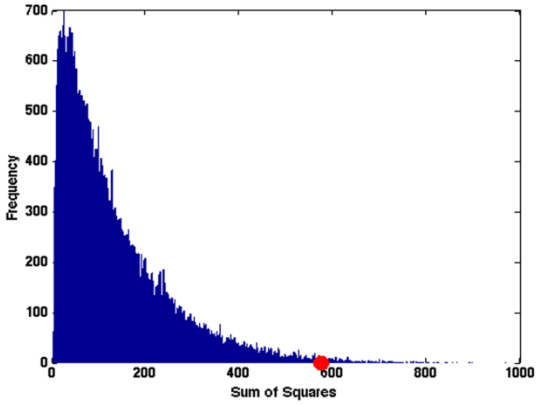

C

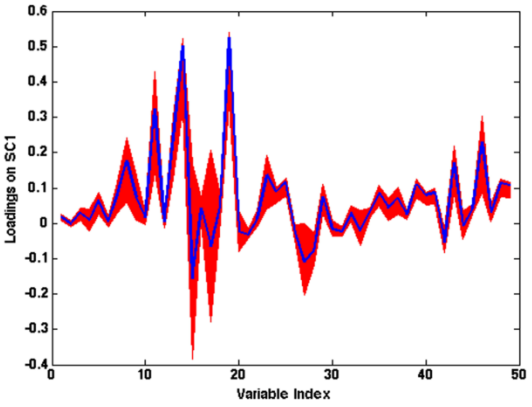

D

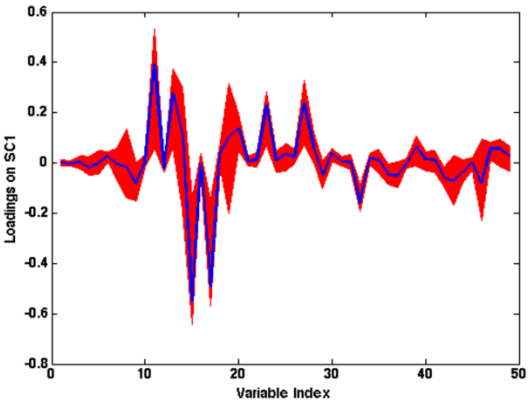

E

Loadings number	Metabolites	Time	Treatment
1	U1		
3	Isoleucine		
5	Valine		
6	U3		
7	Lactate + threonine		
8	Alanine		
9	GABA		
11	Glutamine		
13	Fructose		
14	Sucrose (fructose)		
15	α -Glucose		
16	U4		
17	β -Glucose		
18	U5		
19	Sucrose (glucose)		
20	U6		
21	U7		
23	Epicatechin		
24	U8		
25	U9		
26	U10		
27	Shikimate		
28	U11		
29	U12		
30	Tryptophan		
31	U13		
32	Adenosine		
33	Formate		
34	Trigonelline		
35	DMAPP		
36	U14		
37	U15		
38	U16		
39	U17		
40	U18		
41	U19		
42	Histidine		
43	Benzoyl moiety		
45	Stigmasterol		
46	PUFA		
47	Xanthone		
48	Total xanthones		
49	Other xanthones		

Figure 9. Evaluation of the significance of the multivariate effect of treatment and time of biomass growth. Evaluation of the significance of the multivariate effect of treatment (A), time (B), by means of permutation tests. SCA analysis on the effect matrices for treatment (C) and time (D): variable loadings for the one-component SCA model (blue line) and their 95% confidence intervals (red). Heatmap for loadings metabolites that contribute significantly to the model for time and treatment effects. Red corresponds to the loadings with positive direction (increase); blue corresponds to the loading with negative direction (decrease) (E).

Primary and secondary metabolic variations related to root biomass growth.

The metabolic variations related to root biomass growth concerned levels of flavonoid compounds such as epicatechin and other phenolics, such as shikimic acid and total xanthones that increased. Moreover, a significant correlation between tryptophan and epicatechin levels ($r = 0.78$) was observed.

Regarding the metabolism of aminoacids, opposite trends were observed in γ-aminobutyric acid (GABA), glutamine and histidine levels. In particular, a decrease in GABA and histidine and an increase in glutamine occurred with increasing culture time. A significant correlation between GABA and glutamine levels ($r = -0.72$) was observed.

A decrease in α- and β- glucose and an increase in fructose levels were also observed. Furthermore, fructose levels correlated significantly with shikimate ($r = 0.89$, Pearson's correlation) and with total xanthones ($r = 0.72$), but correlated inversely with histidine ($r = -0.77$). Among the small organic acids, a decrease in formate level was observed.

Finally, significant metabolic variations related to root biomass growth concerned likewise levels of unknown metabolites, such as U3, U6 and U11 that increased and U14 that decreased.

All metabolites (loadings in ASCA analysis) that contribute significantly to the model ASCA were statistically significant also by univariate analysis ($P < 0.05$), (as shown in Figure 4-7).

Primary and secondary metabolic variations related to chitosan treatment.

The metabolic variations related to chitosan treatment concerned levels of phenylpropanoid-derived secondary metabolites. In particular, epicatechin and xanthone levels were two- and eight-fold higher, respectively, than the corresponding control samples at 72 h after elicitation (Figures 4-7). In chitosan-treated roots, the level of shikimate, was lower than in control roots, while benzoyl-moiety levels were ten-fold higher.

A considerable increase in dimethylallyl-pyrophosphate (DMAPP), precursor of the isoprenoid compounds, was observed. DMAPP content in treated roots was seven-fold higher at 24 h and nine-fold higher at 72 h than their respective controls.

Regarding the metabolism of aminoacids, a significant increase in aminoacid levels, such as isoleucine, valine, glutamine, GABA, alanine, were observed together with a decrease in histidine.

Among carbohydrates, significant increase in sucrose and fructose at 24 h and 72 h after elicitation were observed. Moreover, an increase in adenosine and trigonelline levels were observed. In chloroformic extract, high stigmasterol levels as well as high polyunsaturated fatty acids levels were found in chitosan-treated roots. Among the small organic acids, an increase in lactate levels were observed.

Finally, significant metabolic variations related to root biomass growth concerned likewise levels of unknown metabolites, such as U1, U4, U5, U8, U9, U12, U14, U15, U16, U17, U18 and U19 that increase, while U7, U10, U11 and U13 decreased.

All metabolites (loadings in ASCA analysis) that contribute significantly to the model ASCA were statistically significant also by univariate analysis ($P < 0.05$), (as shown in Figure 4-7).

A scheme of the metabolic changes in treated roots is reported in Figure 10.

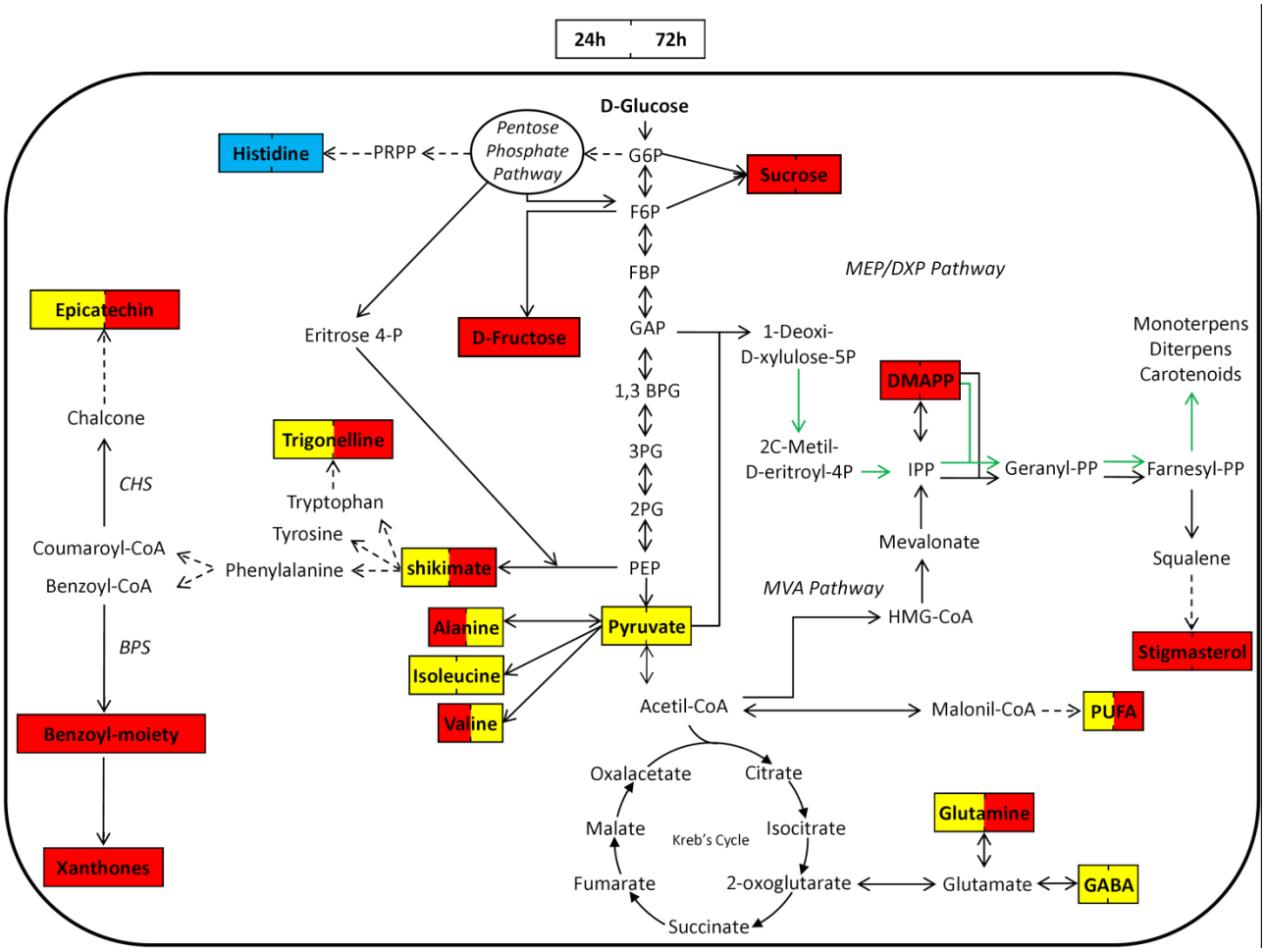

Figure 10. Schematic representation of root metabolic network. The metabolite level changes observed after 24 and 72 h of chitosan elicitation are shown. The significant metabolites as evaluated by ASCA modeling for chitosan treatment effect are represented by coloured boxes. The color code designates changed and unchanged metabolite abundances as follows: red: significantly increased; yellow: not significantly changed; blue: significantly decreased. The significant differences between treated and control at corresponding experimental times were assessed by using Student's t test. Solid arrows in the network diagram specify a single step connecting two metabolites; dashed arrows indicate at least two steps. CHS: chalcone synthase; BPS: benzophenone synthase.

Morpho-anatomical analysis of control and chitosan-treated *Hypericum perforatum* in vitro roots

Histological analysis was carried out to investigate the effect of chitosan elicitation on the morphology and anatomy *Hypericum perforatum in vitro* roots. Chitosan-treated roots, showed morpho-anatomical alterations compared to the control roots, both at 24 h and at 72 h. Morphological analysis after 24 h of treatment with chitosan showed a swelling in the roots in the region of distension and differentiation, after 72 h swelling appeared more pronounced (Figure 11). In response to chitosan elicitation the maximum diameter of the root increased approximately 1.5 times compared to the control, from 256 µm to 375 µm at a distance from the apex of 600 µm. The microscopic analysis revealed that the swelling of the root was mainly due to hypertrophy of the cortical cells, in particular of the first two subepidermal layers. The cell expansion did not involve the rizoderma which subsequently underwent tensile forces such as to cause often thinning and breakage. Furthermore, the direction of stretching of the cortical cells in the elicited roots took place predominantly in the radial direction, thus the opposite than normal. Finally, in addition to the normal anticlinal divisions, in hypertrophic cortical layers were observed frequently periclinal divisions that resulted in any increase in some areas of the cortical layers (Figure 12).

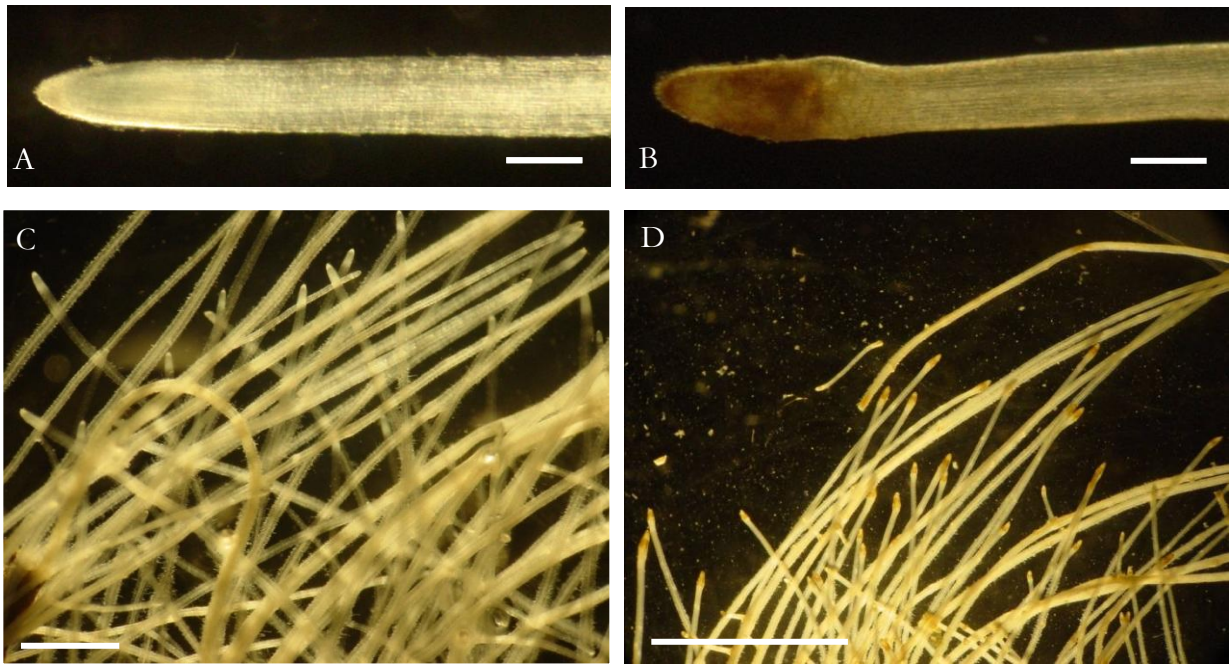

Figure 11. Morphology of *H. perforatum in vitro* roots. Stereomicroscopic view of control (A) and chitosan treated (B) roots at 72 hours. A swelling in the region of distension and differentiation was observed in chitosan treated roots. Bars represent 250 μm (A and B), and 2,5 mm (C and D).

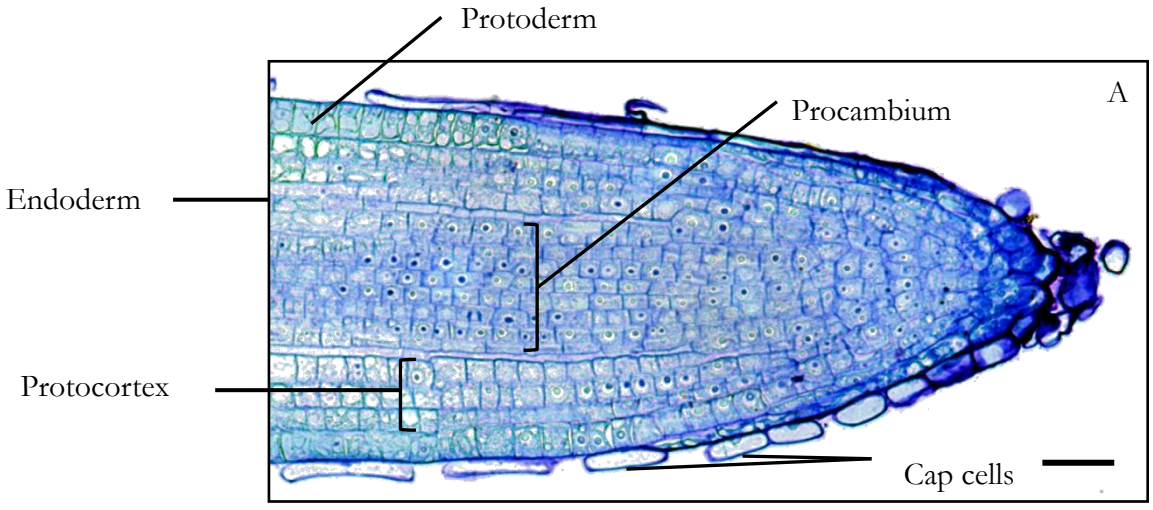

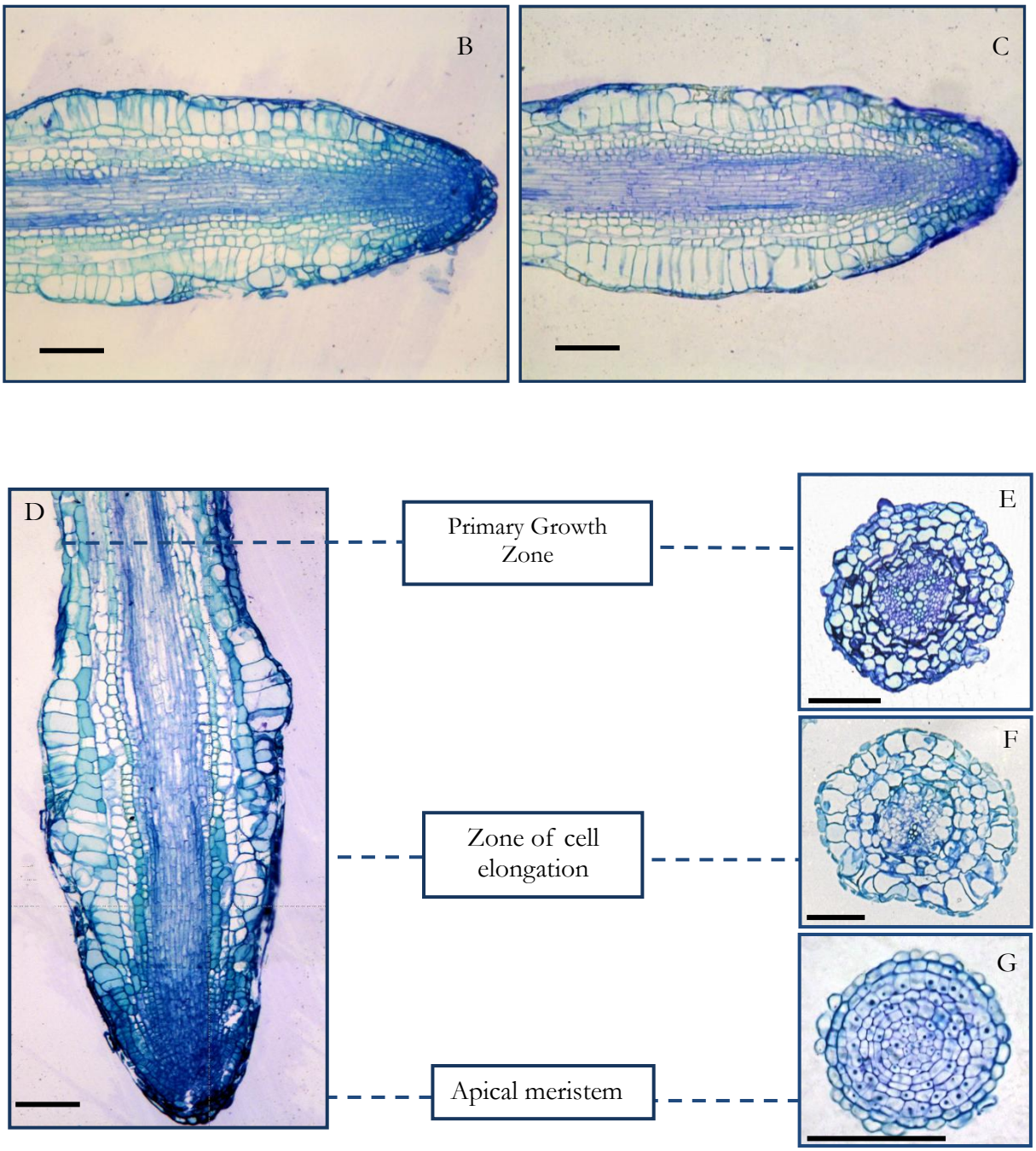

Figure 12. Anatomy of *H. perforatum in vitro* roots. Resin-embebbed sections stained with 0.1% toluidine blue to show the anatomical structure. Longitudinal sections of control (A), and chitosan treated roots at 24 (B) and at 72 (C) hours. Longitudinal section (D) and cross sections (E-G) of chitosan treated root at 72h showing primary growth zone (D), elongation zone (E) and apical meristem (F). Bars represent 100 μm.

The tests with histochemical Nadi reagent conducted on fresh sections revealed the presence of terpenes in the lumen of the secretory ducts, localized at the periphery of the vascular cylinder, both in the roots regenerated in vitro and in those of the seedlings. In the entire roots (not sectioned), purple stain imparted by the Nadi reagent is especially strong in the area of primary structure, while in the apex and in the elongation and differentiation zone the signal was very weak (Figure 13 A). These results suggest that the terpene compounds are present in plant root and *in vitro* regenerated roots, in both control and treated roots, and they accumulated in specific secretory ducts (Figure 13 B), mainly localized in the primary structure zone.

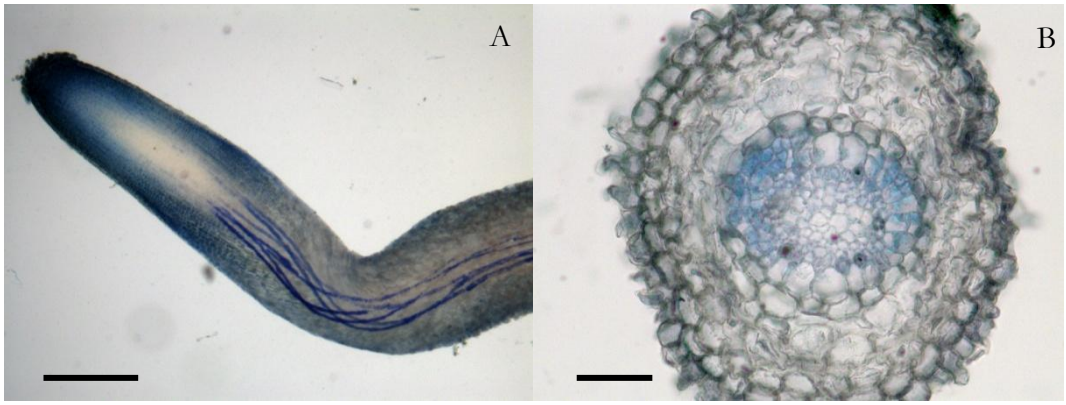

Figure 13. *H. perforatum* control *in vitro* roots stained with Nadi reagent. Secretory ducts showing terpenoid accumulation, stained in violet, are localised in the primary structure zone of the root (A). F fresh cross section of the same root (B). Bars represent 250 μm (A) and 50 μm (B).

3.5 Discussion

NMR–based metabolomics allowed the primary and secondary metabolism of *H. perforatum* regenerated roots to be characterized and the effects due to the increasing biomass density or to the elicitation process to be determined.

The most significant metabolic variations involved levels of amino acids, carbohydrates, phenylpropanoids, lipids, and isoprenoids. In response to chitosan elicitation, valine, isoleucine, glutamine, γ-aminobutyric acid, fructose, sucrose, poly-unsaturated fatty acids, epicatechin, xanthones, dimethylallyl-pyrophosphate, and stigmasterol increased, while histidine decreased.

Effect of root biomass growth on primary and secondary metabolism.

The results of ASCA modelling, associated with the root growth curve data, enable the "time effect" to be defined as the effect of the increase of biomass density in a confined environment. Control roots showed an increase in flavonoid levels, such as epicatechin and other phenolics, such as shikimic acid and total xanthones associated with an increase in biomass density and with a decrease in growth ratio.

The relationship between biomass density, the slowdown in biomass growth and phenol biosynthesis was also observed by Cui et al. (2010) in *H. perforatum* roots cultured in a bioreactor.

In the control roots the significant correlation between tryptophan and epicatechin increased levels was observed and this result pointed to a stimulation of the phenylpropanoid pathway caused by a higher root biomass density in a confined environment.

Regarding the aminoacid metabolism, opposite trends were observed in GABA, histidine, and glutamine levels. The increase in glutamine levels associated with a decrease in GABA levels is of interest. GABA is a ubiquitous non-protein amino acid that in plants has been linked to stress, signalling and storage (Fait et al. 2008). It has long been known that GABA is derived from glutamate, through glutamate decarboxylase (GAD) activity, and is then converted to succinic semialdehyde and succinate, which enters the tricarboxylic acid cycle. GAD activity is confined to

the cytosol, specific for glutamate, and regulated by pH and Ca^{2+}-calmodulin (Shelp et al. 2012). It has been reported that this proton-consuming reaction can limit cytosolic acidosis in certain species during exposure to various stress conditions such as hypoxia (Shelp et al. 2012). The relationship observed between time-related decrease in GABA and increase in glutamine suggests a metabolic flux shift from GABA synthesis towards glutamine synthesis which enhances nitrogen storage.

It is a known fact that the slower growing plants invest more of their total root metabolites in carbon- and nitrogen-storage compounds (Atkinson et al. 2012). In our results the significant increase in glutamine, which plays a role in nitrogen storage, associated to a slight increase in fructose and no significant changes in sucrose levels could be explained by a slowdown in the growth rate.

In control roots, fructose levels correlated significantly with shikimate and with xanthones, but correlated inversely with histidine. This correlation pattern seems to illustrate the biochemical relationship between the synthesis of fructose, through transaldolase or transketolase, and histidine synthesis, starting from other intermediates in the pentose phosphate pathway. A competition between metabolic fluxes involving pentose phosphate pathway intermediates towards fructose/erythrose-4-phosphate (via transketolase and transaldolase reactions), channelled through the biosynthesis of shikimate and phenylpropanoid metabolites and histidine biosynthesis (via oxidative penthose phosphate pathway and isomerase reactions), could be hypothesized.

Effects of chitosan elicitation on primary and secondary metabolism

In elicited roots, the chitosan addition at day 12 caused a sudden slowdown of growth, whereas the growth of the control roots continued. This inhibitory effect of chitosan on biomass growth in root cultures has been also reported for other species such as *Ocimum basilicum* L. (Bais et al. 2002) and *Withania sominifera* (L.) Dunal (Sivanandhan et al. 2012).

In the chitosan-treated roots ASCA results (Figure 9) showed a significant increase in sucrose and fructose but not in glucose levels at 24 h and 72 h after elicitation. Moreover, a significant increase

in aminoacid levels, such as isoleucine, valine, glutamine, GABA, alanine, were observed together with a decrease in histidine.

The observed metabolic profile of root extracts is consistent with slowdown or arrested growth, which causes a metabolic shift towards a storage of carbon and nitrogen compounds, such as sucrose and aminoacids (Atkinson et al. 2012). However, this metabolic profile reflects also a process of adaptation to stress conditions induced by chitosan treatment.

Since it is well known that the early defence responses elicited by chitosan include a raising of cytosolic H^+ and Ca^{2+} concentrations (Zhao et al. 2005), the observed levels of GABA that are higher than control roots, in particular at 24 hours after the chitosan treatment, can be related to a higher GAD activity stimulated by an altered intracellular H^+ and Ca^{2+} homeostasis (Kinnersley et al. 2000, Snedden et al. 1995).

In chitosan-elicited roots, an increase in phenylpropanoid-derived secondary metabolites such as epicatechin and xanthones was displayed by the ASCA model. Xanthones and flavonoids are synthesized from phenylalanine through shikimate pathway. In elicited roots, the level of shikimate, a key intermediate in the phenylpropanoid pathway, was lower than in control roots, while benzoyl-moiety levels were ten-fold higher. These results indicate that both the phenylpropanoid and xanthone pathways were specifically stimulated by chitosan treatment, which is in agreement with previous results obtained using the same experimental system by Tocci et al. (2011). A scheme of the above metabolic pathways is reported in Figure 10.

Chitosan has been extensively studied with regard to its effects on enzymes involved in the phenylpropanoid pathway (Baque et al. 2012, Chakraborty et al. 2009). It is known that chitosan mimics a fungal infection, inducing a non-host resistance through PRR-mediated recognition and priming a systemic acquired immunity (Iriti et al. 2009). The observed increase in xanthones supports the hypothesis proposed by Franklin et al. (Franklin et al. 2009) that these metabolites act as phytoalexines, playing a role in plant chemical defence against pathogen attack.

Also of interest is the increase in DMAPP observed in chitosan elicited roots of *H. perforatum*. DMAPP, together with its isomer isopentenyl pyrophosphate (IPP), is the precursor of the isoprenoid compounds, including molecules such as sterols, dolichols, triterpenes, ubiquinone, components of macromolecules such as prenyl groups, and isopentenylated tRNAs (Sacchettini et al. 1997, Kuzuyama et al. 2003). The diversity of isoprenoids reflects the variety of important biological functions, including electron transport in respiration and photosynthesis, hormone-based signalling, the regulation of transcriptional and post-translational processes that control lipid glycoprotein biosynthesis, protein cleavage degradation, meiosis and apoptosis. The isoprenoids are also important structural components of cell and organelle membranes (Hunter 2007, 2011). In addition, they can play a crucial role as phytoalexins, because many of them exert antibiotic, antiviral and fungitoxic or fungistatic activities (Ahuja et al. 2012). An increase in concentration of the isoprenoid phytoalexins in response to fungal elicitors in the roots has been also observed in *Oryza sativa* L., in which fungal chitin oligosaccharide stimulated the roots to biosynthesize and release several diterpenoids into the medium (Toyomasu et al. 2008).

DMAPP and IPP may be produced through two independent metabolic pathways: the acetate-mevalonate (MVA) pathway and the non-mevalonate pathway (non-MVA), also called the 1-deoxy-D-xylulose-5-phosphate (DXP) or the 2-C-methyl-D-erythritol-4-phosphate (MEP) pathway (Hunter 2007). In plants, the MVA and non-MVA pathways are compartmentalized in the cytoplasm and plastid, respectively. Sesquiterpenes, sterols, and polyterpenes are derived via the cytosolic MVA pathway, whereas isoprene, phytol, carotenoids, and the plant hormones gibberellic and abscisic acid are synthesized via the plastid non-MVA pathway (Hsieh et al. 2005). Mono- and sesquiterpenes were isolated in *Hypericum perforatum* L. roots by GC-MS (Motavalizadehkakhky 2012). It is interesting that high stigmasterol levels have been found in chitosan-treated roots. Stigmasterol is synthesized inside the cytosol through the cytochrome P450 CYP710A1 via C22 desaturation from β-sitosterol originating from reactions involved in the sterol branch of the isoprenoid pathway (Benveniste 2004). Despite an increased synthesis of stigmasterol, the results show that β-sitosterol

levels were found to remain constant at 24 h and 72 h after chitosan treatment, indicating that the chitosan treatment stimulated the *de novo* synthesis of β-sitosterol and its desaturation through the sterol biosynthetic pathway.

An increased synthesis of stigmasterol was found in different plant-pathogen interactions. The conversion of β-sitosterol to stigmasterol in *Arabidopsis thaliana* leaves was observed 10 and 48 h after inoculation of virulent and avirulent *Pseudomonas syringae* strains (Griebel et al. 2010). These authors found that the pathogen-stimulated stigmasterol was triggered by the perception of pathogen-associated molecular patterns (PAMPs) and the generation of reactive oxygen species (ROS) (Griebel et al. 2010). The role of stigmasterol in plants during stress is still poorly understood. Sitosterol and stigmasterol, like brassinosteroids, are involved in the regulatory function of plant development, affecting gene expression involved in cell expansion and division, vascular tissue differentiation and several developmental programs (Sasse 2003). Several reports have proposed the existence of sterol-membrane microdomains, so-called lipid rafts, which may play a role in the recruitment of molecular components involved in plant defence signalling (Bhat et al. 2005). In particular, it has been suggested that a pathogen-induced change in stigmasterol/sitosterol ratio can influence different physicochemical properties of membrane micro-domains and thereby modulate plant defence signalling (Griebel et al. 2010).

Moreover, the increase in polyunsaturated fatty acids observed is in agreement with the results found for *A. thaliana* leaves treated with *P. syringae* (Yaeno et al. 2004).

On the basis of the above evidence, the increase in polyunsaturated fatty acids and the increase in stigmasterol levels suggest a stimulation of a lipid desaturation process that may have altered the membrane microdomains, favouring a change in membrane permeability.

CHAPTER 4

STUDY II

NMR-based metabolomics to evaluate the effects of biomass growth and chitosan elicitation on primary and secondary metabolism of *Hypericum perforatum in vitro* roots after 96 and 192 hours

4.1 Introduction

Plant roots are the potential source of an enormous diversity of metabolites and therefore are considered as the site of unique secondary metabolism of the whole plant.

Recent advances in plant biotechnological research have shown that *in vitro* root cultures are an attractive and alternative method to the whole plant, cell or hairy root culture for biomass and pharmaceutically useful compounds production. Over the last few years, *in vitro* root cultures have gained popularity and interest, especially in the possibility to modify the production of bioactive molecules (Bais et la. 2002, Baque et al. 2012).

Up to now, despite potential advantages of bioactive molecules production by root cultures, only some compounds such as paclitaxel, shikonin, ginsenosides and berberine have been produced on a commercial scale (Sivakumar et al. 2005, Bourgaud et al. 2001, Baque et al. 2012).

In the last years, *in vitro* root cultures of *Hypericum perforatum* (L.) have received great attention, due to the possibility to obtain a wide variety of bioactive compounds such as phenolics, flavonols, xanthones, essential oils and other metabolites, which have been reported to have different pharmacological activities (Crockett et al. 2011, Tocci et al. 2012, 2013).

H. perforatum (St. John's wort) is a traditional medicinal plant that for centuries has been utilized in popular medicine for a range of purposes (Nahrstedt et al. 2010). However, the industrial application of roots of this plant is still in its beginning probably due to the restriction of genetically-modified organisms for medicinal purpose and to a lack of accurate knowledge of action mechanisms of *H. perforatum* root extracts.

It is well known that the production of biomass and metabolites produced by *in vitro* cultures can be greatly affected by various parameters such as inoculum density, medium components, oxygen transfer and mixing, and other physics-chemical factors and that these parameters should be optimized to maximize production of biomass and useful plant metabolites.

Recently, Cui and collaborators (2010) have investigated the effects of different concentrations of auxin and auxin/cytokinin combinations, inoculum sizes and Murashige and Skoog (MS) medium

dilutions on biomass and accumulation of total phenols and flavonoids in adventitious roots of *H. perforatum*. Subsequently, they investigated the effects of inoculum density, aeration volume and culture period on accumulation of both biomass and secondary metabolites in adventitious roots of *H. perforatum* in balloon type airlift bioreactors. This work contributed to optimize and develope the bioreactor technology for root cultures of *H. perforatum* and the production of several bioactive metabolites such as chlorogenic acid, quercetin and hyperoside and demonstrating that scale-up of adventitious root cultures of *H. perforatum* is feasible (Cui et al. 2011).

To investigate and define the important biological functions and roles of plant metabolites in the growth of plant biomass and potentially utilize them for practical purposes, it is essential to have a simple, sensitive, and reliable methodology for their simultaneous quantification in plant.

For instance, an interesting study proposed by Jin et al. (2012) showed an efficient enrichment method using immobilized metal affinity chromatography (IMAC) coupled with LC-MS/MS for sensitive and selective extraction and quantification of sphingolipids, from adventitious roots of *H. perforatum* cultured in bioreactor. Moreover, in this study a particular attention was given at the culture time, another important parameter which affects the performance of plant growth. Cui et al (2011) and Jin et al. (2012) demonstrated that there are not so much advantages culturing the root biomass more then 4 weeks in terms of production of useful secondary metabolites including phenolics, flavonoids and chlorogenic acid, suggesting a relation between the time-dependent growth rate and production of plant metabolites from the adventitious roots. It is reasonable to believe that these secondary metabolites could have a direct role in controlling growth rate of the root biomass. Despite optimization of these parameters for the efficient production of commercially important bioactive compounds, one of the major obstacles in the industrial application of organ culture is the low target product yield. In this context, several strategies have been adopted to improve production of plant-derived secondary metabolites such as elicitation, two-phase and two-stage culture system, genetic transformation, metabolic and bioreactor engineering. Of the various efforts, elicitation is seen as an effective strategy to enhance production of commercially important

bioactive compounds such as anthraquinones (Komaraiah et al. 2005), ginsenosides (Paek et al. 2009), saikosaponin (Chen et al. 2007) and scopolamine (Biondi et al. 2000). Elicitors are compounds from various biotic or abiotic sources that can modulate a plant defense reaction, which may enhance secondary metabolism in plant cell and root cultures (Zhao et al. 2005). The effect of elicitor chitosan has been studied in detail on biosynthesis of xanthones in *H. perforatum* roots (Tocci et al. 2011).

Although several studies have been performed to optimize biomass growth and secondary metabolite production in bioreactor of *H. perforatum* adventitious roots, the effect of culture time and chitosan elicitation on primary and secondary metabolism of *in vitro* regenerated root cultures of *H. perforatum* has to be further investigated. A deeper attention should be addressed to define the culture parameters to achieve the optimal biomass density and the requested secondary metabolite yield. In addition, the qualitative and quantitative characterization of metabolite composition of a plant extract is of crucial importance to obtain standard preparations for their use aims to human health.

In the previous study (STUDY I), the non-targeted metabolomic approach has allowed to characterize the primary and secondary metabolism of *H. perforatum* regenerated roots and the effects due to the increasing biomass density and to the elicitation process.

In particular, NMR-based metabolic profiling associated with ANOVA-simultaneous component analysis allowed to determine the primary metabolic changes and the secondary metabolite production linked to root biomass growth in a confined environment and chitosan elicitation at 0, 24 and 72 hours. On the basis of the obtained results, a further experiment changing the culture conditions has been carried out. In this experiment, we have shortened the pre-elicitation phase from twelve to eight days, by removing a renewal of culture medium, and furthermore we have prolonged the observation time until to sixteen day, corresponding to 192 hours after the chitosan or solvent addition. These conditions were performed to assess the effect of failure to renew of culture medium, such as the renewal of auxins on biomass growth and on the primary and secondary metabolism of the *H. perforatum* roots, and to evaluate the effect of chitosan elicitation at

longer time compared to the previous experiment. Moreover, we have investigated how these changes in culture parameters could affect the primary metabolism and the secondary metabolites yield.

4.2 Objective

The aim of the present study was to characterize the changes in the primary and secondary metabolism of *in vitro* regenerated roots of *H. perforatum* during growth in a confined culture environment and in response to chitosan eliciattion after 96 and 192 h. In this experiment, the effect of an unique renewal of culture medium on time-dependent biomass growth and on chitosan elicitation response at longer times after the elicitation was evaluated by exploring the primary and secondary metabolism of the *H. perforatum* roots. Furthermore, we compared the obtained results on secondary metabolites yield with those of previous experiment. A metabolomic platform integrating non-targeted NMR-based metabolic profiling and multivariate analysis such as Partial Least Square 2 (PLS2) and ANOVA simultaneous component analysis (ASCA) has been used.

As in the first study, an histological analysis was carried out to investigate the effect of chitosan elicitation on the morphology and anatomy of *Hypericum perforatum in vitro* roots after 96 and 192 hours of treatments.

Due to the high levels of DMAPP, precursor of isoprenoid compunds, observed in the first study in the chitosan-treated roots, a preliminary analysis by GC/MS has been carried out to verify the terpene production.

4.3 Material and Methods

Liquid cultures were established inoculating 1 g fresh weight (FW) of roots in magenta vessels containing 80 ml liquid MS medium supplemented with glucose (2,2 g l-1) and IBA (1 mg l-1). The medium was renewed at 4° day. The roots were elicited using chitosan (medium molecular weight; Sigma-Aldrich, Milan, Italy), dissolved in acidified water with HCl (1M), at a final concentration of 200 mg l−1, which was added on the eighth day of culture using 0,22 μm sterile filter. In vitro regenerated roots were harvested at eighth day (time 0), at eleventh day (72 h, time 2), thirteenth day (96 h, time 3) and sixteenth day (192 h, time 4) and divided into seven groups: basal (time 0), control and treated to 72 hours after elicitation (time 1), control and treated at 96 hours after elicitation (time 2) and control and treated at 192 hours after elicitation (time 4). The samples were subjected to metabolic quenching and prepared for the NMR acquisition (as explained in the paragraph 2.1). NMR spectra were acquired and analysed (as explained in the paragraph 2.2).

Multivariate data analysis was carried out using Unscrambler 10 Software (CAMO, Oslo, Norway) and routines operating in a Matlab R2012a environment (The MathWorks, Inc.,Natick, MA).

Spectral data were mean-centered and scaled before analysis. To explore the whole data set and highlight significant differences among sample, inherent clustering and potential outliers, thus obtaining a simple visual idea as to the main relationships between these samples, principal component analysis (PCA) was used. PCA was applied to the data matrix containing data relative to root samples (control and treated) consisting of 30 rows and 66 columns, each row contains the measurements (concentrations) for a given sample and each column the measurement for a given variable (metabolites).

To maximize the covariance between the predictor matrix X (matrix of NMR data) and the response matrix Y (matrix of the information on "external factor" (time and treatment) to which root samples belong), a Partial Least Square 2 (PLS 2) regression model was built. The matrix X contained the concentration of metabolites detected in all samples at all experimental times. Each row represented a sample and each column represented a variable (metabolite). The Y is a "dummy" matrix was

constituted by two columns, represented by the time (hours) and treatment and containing zero for the y variable corresponding to the control and 1 for the y variable corresponding to the treated samples and many rows as were variables (metabolites) considered.

Cross-validation was used to select the optimal number of latent variables (LVs; linear combinations of the measured signals) for PLS 2 model. Statistical validity of the calculated model and the reliability of results were assessed by permutation tests and cross-model validation (Szymanska et al. 2012).

In order to assess whether and how treatment, time and their interaction could have an effect on the metabolic profile of the samples as determined by NMR spectroscopy, ANOVA-Simultaneous component analysis (ASCA) was used (Smilde et al. 2005, Jansen et al. 2005). The data collected at time 0, 72, 96 and 192 h were considered for the analysis. The detailed description of the ASCA model is reported in section 3.3.

Having verified that treatment and time had a significant effect on the metabolic profiles of samples, SCA (after Pareto scaling) was used to model the variation in the two corresponding matrices $X_{treatment}$ and X_{time}. Considering that for N levels can be obtained N-1 components that explain the 100% of the variance and that two levels only were considered for treatment factor (control/treated), a single component explaining 100% of the variance of the individual matrix was obtained. On the other hand, as four levels were considered for time factor (0, 72, 96 and 192 h), three components explaining 100% of the variance of the individual matrix were obtained.

Subsequently, the individual matrices were decomposed into the product of one score and one loading vector. In order to use SCA results for the interpretation of the metabolic effect of treatment and time, the significance of the contribution of the experimental variables to the definition of the models (i.e. the significance of the loadings) had to be assessed (see Section 3.3).

To assess the statistical univariate significance of the metabolic changes among experimental groups, previously individuated by multivariate analysis, a Two-Way ANOVA and Tukey test were applied. Differences showing P-values less then 0.05 were considered statistically significant.

In order to verify the presence of terpenes in *H. perforatum in vitro* roots, control and treated root samples harvested at time 192 h were pulverized in liquid nitrogen and extracted by dichloromethene (DCM). DCM-fractions of the root samples were analyzed by Gas chromatography (GS) associated to Mass Spectrometry (MS). These analyzes were conducted in collaboration with the "Núcleo de Investigações Químico-Farmacêuticas" (NIQFAR), "Universidade do Vale do Itajaí".

To investigate the effect of culture time and chitosan elicitation on root anatomy, sections of fresh samples and fixed samples embedded in resin were analysed. To investigate the effect of culture time and chitosan elicitation on roots morphology, whole roots samples were analysed by a Zeiss stereomicroscope equipped with reflected and transmitted light.

4.4 Results

The growth curve of both elicited and non-elicited *H. perforatum in vitro* roots was measured during the course of sixteen days and is plotted in Figure 1.

In control roots, it was possible observe an exponential phase of growth curve from day 0 to day 12, whereas a decreasing growth rate could be observed from day 13 to day 16.

In elicited roots, the chitosan addition at day 8 caused a sudden slowdown of growth, approaching to the stationary growth phase after the day 12.

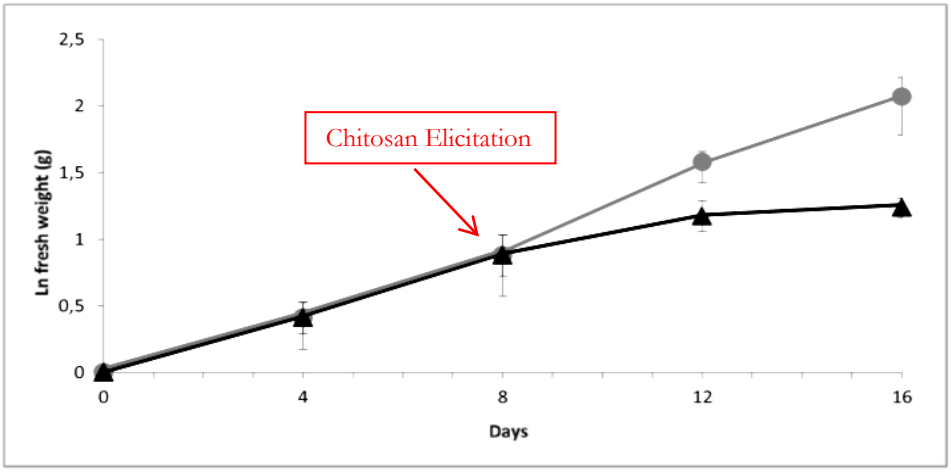

Figure 1. The growth curve of *H. perforatum in vitro* roots over a period of 16 days. Growth is expressed as a natural logarithm of fresh weight biomass. Data are presented as the mean ± standard deviation (SD) of five samples in five independent experiments.

Seventy-six metabolites were identified and assigned. ^{1}H and ^{13}C data are reported in Table 1 (see Study I).

^{1}H-NMR spectra of control and treated roots consisted of a vast array of metabolites including amino acids, carbohydrates, organic acids, polyphenols, isoprenoids, fatty acids and sterols. Among the polyphenols, several furanic rings that can be attributed to xanthone compounds were identified. However, the univocal assignment of these resonances to a specific molecular structure of xanthone was hindered due to the extreme signal overlapping. Nevertheless, these resonance were quantified

by integration and considered for multivariate analysis. Moreover, at 96 and 192 h after chitosan elicitation, it has been possible to identify different signals belonging to Rheediaxanthone and a new xanthone named Brasilixantone B (Figure 2). ^{1}H and ^{13}C data of Brasilixanthone B are reported in Table 2.

Table 2. ^{1}H and ^{13}C data of Brasilixanthone B in chloroformic extracts of chitosan treated roots.

Position	δ ^{1}H	multiplicity (J Hz)	Integral	δ ^{13}C
1	\	\	\	157.8
2	\	\	\	104.4
3	\	\	\	159.9
4	6.26	s	1	93.1
4a	\	\	\	156.5
5	6.84	s	1	101.9
6	\	\	\	153.0
7	\	\	\	136.8
8	\	\	\	119.7
8a	\	\	\	108.5
9	\	\	\	182.5
9a	\	\	\	103.9
10a	\	\	\	150.9
11	6.73	d (10.1)	1	115.6
12	5.57	d (10.1)	1	127.1
13	\	\	\	78.0
14,15	1.47	s	3+3	26.7
21	8.05	d (10.1)	1	157.8
22	5.84	d (10.1)	1	132.2
23	\	\	\	78.1
24,25	1.50	s	3+3	27.3

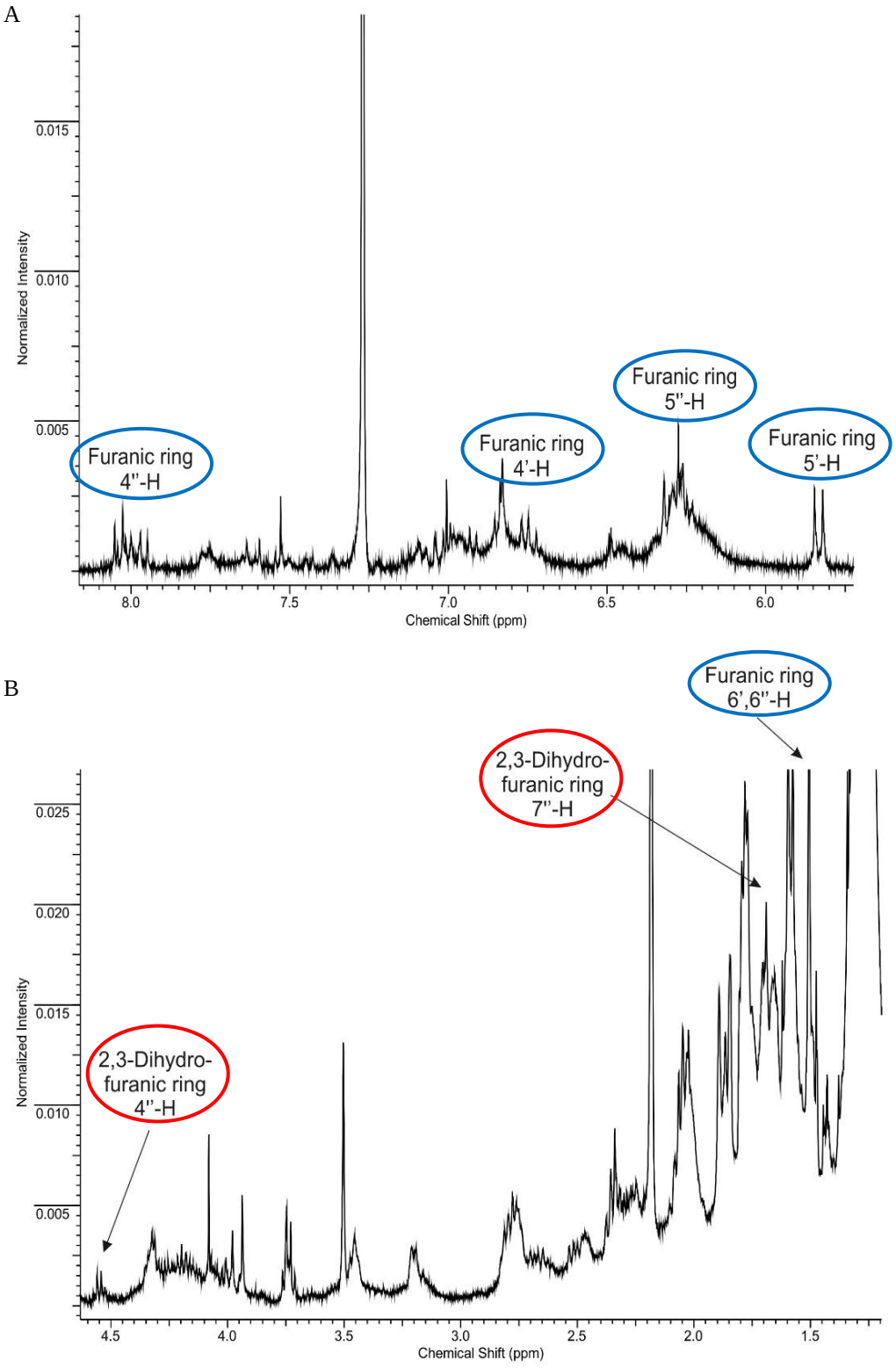

Figure 2. [1]H-NMR spectra of chloroformic phase of treated roots at 192 h. In blue assigned signals of Brasilixanthone B and in red assigned signals of Rheediaxanthone from 8.5 to 5.5 ppm (A) and from 5 to 1 ppm (B).

The concentrations of metabolites measured at time 0 (day 8), 72 h (day 11), 96 h (day 12) and 192 h (day 16) both in the control and the chitosan-elicited roots are reported in Figure 3.

AMINOACIDS

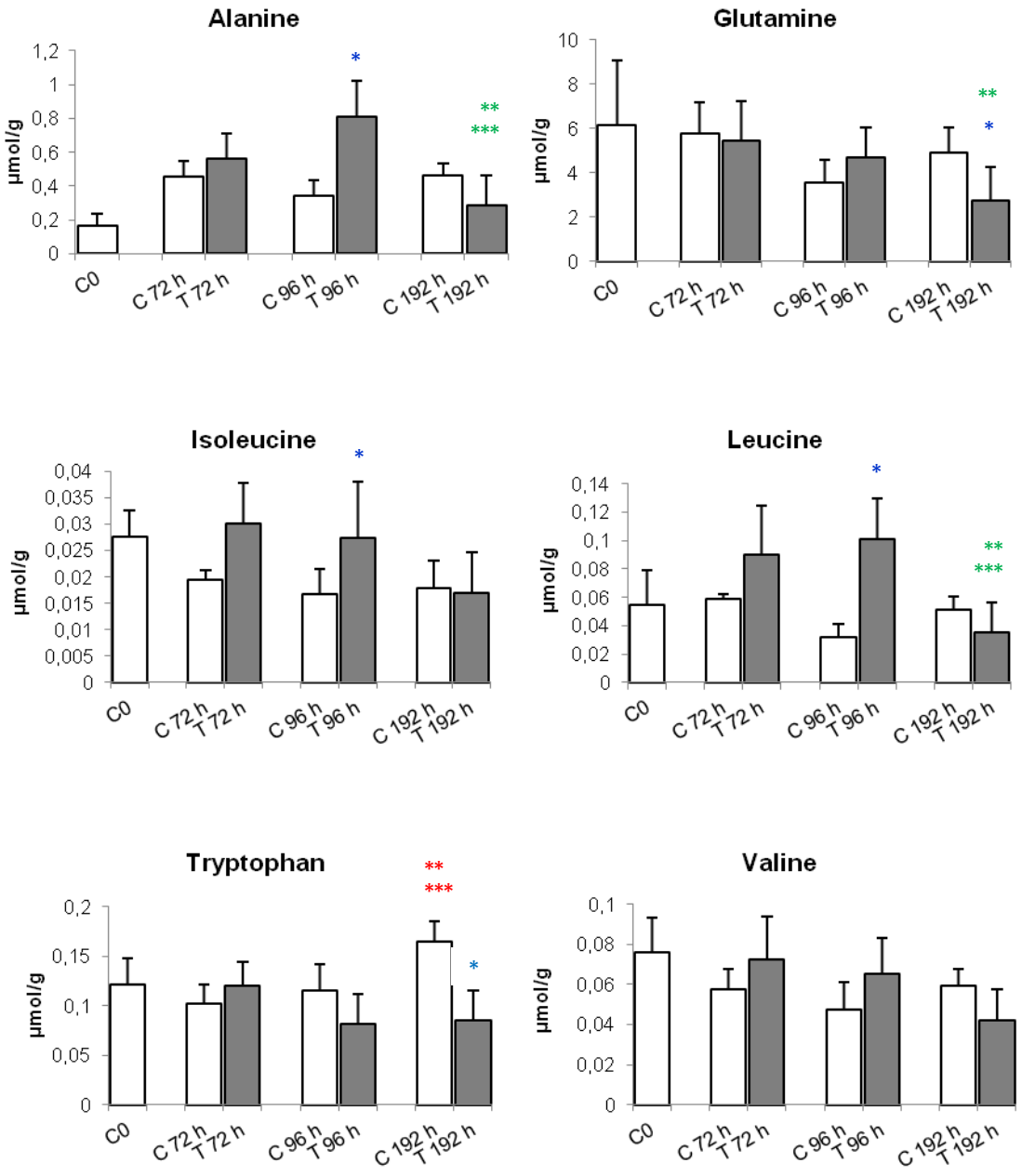

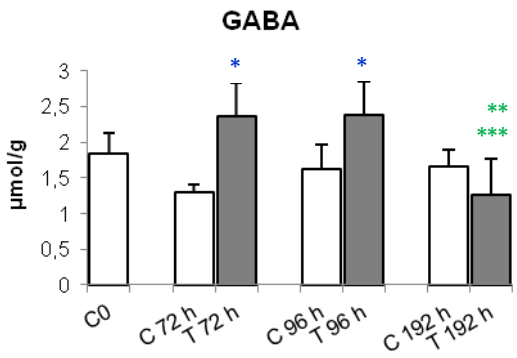

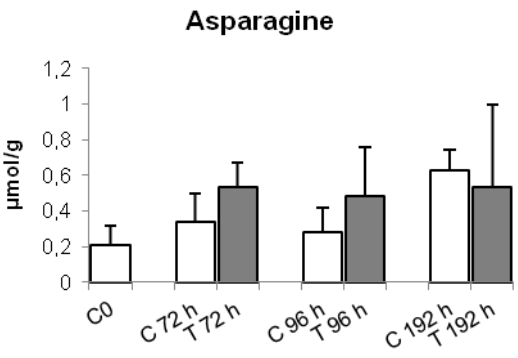

SMALL ORGANIC ACIDS

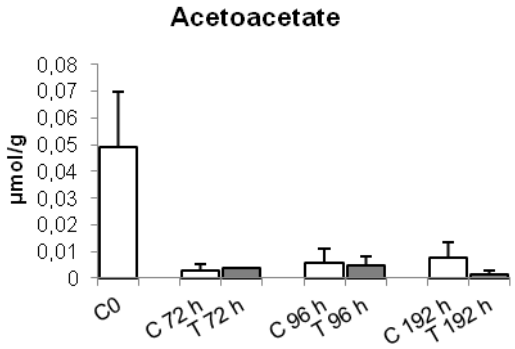

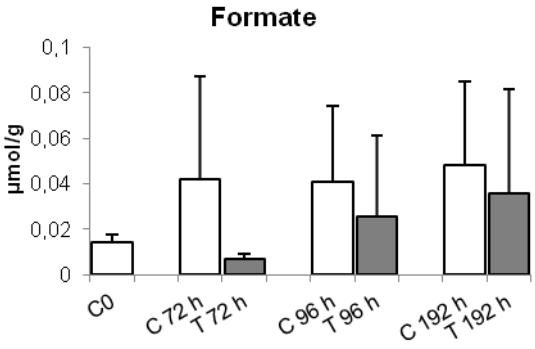

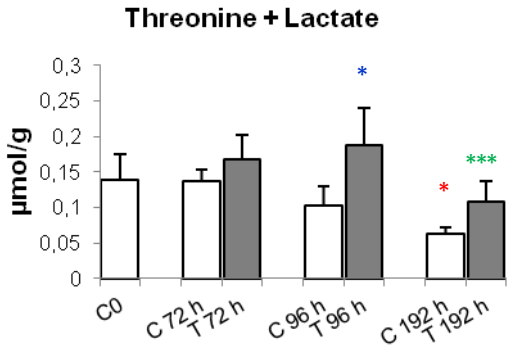

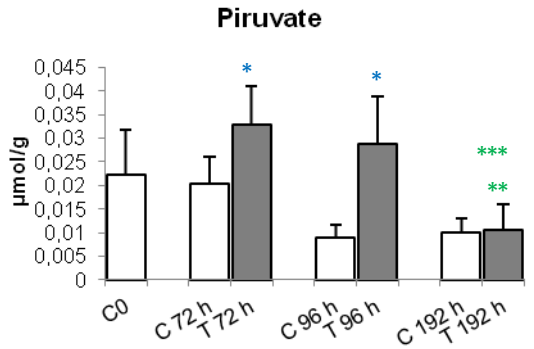

SUGARS

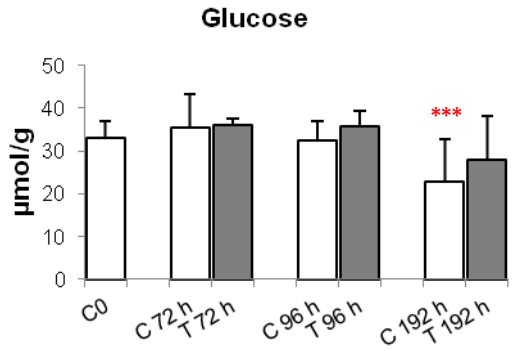
Glucose
µmol/g
50
40
30
20
10
0
***
C0
C 72 h
T 72 h
C 96 h
T 96 h
C 192 h
T 192 h

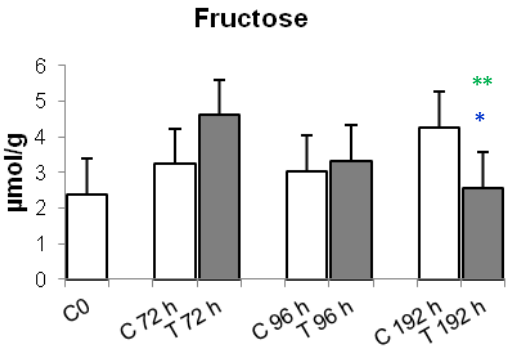
Fructose
µmol/g
6
5
4
3
2
1
0
**
*
C0
C 72 h
T 72 h
C 96 h
T 96 h
C 192 h
T 192 h

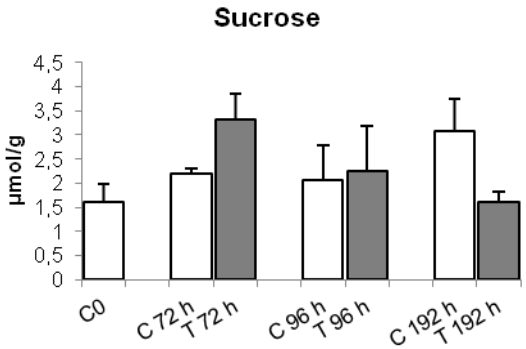
Sucrose
µmol/g
4,5
4
3,5
3
2,5
2
1,5
1
0,5
0
C0
C 72 h
T 72 h
C 96 h
T 96 h
C 192 h
T 192 h

LIPIDS

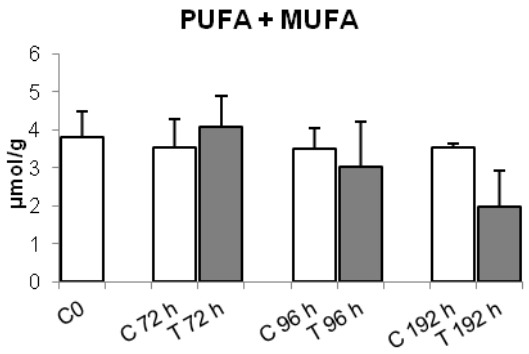
PUFA + MUFA
µmol/g
0
1
2
3
4
5
6
C0
C 72 h
T 72 h
C 96 h
T 96 h
C 192 h
T 192 h

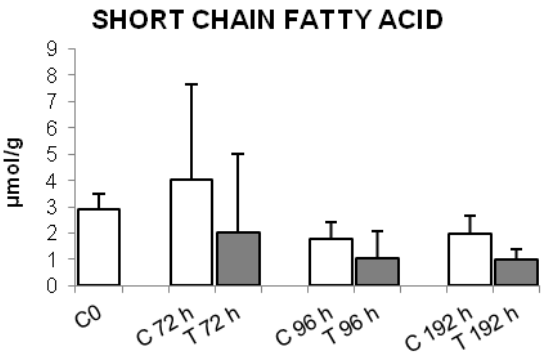
SHORT CHAIN FATTY ACID
µmol/g
0
1
2
3
4
5
6
7
8
9
C0
C 72 h
T 72 h
C 96 h
T 96 h
C 192 h
T 192 h

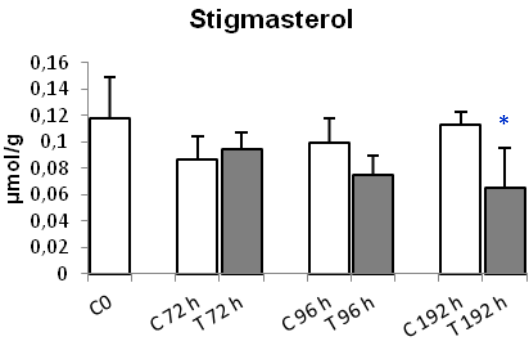
Stigmasterol
µmol/g
0
0,02
0,04
0,06
0,08
0,1
0,12
0,14
0,16
*
C0
C 72 h
T 72 h
C 96 h
T 96 h
C 192 h
T 192 h

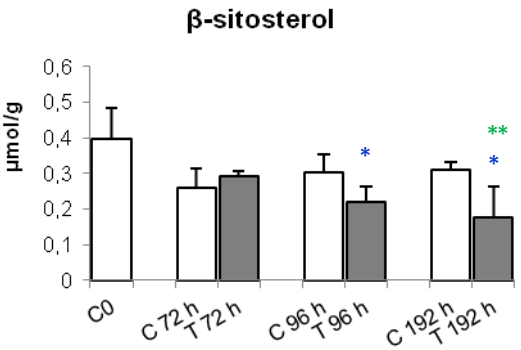
β-sitosterol
µmol/g
0
0,1
0,2
0,3
0,4
0,5
0,6
*
**
*
C0
C 72 h
T 72 h
C 96 h
T 96 h
C 192 h
T 192 h

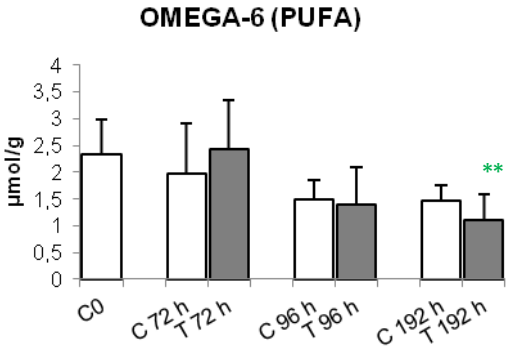
OMEGA-6 (PUFA)
µmol/g
0
0,5
1
1,5
2
2,5
3
3,5
4
**
C0
C 72 h
T 72 h
C 96 h
T 96 h
C 192 h
T 192 h

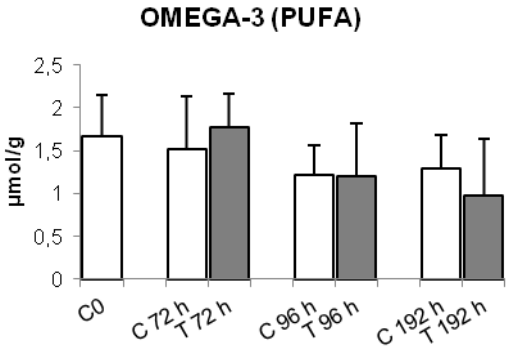
OMEGA-3 (PUFA)
µmol/g
0
0,5
1
1,5
2
2,5
C0
C 72 h
T 72 h
C 96 h
T 96 h
C 192 h
T 192 h

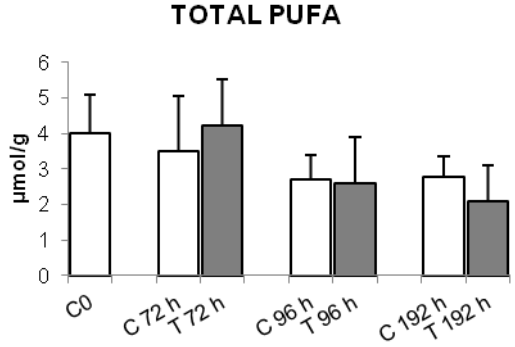
TOTAL PUFA
µmol/g
0
1
2
3
4
5
6
C0
C 72 h
T 72 h
C 96 h
T 96 h
C 192 h
T 192 h

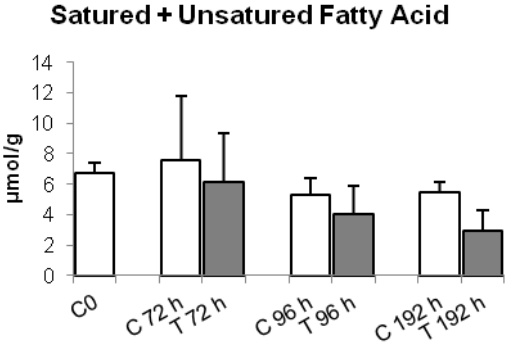
Satured + Unsatured Fatty Acid
µmol/g
0
2
4
6
8
10
12
14
C0
C 72 h
T 72 h
C 96 h
T 96 h
C 192 h
T 192 h

PHENYLPROPANOID PATHWAY

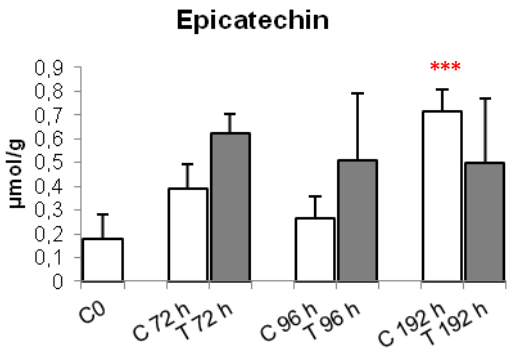

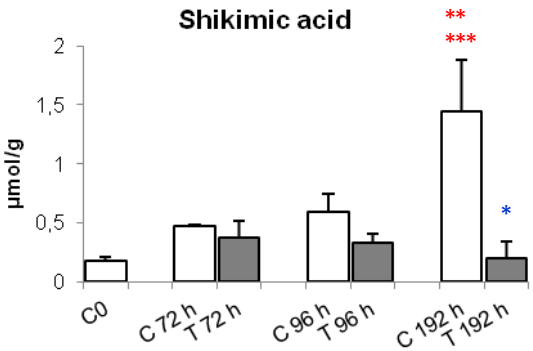

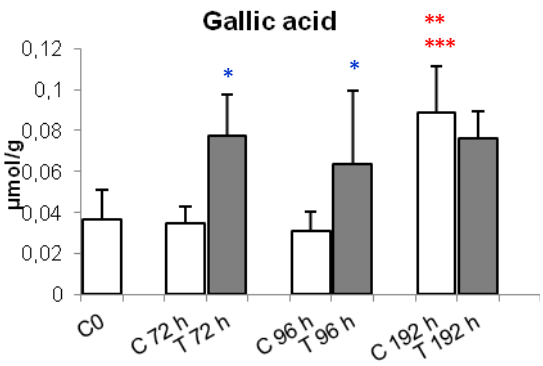

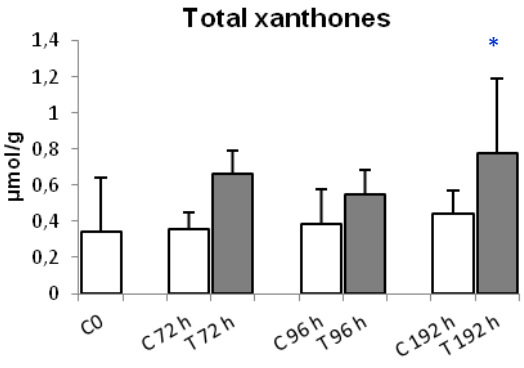

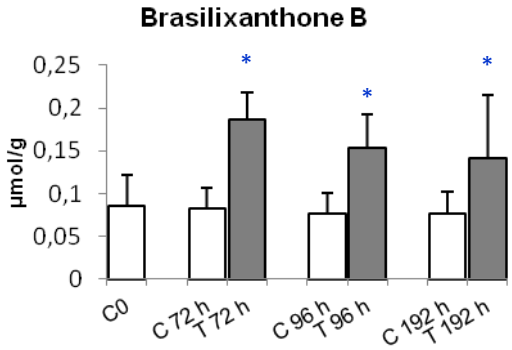

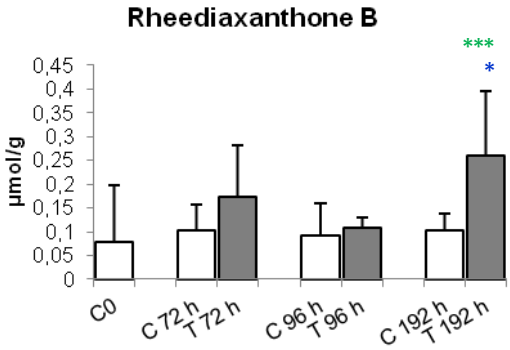

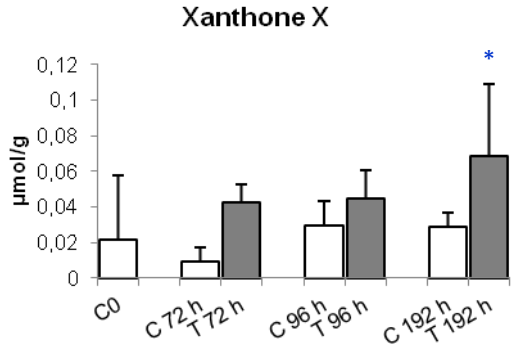

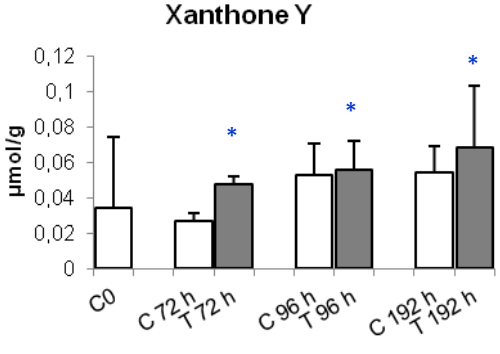

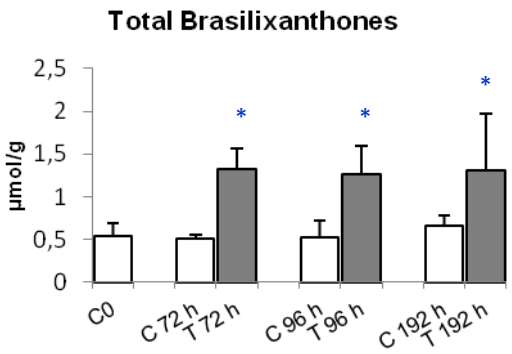

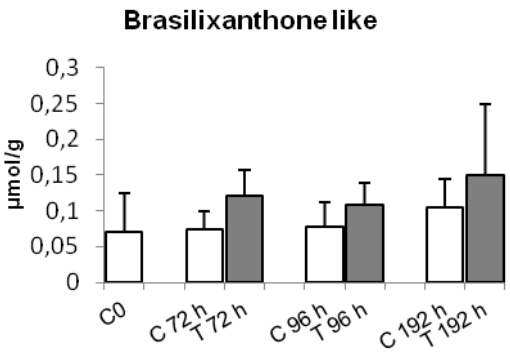

ISOPRENOID PATHWAY

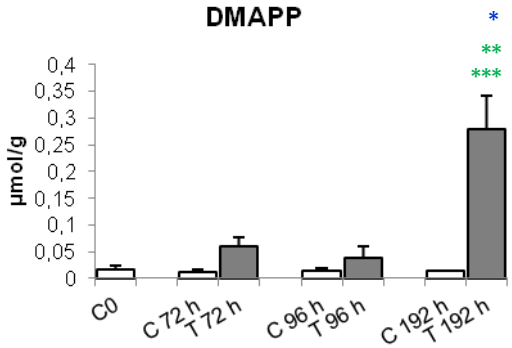

OTHER COMPOUNDS

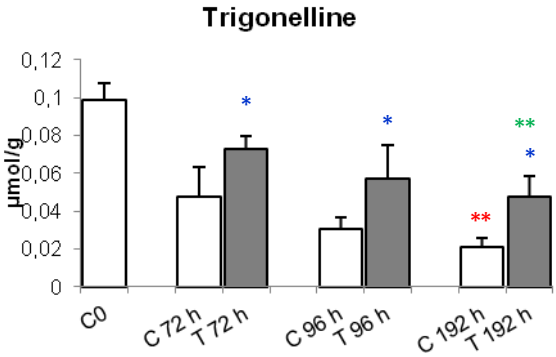

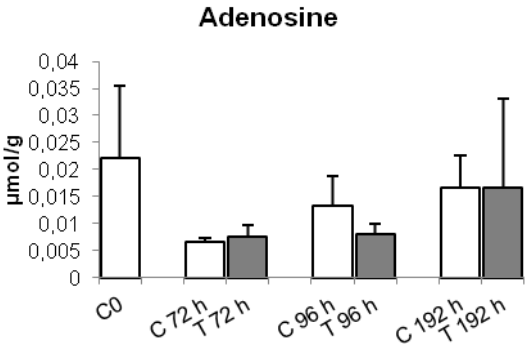

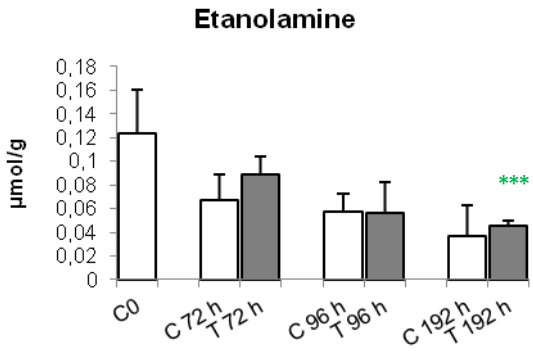

UNKNOWN COMPOUNDS

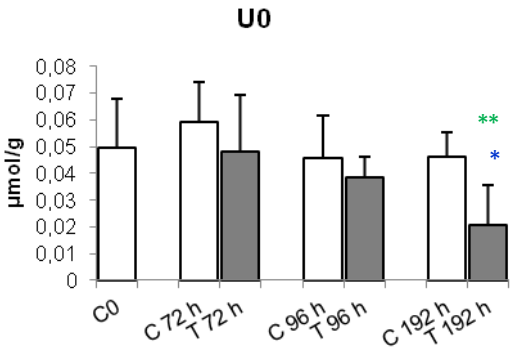

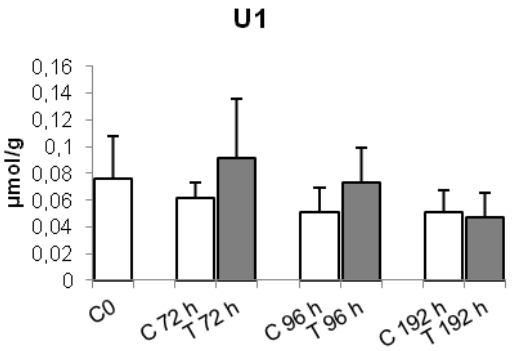

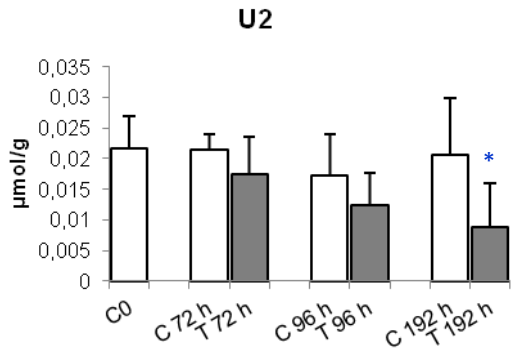

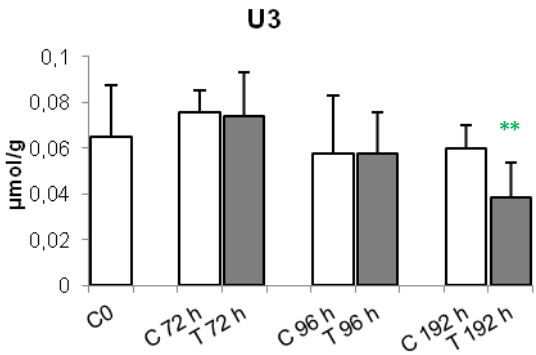

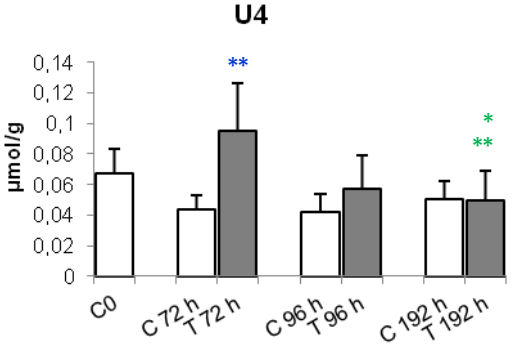

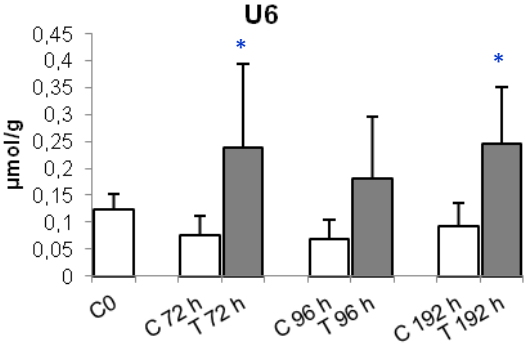

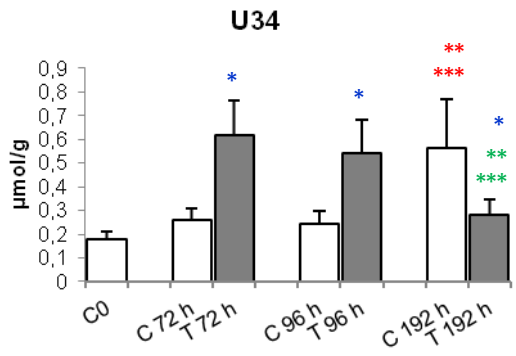
U34
µmol/g
0,9
0,8
0,7
0,6
0,5
0,4
0,3
0,2
0,1
0
C0
C 72 h
T 72 h
C 96 h
T 96 h
C 192 h
T 192 h

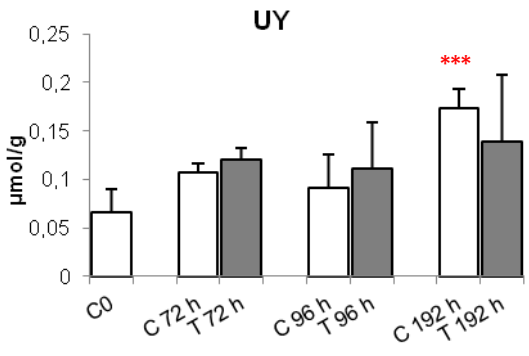
UY
µmol/g
0,25
0,2
0,15
0,1
0,05
0
C0
C 72 h
T 72 h
C 96 h
T 96 h
C 192 h
T 192 h

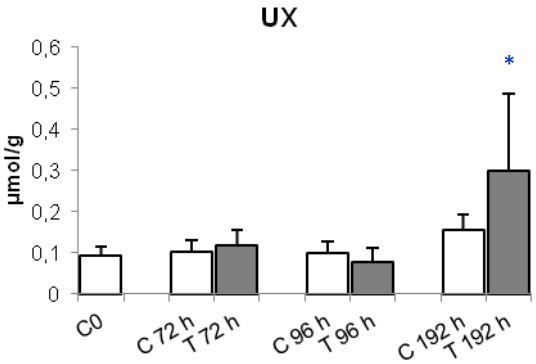
UX
µmol/g
0,6
0,5
0,4
0,3
0,2
0,1
0
C0
C 72 h
T 72 h
C 96 h
T 96 h
C 192 h
T 192 h

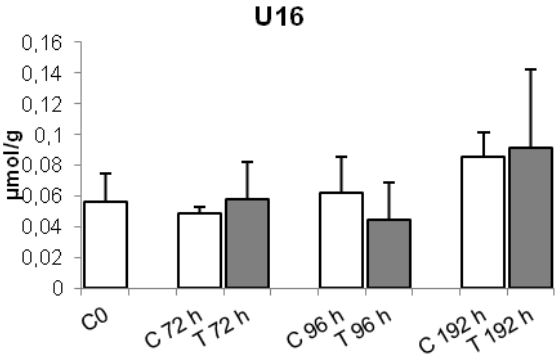
U16
µmol/g
0,16
0,14
0,12
0,1
0,08
0,06
0,04
0,02
0
C0
C 72 h
T 72 h
C 96 h
T 96 h
C 192 h
T 192 h

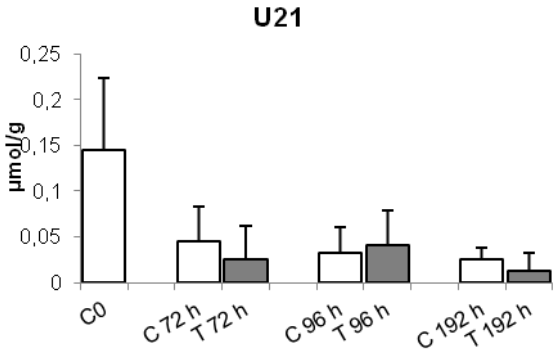
U21
µmol/g
0,25
0,2
0,15
0,1
0,05
0
C0
C 72 h
T 72 h
C 96 h
T 96 h
C 192 h
T 192 h

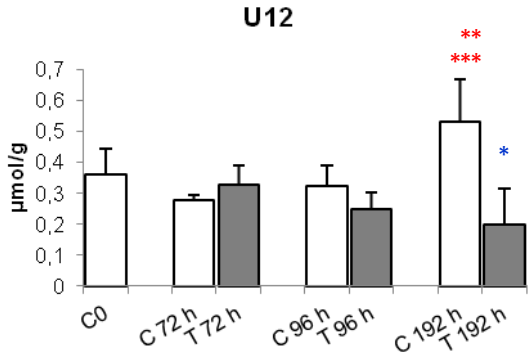
U12
µmol/g
0,7
0,6
0,5
0,4
0,3
0,2
0,1
0
C0
C 72 h
T 72 h
C 96 h
T 96 h
C 192 h
T 192 h

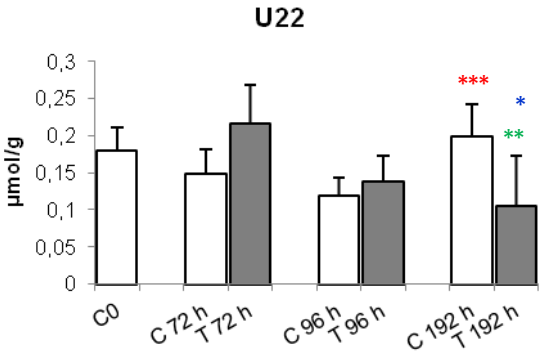
U22
µmol/g
0,3
0,25
0,2
0,15
0,1
0,05
0
C0
C 72 h
T 72 h
C 96 h
T 96 h
C 192 h
T 192 h

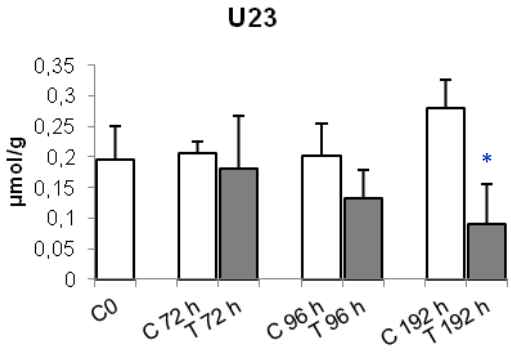
U23
µmol/g
0,35
0,3
0,25
0,2
0,15
0,1
0,05
0
C0
C 72 h
T 72 h
C 96 h
T 96 h
C 192 h
T 192 h

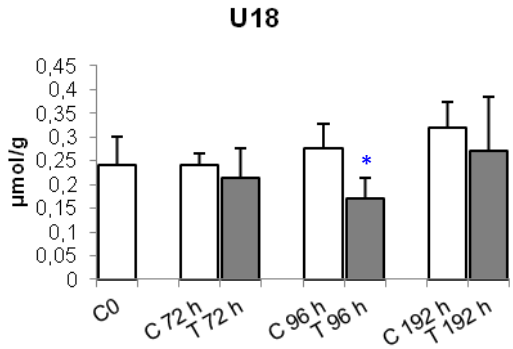
U18
µmol/g
0,45
0,4
0,35
0,3
0,25
0,2
0,15
0,1
0,05
0
*
C0
C 72 h
T 72 h
C 96 h
T 96 h
C 192 h
T 192 h

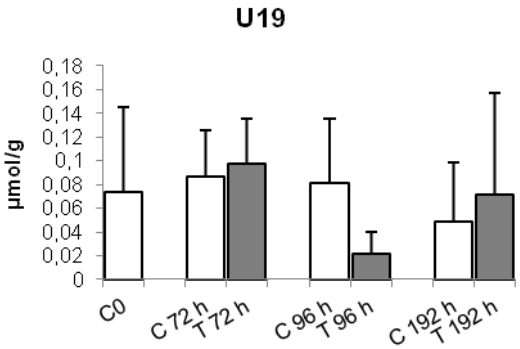
U19
µmol/g
0,18
0,16
0,14
0,12
0,1
0,08
0,06
0,04
0,02
0
C0
C 72 h
T 72 h
C 96 h
T 96 h
C 192 h
T 192 h

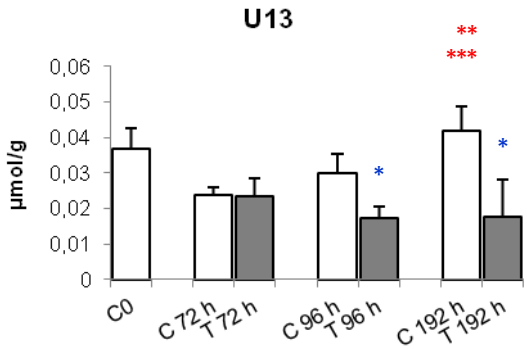
U13
µmol/g
0,06
0,05
0,04
0,03
0,02
0,01
0
**
***
*
*
C0
C 72 h
T 72 h
C 96 h
T 96 h
C 192 h
T 192 h

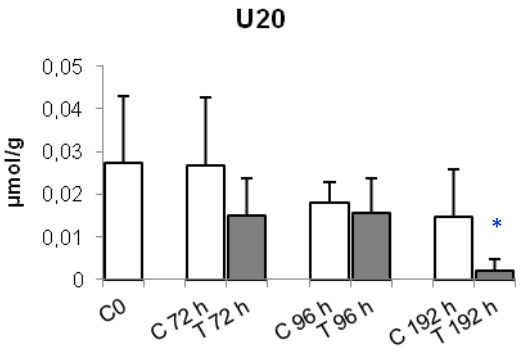
U20
µmol/g
0,05
0,04
0,03
0,02
0,01
0
*
C0
C 72 h
T 72 h
C 96 h
T 96 h
C 192 h
T 192 h

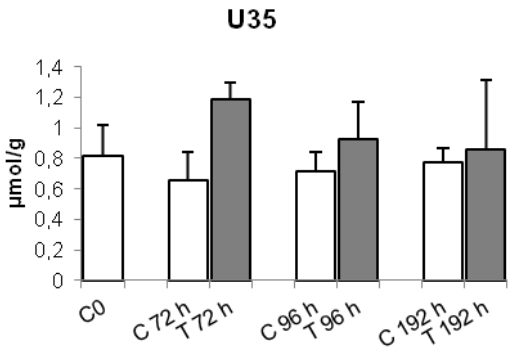
U35
µmol/g
1,4
1,2
1
0,8
0,6
0,4
0,2
0
C0
C 72 h
T 72 h
C 96 h
T 96 h
C 192 h
T 192 h

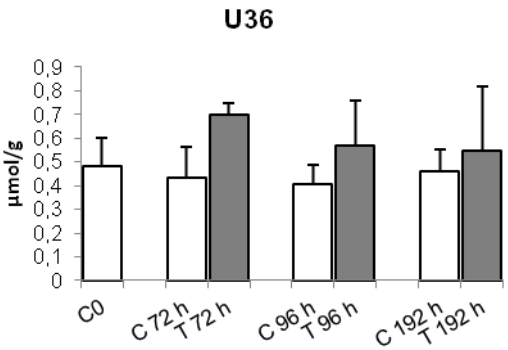
U36
µmol/g
0,9
0,8
0,7
0,6
0,5
0,4
0,3
0,2
0,1
0
C0
C 72 h
T 72 h
C 96 h
T 96 h
C 192 h
T 192 h

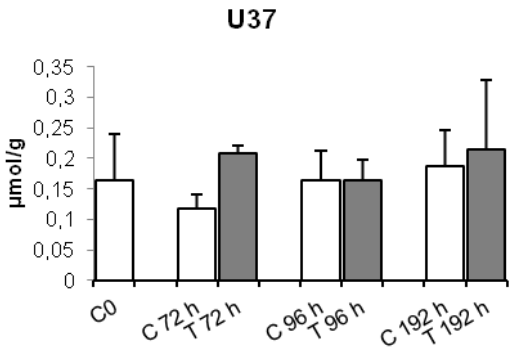
U37
µmol/g
0,35
0,3
0,25
0,2
0,15
0,1
0,05
0
C0
C 72 h
T 72 h
C 96 h
T 96 h
C 192 h
T 192 h

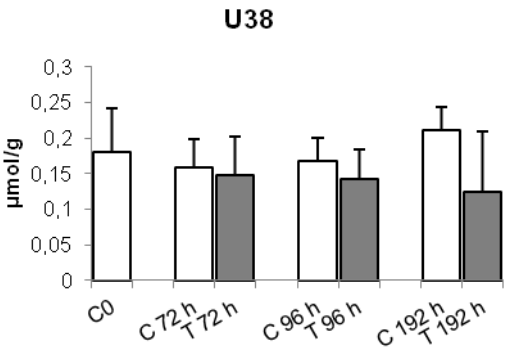
U38
µmol/g
0,3
0,25
0,2
0,15
0,1
0,05
0
C0
C 72 h
T 72 h
C 96 h
T 96 h
C 192 h
T 192 h

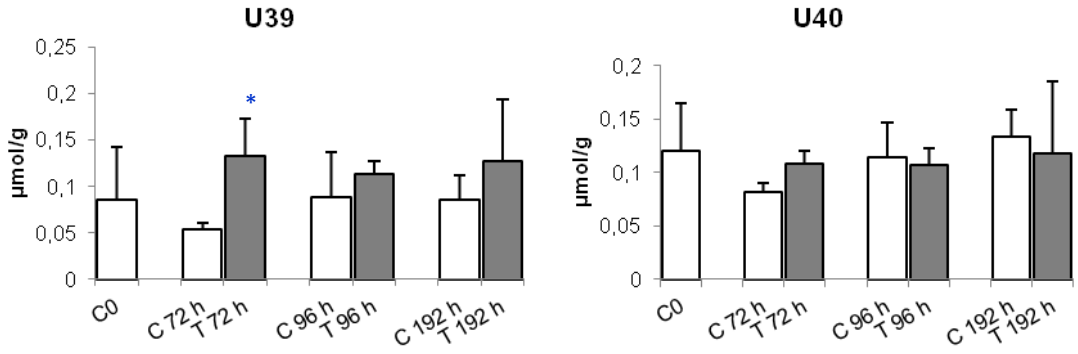

Figure 3. Metabolic composition of the root extracts. Histograms representing the quantitative composition of the assigned metabolites grouped into distinct classes. Data are expressed in µmol/g of fresh weight and are presented as the mean ± standard deviation (SD) of five samples in five independent experiments. White and grey bars represent control and chitosan elicited samples, respectively, at various experimental times. * Significally different from control at the same experimental time. * Significant difference between controls at 72 h and 96 h. ** Significant difference between controls at 72 h and 192 h. *** Significant difference between controls at 96 h and 192 h. * Significant difference between treated at 72 h and 96 h. ** Significant difference between treated at 72 h and 192 h. *** Significant difference between treated at 96 h and 192 h as assessed by Two-Way ANOVA. $P < 0.05$.

An initial exploration of the whole data set to identify a possible clustering of samples and possible outliers was performed by Principal Component Analysis (PCA). PCA was applied on the data set constituted by metabolite concentrations measured at basal time (day 0), 72 h (day 11), 96 h (day 12) and 192 h (day 16) after elicitation, and the resulting score plot is shown in Figure 4.

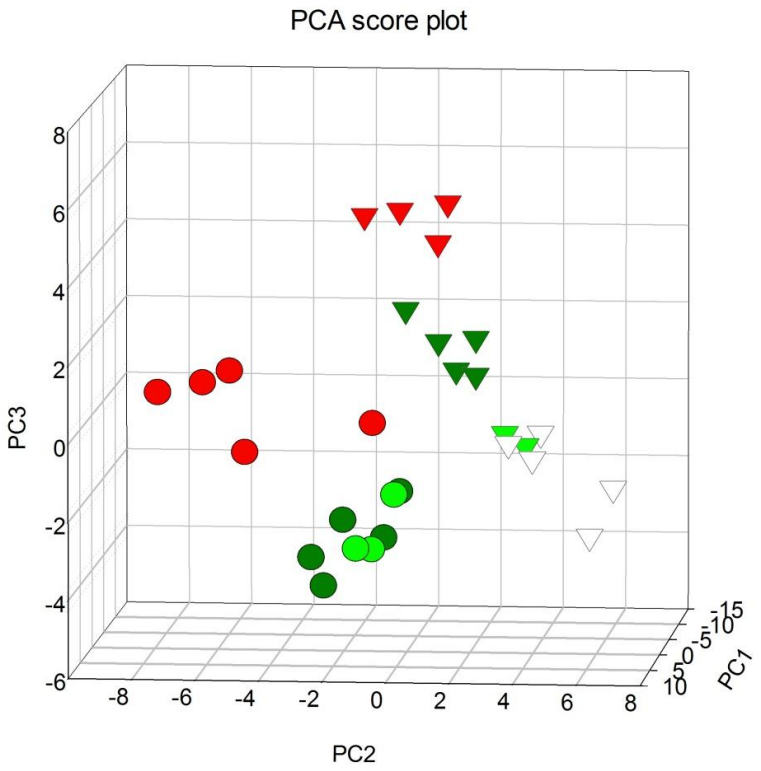

Figure 4. The PC scores plot relative to whole set of *H. perforatum* root data. ▽ basal samples; ▼ control samples at 72 h, ▼ control samples at 96 h; ▼ control samples at 192 h; ● chitosan-elicited samples at 72 h; ● chitosan-elicited samples at 96 h; ● chitosan-elicited samples at 192 h. Total variance explained by PCs was 28%, 19% and 12% for PC1, PC2 and PC3, respectively.

A complete separation between control and treated roots was achieved with 3 PCs explaining 28%, 19% and 12% of the X-variance, respectively.

In particular PC2 and PC3 scores corresponding to chitosan elicitation- and biomass growth-related changes, respectively, whereas PC1 score represents the high variability does not related to time and treatment. In particular, PC2 and PC3 separated the samples on the basis of treatment with chitosan and time of biomass growth, while PC1 does not seem to be linked to any of the considered factors (time and treatment). The latter represents the high variability due to sample size and to large number of variables. The PCA highlights that the total variability for the discrimination of the factors (time and treatment) is less and in other words, a smaller number of variables are involved in the description of principal component compared to the first experiment (see study I).

In order to disentangle the contribution of metabolic variations related to root biomass growth in a confined environment from that depending on chitosan elicitation, a multivariate regression such as partial least squares 2 (PLS2) model has been applied.

The obtained model were constituted on four significant latent variables for PLS2 model (Figure 5) explaining 98.3% of the Y variance, with a cross-validation Q^2 of 0.928 (time effect), and 81.6% with a cross-validation Q^2 of 0.745 (treatment effect).

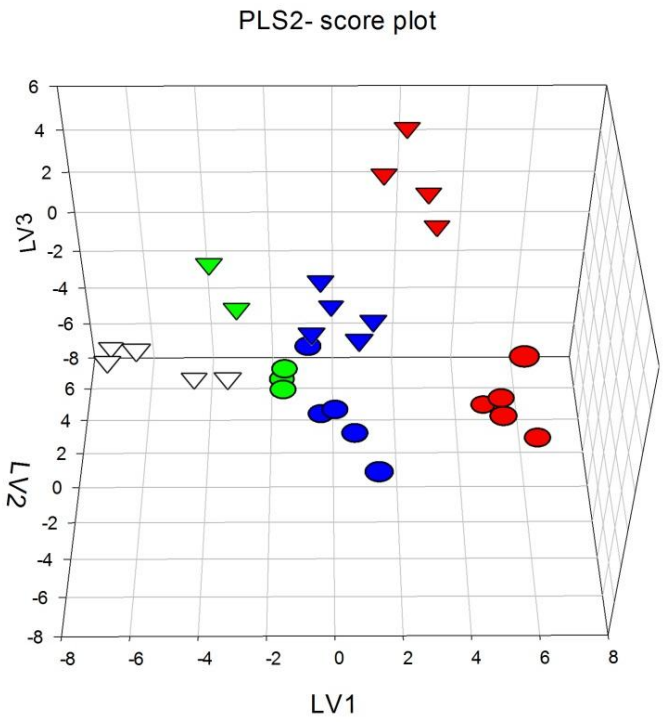

Figure 4. PLS2 score plot

- Samples at time 0 (day 8)
- control samples at 72 h (day 11)
- control samples at 96 h (day 12)
- control samples at 192 h (day 16)
- chitosan-elicited samples at 72 h
- chitosan-elicited samples at 96 h
- chitosan-elicited samples at 192 h

Figure 5. The PLS2 model were constituted on four significant latent variables for PLS2 model explaining 98.3% of the Y variance for the time effect and 81.6% of the Y variance for the treatment effect.

The PLS2 model show to be able to separate the time-dependent trajectories on the LVs planes of elicited and not-elicited root samples. In particular, the PLS2 model built on control and treated root sample identified significant differences related to a "time effect" and "treatment effect". However, the metabolic variations induced by the different factors (treatment and time) distinguishing "between" and "within" of factors identified cannot be easily interpreted by loading regression analysis.

For this reason, in order to discriminate the metabolic variations related to root biomass growth and to chitosan treatment, and to their interaction, ASCA modelling was applied.

ASCA modelling showed that only the effects of chitosan treatment and time were significant (the *p*-values for treatment and time were 0.03618 and 0.00194, respectively), while the effect of the their interaction was not statistically different from zero ($p>0.87$) Figure 6 A, B and C.

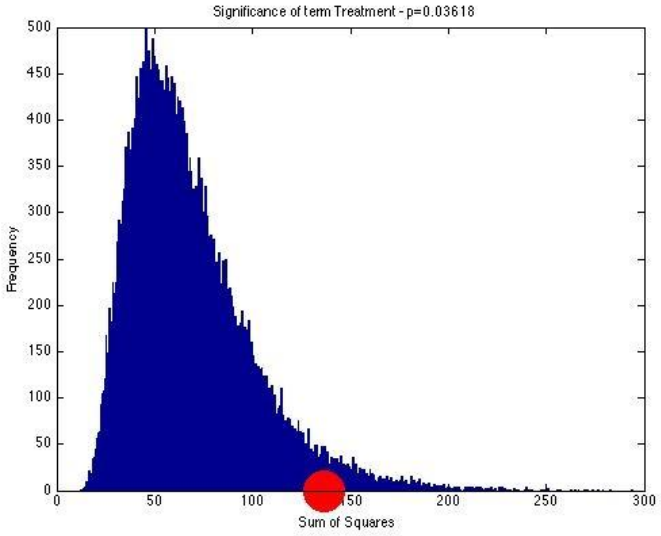

Figure 6 A. Evaluation of the significance of the multivariate effect of treatment by means of permutation tests.

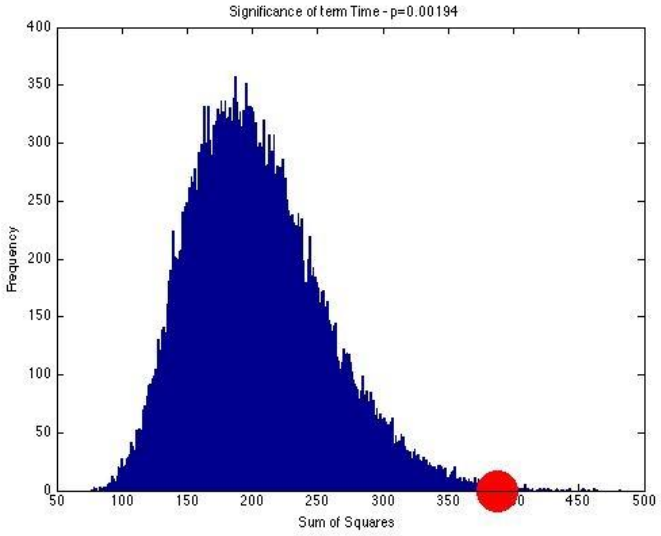

Figure 6 B. Evaluation of the significance of the multivariate effect of time by means of permutation tests.

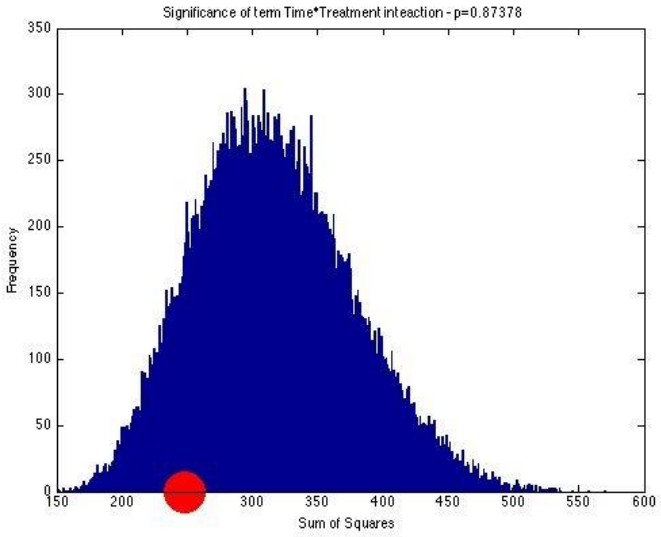

Figure 6 C. Evaluation of the significance of the multivariate effect of treatment-time interaction by means of permutation tests.

Having verified that treatment and time had a significant effect on the metabolic profiles of *H. perforatum* roots, simultaneous component analysis (SCA) was used (after Pareto scaling) to model the variation in the two corresponding matrices $\mathbf{X}_{treatment}$ and $\mathbf{X}_{time}$.

Effect of the chitosan treatment on *H. perforatum* root metabolism as revealed by ASCA analysis

As described in section 4.3, a single component (SC1) was calculated by SCA model and the corresponding score plot is shown in Figure 7.

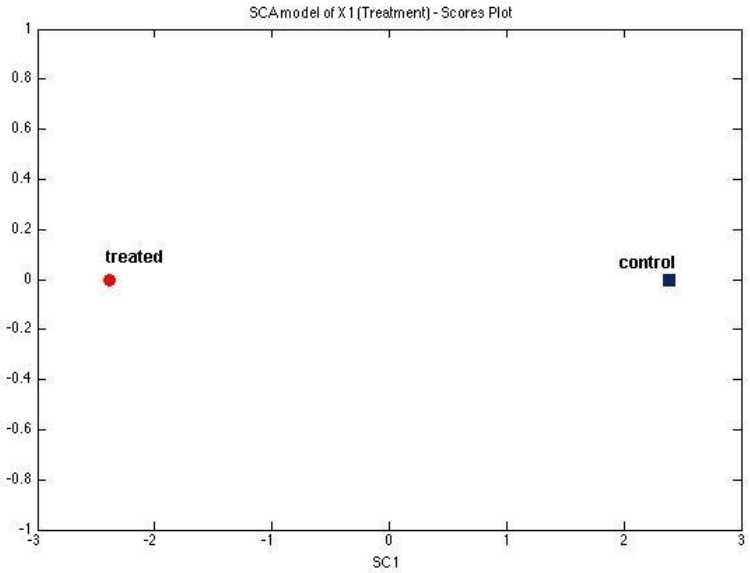

Figure 7. SCA score plot for effect of treatment: SC1 shows the significant effect of the chitosan elicitation.

Along SC1, control samples were placed at positive values whereas the treated samples were placed at negative values of SC1 (figure 7). The distribution of the loadings for the SCA model of the treatment effect is reported in Figure 8.

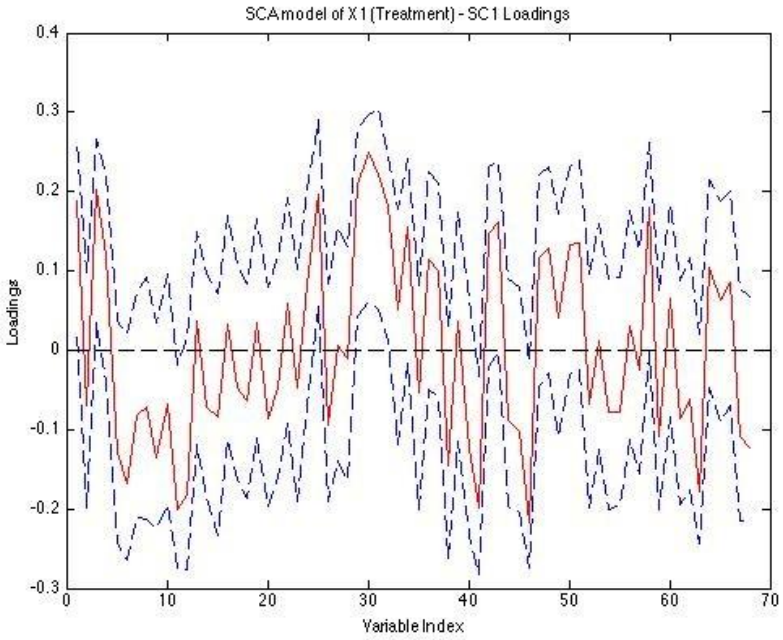

Figure 8. SCA analysis on the effect matrix for treatment: variable loadings for the one-component SCA model (blue line) and their 95% confidence intervals (red).

Considering that control samples were placed at positive values of SC1, variables with positive loadings were higher in control then treated roots. Conversely, chitosan treated samples were placed at negative values of SC1 therefore, variables with negative loadings were higher in treated then control samples. The SC1 identified as significant metabolites for SCA model: shikimic acid, tryptophan and five unknown metabolites such as U0, U2, U12, U23 and U18 that were higher in control then in elicited roots and DMAPP, total brasilixanthones, and U6 that were higher in elicited then in control roots.

Effect of the time on *H. perforatum* root metabolism as revealed by ASCA analysis

As described in section 4.3, two component (SC1 and SC2) were resulted significant for the SCA model and the corresponding score plot is shown in Figure 9A.

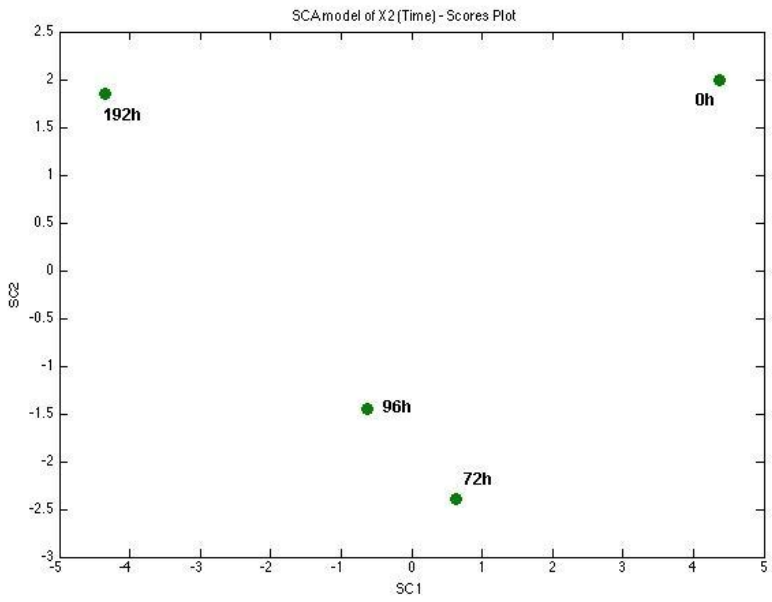

Figure 9A. SCA score plot for the effect of time: SC1 and SC2 show the significant effect of time.

In order to better understand the evolution of the scores in function of time, a score plot with the distribution of the scores for each of the two components (SC1 and SC2) is reported in Figure (9B).

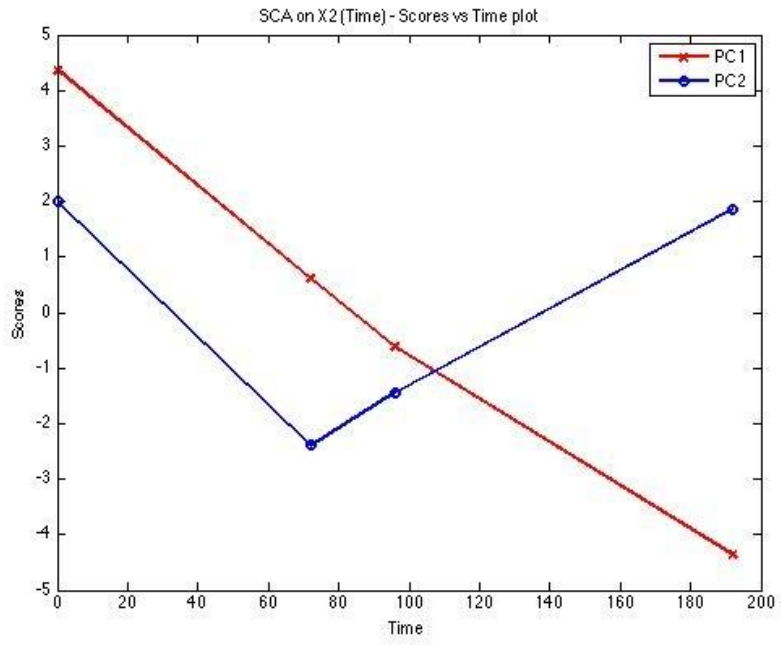

Figure 9B. SCA score plot for the effect of time: SC1 and SC2 show the significant effect of time.

The two components SC1 and SC2 show two metabolic events which contribute to the total variance in two different ways, explaining the 65% and 20% respectively.

In particular, SC1 displays a monotonous trajectory in function of time: the scores decreased with the time went until reaching a minimum. Consequently, the variables with positive loading systematically decreased whereas the variables with negative loading systematically increased along this component. In order to explain this difference loading analysis was performed. The distribution of the loadings for the SCA model of the time effect along the SC1 is reported in Figure 10.

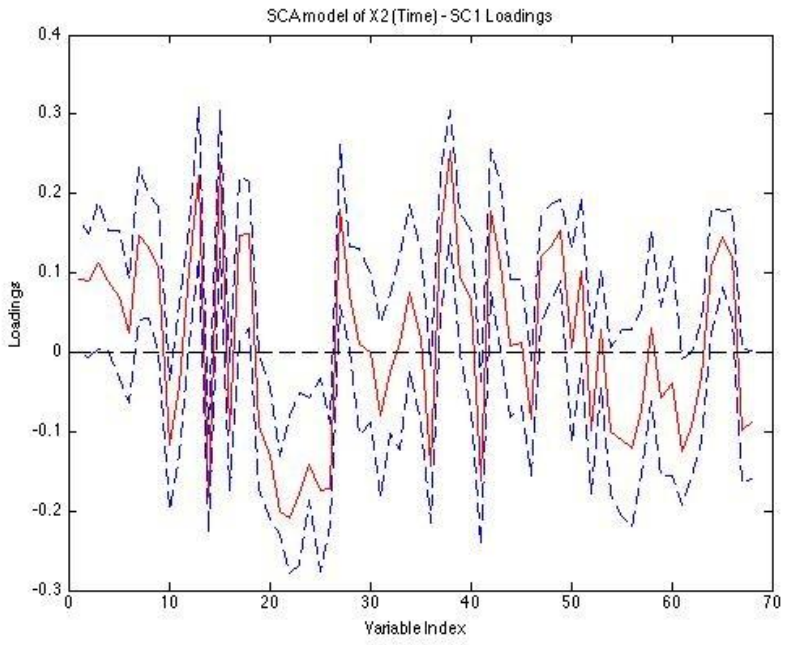

Figure 10. SCA analysis on the effect matrix for time along SC1: variable loadings for the one-component SCA model (blue line) and their 95% confidence intervals (red).

The significant metabolites that decreased were isoleucine, valine, threonine + lactate, pyruvate, acetoacetate, etanolamine, α- and β-glucose, trigonelline, sitosterol, stigmasterol, PUFA + MUFA, satured and unsatured fatty acid, omega-6, short fatty acids, total PUFA, Omega 3 and two unknown metabolites such as U2 and U3. The significant metabolites that increased were alanine, asparagine, fructose, sucrose, epicatechin, shikimic acid, gallic acid, formate, DMAPP, total brasilixanthones, brasilixanthone B, brasilixanthone like, and four unknown metabolites such as U34, UY, UX and U16.

Conversely, SC2 displays a perturbation that evolves over time returning to the starting point: the scores decreased until 72 h and then progressively increased until returning to the initial values. Consequently, the variables with positive loading decreased and then increased whereas the variables with negative loading increased and then decrease. In order to explain this difference loading analysis was performed. The distribution of the loadings for the SCA model of the time effect along the SC2 is reported in Figure 11.

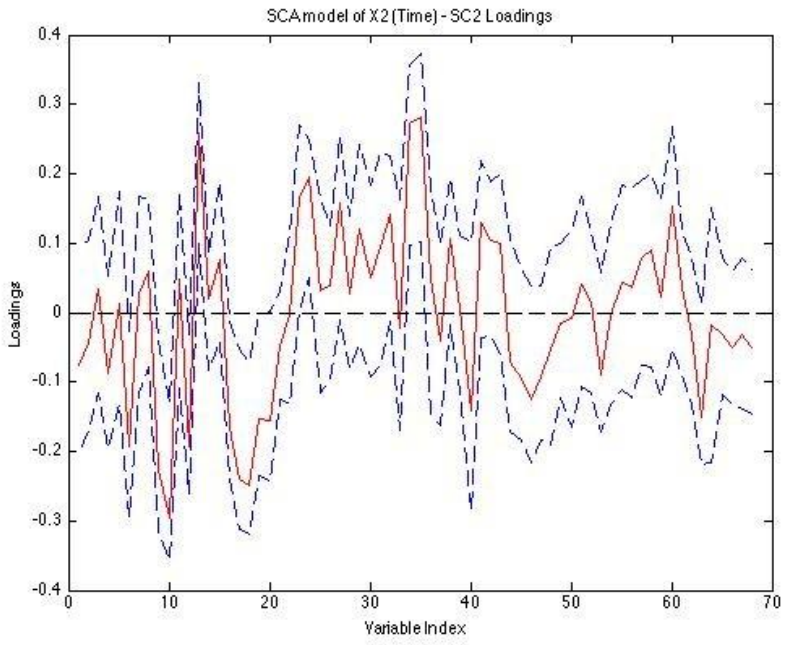

Figure 11. SCA analysis on the effect matrix for time along SC2: variable loadings for the one-component SCA model (blue line) and their 95% confidence intervals (red).

The significant metabolites that decreased and then increased were acetoacetate, adenosine and three unknown metabolites such as UX, U16, U13. The significant metabolites that increased and then decreased were leucine, threonine + lactate, alanine, pyruvate, fructose, α- and β-glucose, and sucrose.

To summarize the loadings metabolites that contribute significantly to the model for time and treatment effects an heatmap has been built and is shown in Figure 12.

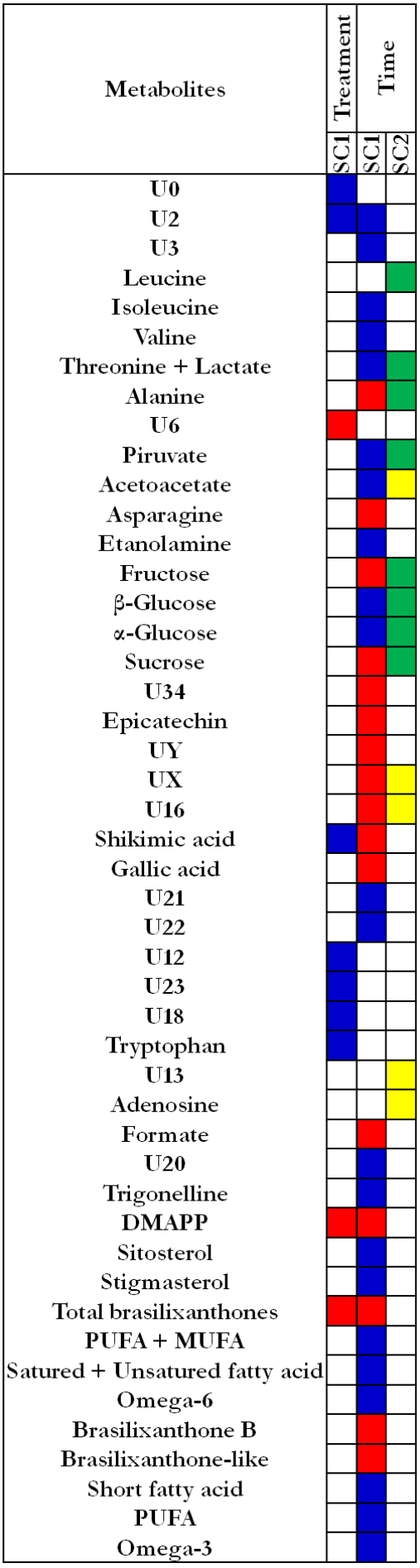
Metabolites
Treatment
Time
SC1
SC1
SC2
U0
U2
U3
Leucine
Isoleucine
Valine
Threonine + Lactate
Alanine
U6
Piruvate
Acetoacetate
Asparagine
Etanolamine
Fructose
β-Glucose
α-Glucose
Sucrose
U34
Epicatechin
UY
UX
U16
Shikimic acid
Gallic acid
U21
U22
U12
U23
U18
Tryptophan
U13
Adenosine
Formate
U20
Trigonelline
DMAPP
Sitosterol
Stigmasterol
Total brasilixanthones
PUFA + MUFA
Satured + Unsatured fatty acid
Omega-6
Brasilixanthone B
Brasilixanthone-like
Short fatty acid
PUFA
Omega-3

Figure 12. Heatmap for loadings metabolites that contribute significantly to the model for time and treatment effects. Treatment effect: blue corresponds to the loading with positive direction (increase) in control roots; red corresponds to the loadings with negative direction (increase) in treated roots. Time effect: for the SC1, blue corresponds to the loading with positive direction (decrease); red corresponds to the loading with negative direction (increase). For the SC2, yellow corresponds to the loading with positive direction (decreased and then increased); green corresponds to the loading with negative direction (increased and then decrease).

Histological analysis of control and chitosan-treated *Hypericum perforatum* in vitro roots at 96 and 192 h

Histological analysis was carried out to investigate the effect of chitosan elicitation on the morphology and anatomy of roots of *Hypericum perforatum* at time 96 and 192 hours after chitosan elicitation. The marked morpho-anatomical alterations already observed at 72 hours remained unchanged at 96 and 192 h (Figure 13).

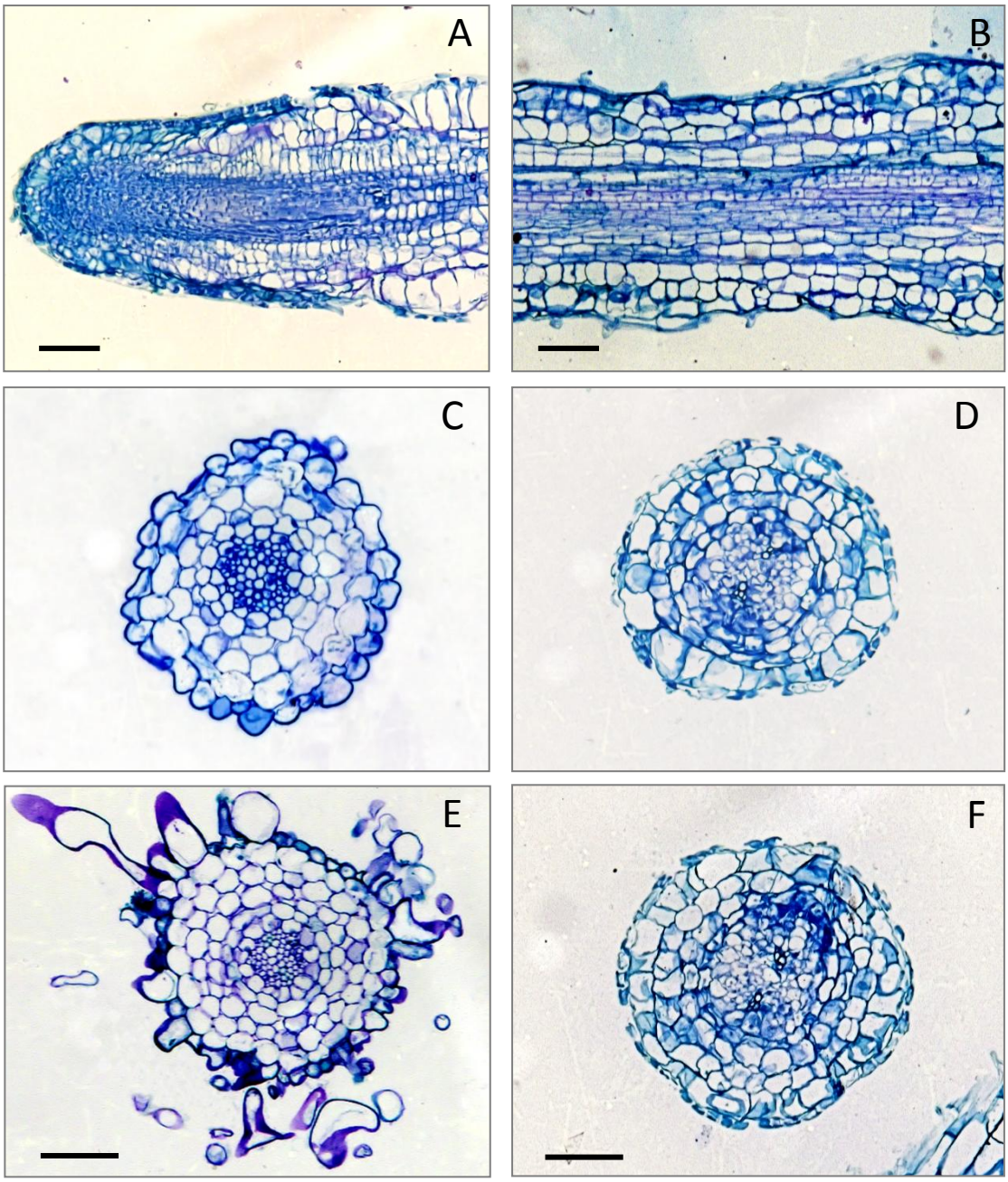

Figure 13. Resin-embedded longitudinal sections of chitosan treated roots (A and B). Cross sections of control roots at 96 h (C) and at 192 h (E) and of chitosan treated roots at 96 h (D) and 192 h (F) stained with 0.1% toluidine blue. Bars represent 100 μm.

Analysis of isoprenoid comopounds by GC/MS

The main compounds observed by GC/MS analysis of root samples were acids/esters of long chain and steroids such as butyric acid (92 % similarity), palmitic acid (88 % similarity), linoleic acid (93 % similarity), n-Heptadecane (90 % similarity), di-n-octyl-phthalate (95 % similarity), stigmasterol (87 % similarity) and γ-sitosterol (94 % similarity). Terpenes compounds were not observed as revealed by chromatograms shown in Figure 14.

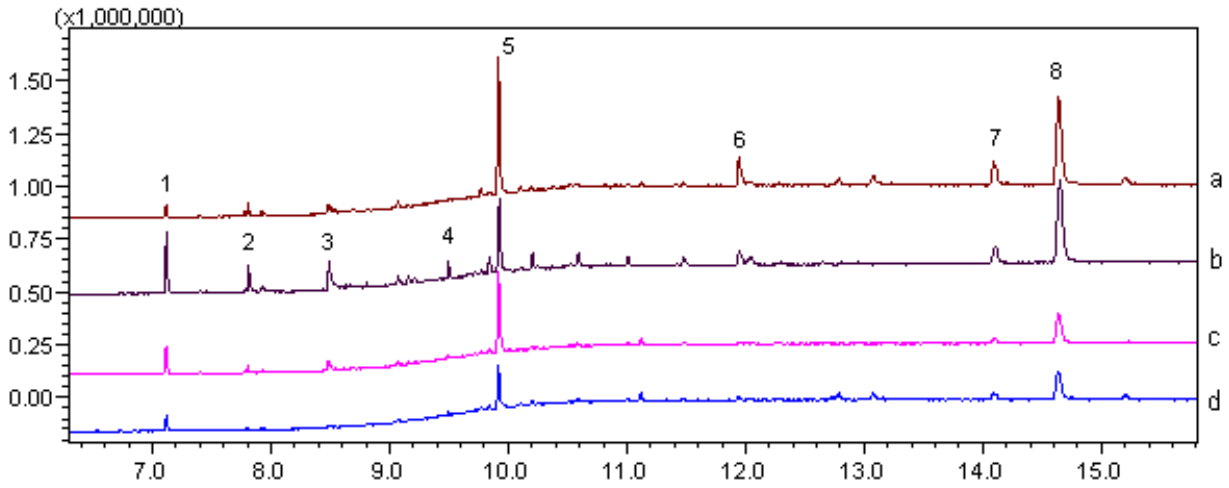

Figure 14. Overlapping chromatograms of root samples: a and d represent treated roots harvested at 192 h; b and c represent control roots harvested at 192 h. The identified compounds are numbered from 1 to 8 as follows: 1) Butyric acid, 2) Palmitic acid, 3) Linoleic acid, 4) n-Heptadecane, 5) Di-n-octyl-phthalate, 6) Unknow compound, 7) Stigmasterol, 8) γ-sitosterol.

4.5 Discussion

Comparing the growth curves of *H. perforatum* control roots from STUDY I and II, it is possible to observe that the shortening of culture time which precedes the elicitation (STUDY II), starting with the same amount of inoculum, an equal biomass density has been obtained. In particular, an equal biomass density has been obtained in both experiments at day 12 and at the end of culture time (day 15 for the first experiment and 16 day for the second one).

Specifically, the removal of a single renewal of culture medium during the exponential phase of the biomass growth, did not influence the growth rate and biomass yield, demonstrating that culture medium composition is not a limiting factor on the root growth rate in the considered experimental times. Conversly, the comparison between the metabolic profiles obtained from the two different culture conditions (STUDY I and II), showed deeply different responses in primary and secondary metabolism of *H. perforatum* control roots. Analogously to the previous study, the biomass growth in a confined environment stimulated the phenylpropanoid metabolism, as revealed by the increase in epicatechin, gallic and shikimic acid levels.

As an effect, a significant positive correlation between shikimic acid and epicatechin (Pearson coefficient r = 0,89) and gallic acid and epicatechin (r= 0,88) levels was observed, and furthermore a significant increase in tryptophan level was observed with the time went. These results confirm the existing relationship between increase in biomass density, growth slowdown and phenol biosynthesis, as proposed by Cui et al. (2010) in *H. perforatum* roots cultured in a bioreactor and already discussed in the previous study. Although xanthone levels did not significantly change over time, it is interesting to observe that control roots showed tenfold higher total xanthone levels in this experiment compared to the first study. The relative amounts of total xanthones in different days of culture were: 0.35 μmol/g (day 11), 0.38 μmol/g (day 12), 0.44 μmol/g (day 16) in the second experiment, and 0.02 μmol/g (day 12) and 0.03 μmol/g (day 15) in the first experiment.

These results demonstrate that a removal of a renewal of culture medium did not affect the biomass growth, but heavily modified the secondary metabolite production. We hypotesize that this effect is

due to the lower auxin (IBA) level to which the roots were exposed with the respect of protocol with double culture medium renewal (first study). Tocci et al (2011) demonstrated that different concentrations of IBA influenced xanthone production in *in vitro* regenerated roots of *H. perforatum*. However, further investigations are requested to clarify molecolar mechanisms underlying these effects.

In elicited roots, the chitosan addition at day 8 caused a sudden slowdown of growth, as observed also in the previous study.

The PLS2 regression model identified significant differences attributable to a time effect and to a chitosan treatment but did not allow to detect possible interactions between the two factors. Applying ASCA model the significance of time and treatment factors and the absence of an interaction between two effects has been highlighted.

As revealed by ASCA model, the metabolic signature defining chitosan treatment effect consisted of changes in the level of primary and secondary metabolites associated with phenylpropanoid and isoprenoid pathways.

The increase in DMAPP and Total Brasilixanthones associated to a decrease in shikimic acid and tryptophan levels suggests a adaptation response to stress conditions induced by elicitation with a specific stimulation of secondary metabolism, in agreement with previous results obtained using the same experimental system by Tocci et al. (2011).

The highest level of DMAPP was measured in chitosan elicited roots at 192 h confirming that the chitosan elicitation induced a stimulation of isoprenoid pathway. Despite the considerable increase in DMAPP levels, GC/MS analysis of extracts of *in vitro* roots of *H. perforatum* elicited with chitosan did not reveal the presence of terpenes. Therefore the increase in DMAPP levels can be associated to other isoprenoid compounds, such as sitosterol and stigmasterol, identified both trough NMR and GS/MS analyses. Concerning xanthones, they were qualitatively and quantitatively higher in the present study. In particular, in chitosan elicited roots the total xanthones after 72 h were 0.66 μmol/g and 0.20 μmol/g, in the experiment with a single and double medium renewal, respectively.

Therefore, in chitosan elicited roots of *H. perforatum*, the yield of xanthones was influenced by renewal of the culture medium and probably by a different IBA level during the interval time after elicitation, analogously to that observed for non elicited roots.

Moreover, at 96 and 192 h after chitosan elicitation, it has been possible to identify molecular structures relative to brasilixantone B and rheediaxanthone. The brasilixantone B, already isolated from roots and stems of *Tovomita brasiliensis* (Marques et al. 2000), has been recently identified in adventitious roots of *H. perforatum* (Li et al. 2013). An antibacterial activity of brasilixanthone has been demonstrated against *Staphylococcus aureus* in twigs of Garcinia nigrolineata (Rukachaisirikul et al. 2005). The rheediaxanthone, previously isolated from the roots of *Hypericum roeperanum* (Rath et al. 1996) and from other species such as *Metaxya rostrata* has been demonstrated induce active cell death in colorectal tumore cells (Kainz KP et al. 2013).

In this study, epicatechin levels did not significantly increase in response to chitosan elicitation. Nevertheless in both experiments (STUDY I and II) epicatechin levels appeared to be higher in treated roots when compared to the respective controls, except in those measured at 192 h which were lower than in the respective control roots. Considering elicited roots at 72 h, the epicatechin and shikimic acid levels were higher in the first than in the second experiment. In particular, in the first experiment, the epicatechin and shikimic acid amounts were 1.15 μmol/g and 0.8 μmol/g respectively, whereas in the second experiment were 0.52 μmol/g and 0.38 μmol/g, respectively.

The modification of the experimental protocol, in term of a single or double culture medium renewal, appears to influence the secondary metabolic response to chitosan elicitation, and therefore the epicatechin or xanthone yield.

Despite the observed metabolic changes, the morpho-anatomical alterations ramained unchanged after 72 h of elicitation demonstrating that the root structure modifications induced by chitosan are a precocious event.

CHAPTER 5

FINAL CONCLUSIONS

Final conclusions

Non targeted NMR-based metabolomics has been used to explore the primary and secondary metabolism of *in vitro* regenerated roots of *Hypericum perforatum*. The approach based on metabolic profiling and multivariate data analysis such as ANOVA Simultaneous Component Analysis and Partial Least Square has allowed to discriminate the metabolic effects due to an increase in biomass and chitosan elicitation.

In the second study, the modification of experimental protocol (a single vs double renewal of culture medium) did not affect the biomass growth rate and the biomass weight and density reached the same values at same culture times. However, the single renewal of the culture medium had a strong impact on primary and secondary metabolism both in control and elicited *H. perforatum* roots.

The metabolomics approach proposed can be considered an efficient tool for setting up an *H. perforatum* root culture system for large-scale production of specific secondary metabolites useful for pharmacological applications, such as epicatechin and xanthones.

In this context, the obtained results suggest that it is essential to consider that the metabolic profile of an extract of *in vitro* root culture depends on achieved biomass density and on the used culture protocols. The auxin levels are reported to have an important role for the improvement of the root biomass yield, but they also appear have a strong impact in the qualitative/quantitative definition of secondary metabolite production. It is worth considering that the influence of auxin on root metabolism in culture should be deeply investigated.

This information is important from an applicative point of view in order to obtain standardized extracts useful for the human health.

Furthermore, it should be taken into account that variations in the experimental protocols can lead to deep changes in the ingredients of the extract and consequently, the biological efficacy migth be compromised or at least changed. Finally, studying the biological properties of different mixtures of metabolites that can be obtained varying the experimental culture conditions will be able to rationalize the production of the metabolite/s of interest.

CHAPTER 6

BIBLIOGRAPHY

1) Agnolet S, Jaroszewski JW, Verpoorte R, Staerk D. 1H-NMR-based metabolomics combined with HPLC-PDA-MS-SPE-NMR for investigation of standardized Ginkgo biloba preparations. *Metabolomics.* 2010; 6: 292-302.

2) Ahuja I, Kissen R, Bones AM. Phytoalexins in defense against pathogens. *Trends Plant Sci.* 2012; 17: 73-90.

3) Allwood JW, Ellis DI, Goodacre R. Metabolomic technologies and their application to the study of plants and plant-host interactions. *Physiol Plant.* 2008; 132: 117-35.

4) Astarita G, Langridge J. An Emerging Role for Metabolomics in Nutrition Science. *J Nutrigenet Nutrigenomics.* 2013; 6 :181-200.

5) Atkinson RR, Burrell MM, Osborne CP, Rose KE, Rees M. A non-targeted metabolomics approach to quantifying differences in root storage between fast- and slow-growing plants. *New Phytol.* 2012; 196: 200-11.

6) Bais HP, Walker TS, Schweizer HP, Vivanco JM. Root specific elicitation and antimicrobial activity of rosmarinic acid in hairy root cultures of *Ocimum basilicum. Plant Physiology and Biochemistry.* 2002; 40: 983-995.

7) Baque MA, Moh SH, Lee EJ, Zhong JJ, Paek KY. Production of biomass and useful compounds from adventitious roots of high-value added medicinal plants using bioreactor. *Biotechnol Adv.* 2012; 30: 1255-67.

8) Barding GA Jr, Béni S, Fukao T, Bailey-Serres J, Larive CK. Comparison of GC-MS and NMR for metabolite profiling of rice subjected to submergence stress. *J Proteome Res.* 2013; 12: 898-909.

9) Barnes J, Anderson LA, Phillipson JD. St John's wort (Hypericum perforatum L.): a review of its chemistry, pharmacology and clinical properties. *J Pharm Pharmacol.* 2001; 53: 583-600.

10) Benveniste P. Biosynthesis and accumulation of sterols. *Annu Rev Plant Biol.* 2004; 55: 429-57.

11) Bhat RA, Panstruga R. Lipid rafts in plants. *Planta.* 2005; 223: 5-19.

12) Biondi S, Fornale S, Oksman-Caldentey KM, Eeva M, Agontanim S, Bagni N. Jasmonates induce over accumulation of methylputrescine and conjugated polyamines in *Hyoscyamus muticus* L. root cultures. *Plant Cell Rep.* 2000; 19: 691-697.

13) Birt DF, Widrlechner MP, Hammer KD, Hillwig ML, Wei J, Kraus GA, Murphy PA, McCoy J, Wurtele ES, Neighbors JD, Wiemer DF, Maury WJ, Price JP. Hypericum in infection: Identification of anti-viral and anti-inflammatory constituents. *Pharm Biol.* 2009; 47: 774-782.

14) Bourgaud F, Gravot A, Milesi S, Gontier E. Production of plant secondary metabolites: a historical perspective. *Plant Science.* 2001; 161: 839-851.

15) Bouteille R, Gaudet M, Lecanu B, This H. Monitoring lactic acid production during milk fermentation by in situ quantitative proton nuclear magnetic resonance spectroscopy. *J Dairy Sci.* 2013; 96: 2071-80.

16) Brereton RG. Chemometrics: Data Analysis for the Laboratory and Chemical Plant. 2003; John Wiley & Sons, Ltd.

17) Bukhari IA, Dar A Behavioral profile of Hypericum perforatum (St. John's Wort) extract. A comparison with standard antidepressants in animal models of depression. *Eur Rev Med Pharmacol Sci.* 2013; 17: 1082-9.

18) Butterweck V, Schmidt M. St. John's wort: role of active compounds for its mechanism of action and efficacy. *Wien Med Wochenschr.* 2007; 157: 356-61.

19) Butterweck V: Mechanism of action of St John's wort in depression: what is known? *CNS Drugs.* 2003; 17: 539-62.

20) Capitani D, Mannina L, Proietti N, Sobolev AP, Tomassini A, Miccheli A, Di Cocco ME, Capuani G, De Salvador R, Delfini M. Monitoring of metabolic profiling and water status of Hayward kiwifruits by nuclear magnetic resonance. *Talanta.* 2010; 82: 1826-38.

21) Caraci F, Crupi R, Drago F, Spina E. Metabolic drug interactions between antidepressants and anticancer drugs: focus on selective serotonin reuptake inhibitors and hypericum extract. *Curr Drug Metab.* 2011; 12: 570-7.

22) Carreno-Quintero N, Acharjee A, Maliepaard C, Bachem CW, Mumm R, Bouwmeester H, Visser RG, Keurentjes JJ. Untargeted metabolic quantitative trait loci analyses reveal a relationship between primary metabolism and potato tuber quality. *Plant Physiol.* 2012; 158:1306-18.

23) Cevallos-Cevallos JM, Reyes-De-Corcuera JI. Metabolomics in food science. *Adv Food Nutr Res.* 2012; 67:1-24.

24) Chakraborty M, Karun A, Mitra A. Accumulation of phenylpropanoid derivatives in chitosan-induced cell suspension culture of Cocos nucifera. *J Plant Physiol.* 2009; 166: 63-71.

25) Chen JA, Papakostas GI, Youn SJ, Baer L, Clain AJ, Fava M, Mischoulon D. Association between patient beliefs regarding assigned treatment and clinical response: reanalysis of data from the Hypericum Depression Trial Study Group. *J Clin Psychiatry*. 2011; 72: 1669-76.

26) Chen LR, Chen YJ, Lee CY, Lin TY. Methyl jasmonate induced transcriptional changes in adventitious roots of *Bupleurum kaoi*. *Plant Sci.* 2007; 173: 12-24.

27) Choi YH, Tapias EC, Kim HK, Lefeber AW, Erkelens C, Verhoeven JT, Brzin J, Zel J, Verpoorte R. Metabolic discrimination of Catharanthus roseus leaves infected by phytoplasma using 1H-NMR spectroscopy and multivariate data analysis. *Plant Physiol.* 2004; 135: 2398-410.

28) Ciccarelli D, Andreucci AC, Pagni AM. Translucent Glands and Secretory Canals in Hypericum perforatum L. (Hypericaceae): Morphological, Anatomical and Histochemical Studies During the Course of Ontogenesis. *Annals of Botany.* 2001; 88: 637-644.

29) Clasquin MF, Melamud E, Singer A, Gooding JR, Xu X, Dong A, Cui H, Campagna SR, Savchenko A,Yakunin AF, Rabinowitz JD, Caudy AA. Riboneogenesis in yeast. *Cell.* 2011; 145: 969-80.

30) Crockett SL, Robson NK. Taxonomy and Chemotaxonomy of the Genus Hypericum. *Med Aromat Plant Sci Biotechnol.* 2011; 5: 1-13.

31) Crockett SL, Poller B, Tabanca N, Pferschy-Wenzig EM, Kunert O, Wedge DE, Bucar F. Bioactive xanthones from the roots of *Hypericum perforatum* (common St John's wort). *J Sci Food Agric.* 2011; 91:428-34.

32) Crupi R, Mazzon E, Marino A, La Spada G, Bramanti P, Battaglia F, Cuzzocrea S, Spina E. Hypericum perforatum treatment: effect on behaviour and neurogenesis in a chronic stress model in mice. *BMC Complement Altern Med.* 2011; 11:7.

33) Cui XH, Chakrabarty D, Lee EJ, Paek KY. Production of adventitious roots and secondary metabolites by *Hypericum perforatum* L. in a bioreactor. *Bioresour Technol.* 2010; 101: 4708-16.

34) Cui XH, Murthy HN, Jin YX, Yim YH, Kim JY, Paek KY. Production of adventitious root biomass and secondary metabolites of Hypericum perforatum L. in a balloon type airlift reactor. *Bioresour Technol.* 2011; 102: 10072-9.

35) Dais P, Hatzakis E. Quality assessment and authentication of virgin olive oil by NMR spectroscopy: a critical review. *Anal Chim Acta.* 2013; 765:1-27.

36) David R, Carde JP. Coloration differentielle des pseudophylles de Pin maritime au moyen du reactif de Nadi. 1964. Comptes Rendus de l'Academie des Sciences Paris, SeÂrie D 258: 1338-1340.

37) De Marchis GM, Bürgi S, Kientsch U, Honegger UE. Vitamin E reduces antidepressant-related beta-adrenoceptor down-regulation in cultured cells. Comparable effects on St. John's wort and tricyclic antidepressant treatment. *Planta Med.* 2006; 72: 1436-7.

38) Duke JA, Ayensu ES. Medicinal Plants of China. *Journal of Botanical Taxonomy and Geobotany.* 1985; 98: 398.

39) Fait A, Fromm H, Walter D, Galili G, Fernie AR. Highway or byway: the metabolic role of the GABA shunt in plants. *Trends Plant Sci.* 2008; 13: 14-9.

40) Falasca A, Melck D, Paris D, Saviano G, Motta A, Iorizzi M. Seasonal changes in the metabolic fingerprint of *Juniperus communis* L. berry extracts by ^{1}H-NMR-based metabolomics. *Metabolomics.* 2013; DOI 10.1007/s11306-013-056-1.

41) Ferrari F, Pasqua G, Monacelli B, Cimino P, Botta B. Xanthones from calli of *Hypericum perforatum* subsp. *perforatum*. *Nat Prod Res*. 2005; 19: 171-6.

42) Fiehn O. Metabolomics--the link between genotypes and phenotypes. *Plant Mol Biol.* 2002; 48: 155-71.

43) Flores-Sanchez IJ, Choi YH, Verpoorte R. Metabolite analysis of Cannabis sativa L. by NMR spectroscopy. *Methods Mol Biol.* 2012; 815: 363-75.

44) Fotakis C, Christodouleas D, Kokkotou K, Zervou M, Zoumpoulakis P, Moulos P, Liouni M, Calokerinos A. NMR metabolite profiling of Greek grape marc spirits. *Food Chem.* 2013; 138: 1837-46.

45) Franklin G, Conceição LF, Kombrink E, Dias AC. Xanthone biosynthesis in Hypericum perforatum cells provides antioxidant and antimicrobial protection upon biotic stress. *Phytochemistry.* 2009; 70: 60-8.

46) Gad HA, El-Ahmady SH, Abou-Shoer MI, Al-Azizi MM. Application of chemometrics in authentication of herbal medicines: a review. *Phytochem Anal.* 2013; 24: 1-24.

47) Gaufichon L, Reisdorf-Cren M, Rothstein SJ, Chardon F, Suzu A. Biological functions of asparagine synthetase in plants. *Plant Science.* 2010; 179: 141-153.

48) Gibson SI. Control of plant development and gene expression by sugar signaling. *Curr Opin Plant Biol.* 2005; 8: 93-102.

49) Gomez-Casati DF, Zanor MI, Busi MV. Metabolomics in plants and humans: applications in the prevention and diagnosis of diseases. *Biomed Res Int.* 2013; doi: 10.1155/2013/792527.

50) Greene T. The Universal Herbal, Caxton Press, London. 1824.

51) Griebel T, Zeier J. A role for beta-sitosterol to stigmasterol conversion in plant-pathogen interactions. *Plant J.* 2010; 63: 254-68.

52) Griffith TN, Varela-Nallar L, Dinamarca MC, Inestrosa NC. Neurobiological effects of Hyperforin and its potential in Alzheimer's disease therapy. *Curr Med Chem.* 2010; 17: 391-406.

53) Guarnerio CF, Fraccaroli M, Gonzo I, Pressi G, Dal Toso R, Guzzo F, Levi M Metabolomic analysis reveals that the accumulation of specific secondary metabolites in Echinacea angustifolia cells cultured in vitro can be controlled by light. *Plant Cell Rep.* 2012; 31: 361-7.

54) Hall RD. Plant metabolomics: from holistic hope, to hype, to hot topic. *New Phytol.* 2006; 169: 453-68.

55) Hasunuma T, Sanda T, Yamada R, Yoshimura K, Ishii J, Kondo A. Metabolic pathway engineering based on metabolomics confers acetic and formic acid tolerance to a recombinant xylose-fermenting strain of Saccharomyces cerevisiae. *Microb Cell Fact.* 2011; 10: 2.

56) Hill J. The Family Herbal, C. Brightly & T. Kinnersley, Bungay. 1808.

57) Hsieh MH, Goodman HM. The Arabidopsis IspH homolog is involved in the plastid non mevalonate pathway of isoprenoid biosynthesis. *Plant Physiol.* 2005; 138: 641-53.

58) Huang N, Rizshsky L, Hauck C, Nikolau BJ, Murphy PA, Birt DF. Identification of anti-inflammatory constituents in Hypericum perforatum and Hypericum gentianoides extracts using RAW 264.7 mouse macrophages. *Phytochemistry.* 2011; 72: 2015-23.

59) Hunter P. Reading the metabolic fine print. The application of metabolomics to diagnostics, drug research and nutrition might be integral to improved health and personalized medicine. *EMBO Rep.* 2009; 10: 20-3.

60) Hunter WN. Isoprenoid precursor biosynthesis offers potential targets for drug discovery against diseases caused by apicomplexan parasites. *Curr Top Med Chem.* 2011; 11: 2048-59.

61) Hunter WN. The non-mevalonate pathway of isoprenoid precursor biosynthesis. *J Biol Chem.* 2007; 282: 21573-7.

62) Huntosova V, Nadova Z, Dzurova L, Jakusova V, Sureau F, Miskovsky P. Cell death response of U87 glioma cells on hypericin photoactivation is mediated by dynamics of hypericin subcellular distribution and its aggregation in cellular organelles. *Photochem Photobiol Sci.* 2012; 11: 1428-36.

63) Inui T, Tsuchiya F, Ishimaru M, Oka K, Komura H. Different beers with different hops. Relevant compounds for their aroma characteristics. *J Agric Food Chem.* 2013; 61: 4758-64.

64) Iriti M, Faoro F. Chitosan as a MAMP, searching for a PRR. *Plant Signal Behav.* 2009; 4: 66-8.

65) Isacchi B, Bergonzi MC, Carnevali F, van der Esch SA, Vincieri FF, Bilia AR. Analysis and stability of the constituents of St. John's wort oils prepared with different methods. *J Pharm Biomed Anal.* 2007; 45: 756-61.

66) Istikoglou CI, Mavreas V, Geroulanos G. History and therapeutic properties of Hypericum Perforatum from antiquity until today. *Psychiatrike.* 2010; 21: 332-8.

67) Jahangir M, Kin HK, Choi YH, Verpoorte R. Metabolomic response of *Brassica rapa* submitted to pre-harvest bacterial contamination. *Food Chemistry.* 2008; 107: 362-368.

68) Jansen JJ, Hoefsloot HCJ, Greef van der J, Timmerman ME, Westerhuis JA, Smilde AK. ASCA: analysis of multivariate data obtained from an experimental design. *J Chemom.* 2005; 19:469-481.

69) Jiang M, Wang C, Zhang Y, Feng Y, Wang Y, Zhu Y. Sparse Partial-least-squares Discriminant Analysis for Different Geographical Origins of Salvia miltiorrhiza by (1) H-NMR-based Metabolomics. *Phytochem Anal.* 2014; 25: 50-8.

70) Jin YX, Cui XH, Paek KY, Yim YH. A strategy for enrichment of the bioactive sphingoid base-1-phosphates produced by Hypericum perforatum L. in a balloon type airlift reactor. *Bioresour Technol.* 2012; 123: 284-9.

71) Jürgenliemk G, Nahrstedt A. Phenolic compounds from Hypericum perforatum. *Planta Med.* 2002; 68: 88-91.

72) Kainz KP, Krenn L, Erdem Z, Kaehling H, Zehl M, Bursch W, Berger W, Marian B. 2-deprenyl-rheediaxanthone B isolated from Metaxya rostrata induces active cell death in colorectal tumor cells. *Plos One.* 2013; 8: e65745.

73) Kasper S, Gastpar M, Möller HJ, Müller WE, Volz HP, Dienel A, Kieser M. Better tolerability of St. John's wort extract WS 5570 compared to treatment with SSRIs: a

reanalysis of data from controlled clinical trials in acute major depression. *Int Clin Psychopharmacol.* 2010; 25: 204-13.

74) Kiers HA, ten Berge JM. Hierarchical relations between methods for simultaneous component analysis and a technique for rotation to a simple simultaneous structure. *British Journal of Mathematical and Statistical Psychology*. 1994; 47: 109-126.

75) Kim HK, Choi YH, Verpoorte R. NMR-based plant metabolomics: where do we stand, where do we go? *Trends Biotechnol.* 2011; 29: 267-75.

76) Kim HK, Choi YH, Verpoorte R. Profiling the jasmonic acid responses by nuclear magnetic resonance-based metabolomics. *Methods Mol Biol.* 2013; 1011: 267-75.

77) Kim HK, Verpoorte R. Sample preparation for plant metabolomics. *Phytochem Anal.* 2010, 21: 4-13.

78) Kim N, Kim K, Choi BY, Lee D, Shin YS, Bang KH, Cha SW, Lee JW, Choi HK, Jang DS, Lee D. Metabolomic approach for age discrimination of Panax ginseng using UPLC-Q-Tof MS. *J Agric Food Chem.* 2011; 59: 10435-41.

79) Kim N, Kim K, Lee D, Shin YS, Bang KH, Cha SW, Lee JW, Choi HK, Hwang BY, Lee D. Non-targeted metabolomics approach for age differentiation and structure interpretation of age-dependent key cons*tituents in* hairy roots of Panax ginseng. *J Nat Prod.* 2012; 75: 1777-84.

80) Kinnersley AM and Turano FJ. Gamma Aminobutyric Acid (GABA) and Plant Responses to Stress. *Critical Reviews in Plant Sciences*. 2000; 19: 479-509.

81) Kinross JM, Drymousis P, Jiménez B, Frilling A. Metabonomic profiling: a novel approach in neuroendocrine neoplasias. *Surgery.* 2013; 154: 1185-92.

82) Kitano H. Systems biology: a brief overview. *Science.* 2002; 295: 1662-4.

83) Komaraiah P, Kavi Kishor PV, Carlsson M, Magnusson KE, Mandenius CF. Enhancement of anthraquinone accumulation in *Morinda citrifolia* Suspension cultures. *Plant Sci.* 2005; 168: 1337-1344.

84) Kusano M, Fukushima A. Current challenges and future potential of tomato breeding using omics approaches. *Breed Sci.* 2013; 63: 31-41.

85) Kuzuyama T, Seto H. Diversity of the biosynthesis of the isoprene units. *Nat Prod Rep.* 2003; 20: 171-83.

86) Kwon Y, Yu SI, Lee H, Yim JH, Zhu JK, Lee BH. Arabidopsis serine decarboxylase mutants implicate the roles of ethanolamine in plant growth and development. *Int J Mol Sci.* 2012; 13:3176-88.

87) Li W, Sun YN, Yan XT, Yang SY, Choi CW, Hyun JW, Kang HK, Paek KY, Kim YH. Isolation of xanthones from adventitious roots of St. John's Wort (*Hypericum perforatum* L.) and their antioxidant and cytotoxic activities. *Food Science and Biotechnology.* 2013; 22: 945-949.

88) Li ZY, Zhi HJ, Zhang FS, Sun HF, Zhang LZ, Jia JP, Xing J, Qin XM. Metabolomic profiling of the antitussive and expectorant plant Tussilago farfara L. by nuclear magnetic resonance spectroscopy and multivariate data analysis. *J Pharm Biomed Anal.* 2013; 75: 158-64.

89) Lian ML, Chakrabarty D, Paek KY: Effect of plant growth regulators and medium composition on cell growth and saponin production during cell suspension culture of mountain ginseng (Panax ginseng C.A. Mayer). *J .Plant Biol.* 2002; 45:201-206.

90) Lindon JC, Holmes E, Nicholson JK. Pattern recognition methods and applications in biomedical magnetic resonance. *Prog Nucl Magn Reson Spectrosc.* 2001; 39: 1-40.

91) Liu C, Pan D, Ye Y, Cao J. ^{1}H NMR and multivariate data analysis of the relationship between the age and quality of duck meat. *Food Chem.* 2013; 141: 1281-6.

92) Manetti C, Bianchetti C, Casciani L, Castro C, Di Cocco ME, Miccheli A, Motto M, Conti F: A metabonomic study of transgenic maize (Zea mays) seeds revealed variations in osmolytes and branched amino acids. *J Exp Bot.* 2006, 57:2613-25.

93) Manetti C, Bianchetti C, Bizzarri M, Casciani L, Castro C, D'Ascenzo G, Delfini M, Di Cocco ME, Laganà A, Miccheli A, Motto M, Conti F: NMR-based metabonomic study of transgenic maize. *Phytochemistry.* 2004; 65: 3187-98.

94) Mannina L, Sobolev AP, Capitani D. Applications of NMR metabolomics to the study of foodstuffs: truffle, kiwifruit, lettuce, and sea bass. *Electrophoresis.* 2012; 33: 2290-313.

95) Marques VL, De Oliveira FM, Conserva LM, Brito LM, Guilhon GM. Dichromenoxanthones from Tovomita brasiliensis. *Phytochemistry.* 2000; 55: 815-8.

96) Matsuda F, Ishihara A, Takanashi K, Morino K, Miyazawa H, Wakasa H, Miyagawa H. Metabolic profiling analysis of genetically modified rice seedlings that overproduce tryptophan reveals the occurrence of its inter-tissue translocation. *Plant Biotechnol.* 2010; 27: 17–27.

97) Menichini G, Alfano C, Marrelli M, Toniolo C, Provenzano E, Statti GA, Nicoletti M, Menichini F, Conforti F. Hypericum perforatum L. subsp. perforatum induces inhibition of free radicals and enhanced phototoxicity in human melanoma cells under ultraviolet light. *Cell Prolif.* 2013; 46: 193-202.

98) Merhi F, Tang R, Piedfer M, Mathieu J, Bombarda I, Zaher M, Kolb JP, Billard C, Bauvois B. Hyperforin inhibits Akt1 kinase activity and promotes caspase-mediated apoptosis involving Bad and Noxa activation in human myeloid tumor cells. *PLoS One.* 2011; 6: e25963. doi

99) Miccheli A, Aureli T, Delfini M, Di Cocco ME, Viola P, Gobetto R, Conti F: Study on influence of inactivation enzyme techniques and extraction procedures on cerebral phosphorylated metabolite levels by 31P NMR spectroscopy. *Cell Mol Biol.* 1988; 34: 591-603.

100) Modarai M, Yang M, Suter A, Kortenkamp A, Heinrich M. Metabolomic profiling of liquid Echinacea medicinal products with in vitro inhibitory effects on cytochrome P450 3A4 (CYP3A4). *Planta Med.* 2010; 76: 378-85.

101) Motavalizadehkakhky A. Antimicrobial activity and chemical composition of essential oils of four Hypericum from Khorasan, Iran. *Journal of Medicinal Plants Research.* 2012; 6: 2478-2487.

102) Nahrstedt A, Butterweck V: Lessons learned from herbal medicinal products: the example of St. John's Wort (perpendicular). *J Nat Prod.* 2010; 73: 1015-21.

103) Nakanishi Y, Fukuda S, Chikayama E, Kimura Y, Ohno H, Kikuchi J. Dynamic omics approach identifies nutrition-mediated microbial interactions. *J Proteome Res.* 2011; 10: 824-36.

104) Newall CA, Anderson LA, Phillipson JD. Herbal Medicines: A Guide for Health-Care Professionals. London: The Pharmaceutical Press. 1996.

105) Nicholson JK, Lindon JC, Holmes E. 'Metabonomics': understanding the metabolic responses of living systems to pathophysiological stimuli via multivariate statistical analysis of biological NMR spectroscopic data. *Xenobiotica.* 1999; 29: 1181-9.

106) Nicholson JK, Lindon JC. Systems biology: Metabonomics. *Nature.* 2008; 455: 1054-6.

107) Novelli M, Beffy P, Menegazzi M, De Tata V, Martino L, Sgarbossa A, Porozov S, Pippa A, Masini M, Marchetti P, Masiello P. St. John's wort extract and hyperforin protect rat and human pancreatic islets against cytokine toxicity. *Acta Diabetol.* 2013; [Epub ahead of print].

108) Nürk, NM, Madriñán S, Carine MA, Chase MW, Blattner FR. Molecular phylogenetics and morphological evolution of St. John's wort (Hypericum; Hypericaceae). *Mol Phylogenet Evol.* 201*3*; 66: 1-16.

109) Ochi H, Sakai Y, Koishihara H, Abe F, Bamba T, Fukusaki E. Monitoring the ripening process of Cheddar cheese based on hydrophilic component profiling *using gas chromatog*raphy-mass spectrometry. *J Dairy Sci.* 2013; 96: 7427-41.

110) Oliver SG, Winson MK, Kell DB, Baganz F. Systematic functional analysis of the yeast genome. *Trends Biotechnol.* 1998; 16: 373-8.

111) Paek KY, Murthy HN, Hahn EJ, Zhong JJ. Large scale culture of ginseng adventitious roots for production of ginsenosides. *Adv Biochem Eng Biotechnol.* 2009; 113: 151-76.

112) Pan Q, Dai Y, Nuringtyas TR, Mustafa NR, Schulte AE, Verpoorte R, Choi YH. Investigation of the Chemomarkers Correlated with Flower Colour in Different Organs of Catharanthus roseus Using NMR-based Metabolomics. *Phytochem Anal.* 2014; 25: 66-74.

113) Pang R, Tao J, Zhang S, Zhu J, Yue X, Zhao L, Ye P, Zhu Y. In vitro anti-hepatitis B virus effect of Hypericum perforatum L. *J Huazhong Univ Sci Technolog Med Sci.* 2010; 30: 98-102.

114) Pasqua G, Avato P, Monacelli B, Santamaria AR, Argentieri MP. Metabolites in cell suspension cultures, calli, and in vitro regenerated organs of *Hypericum perforatum* cv. Top *Plant Sci.* 2003; 165: 977–982.

115) Pauling L, Robinson AB, Teranishi R, Cary P. Quantitative analysis of urine vapor and breath by gas-liquid partition chromatography. *Proc Natl Acad Sci* U S A. 1971; 68: 2374-6.

116) Pétriacq P, De Bont L, Tcherkez G, Gakière B. NAD Not just a pawn on the board of plant-pathogen interactions. *Plant Signal Behav.* 2013; 8: e22477.

117) Porzel A, Farag MA, Mülbradt J, Wessjohann LA. Metabolite profiling and fingerprinting of *Hypericum* species: a comparison of MS and NMR metabolomics. *Metabolomics.* 2013; DOI 10.1007/s11306-013-0609-7.

118) Putri SP, Yamamoto S, Tsugawa H, Fukusaki E. Current metabolomics: technological advances. *J Biosci Bioeng.* 2013; 116: 9-16.

119) Radusiene J, Judzentiene A, Bernotiene G. Essential oil composition and variability of *Hypericum perforatum* L. growing in Lithuania. *Biochemical Systematics and Ecology.* 2005; 33: 113-124.

120) Rao SR, Ravishankar GA. Plant cell cultures: chemical factories of secondary metabolites. *Biotechnol Adv.* 2002; 20: 101-53.

121) Rasmussen B, Cloarec O, Tang H, Staerk D, Jaroszewski JW. Multivariate analysis of integrated and full-resolution ^{1}H-NMR spectral data from complex pharmaceutical preparations: St. John's wort. *Planta Med.* 2006; 72: 556-63.

122) Rasmussen S, Parsons AJ, Jones CS. Metabolomics of forage plants: a review. *Ann Bot.* 2012; 110: 1281-90.

123) Rath G, Potterat O, Mavi , Hostettmann K. Xanthones from *Hypericum roeperanum*. *Phytochemistry.* 1996; 43: 513-20.

124) Rukachaisikul V, Tadpetch K, Watthanaphanit A, Saengsanae N, Phongpaichit S. Benzopyran, biphenyl, and tetraoxygenated xanthone derivatives from the twigs of Garcinia nigrolineata. *J Nat Prod.* 2005; 68: 1218-21.

125) Sacchettini JC, Poulter CD. Creating isoprenoid diversity. *Science.* 1997; 277: 1788-9.

126) Saddiqe Z, Naeem I, Maimoona A. A review of the antibacterial activity of Hypericum perforatum L. *J Ethnopharmacol.* 2010; 131: 511-21.

127) Sardans J, Gargallo-Garriga A, Pérez-Trujillo M, Parella TJ, Seco R, Filella I, Peñuelas J Metabolic responses of Quercus ilex seedlings to wounding analysed with nuclear magnetic resonance profiling. *Plant Biol (Stuttg).* 2013; doi: 10.1111/plb.12032.

128) Sasse JM. Physiological Actions of Brassinosteroids: An Update. *J Plant Growth Regul.* 2003; 22: 276-288.

129) Schempp CM, Kirkin V, Simon-Haarhaus B, Kersten A, Kiss J, Termeer CC, Gilb B, Kaufmann T, Borner C, Sleeman JP, Simon JC. Inhibition of tumour cell growth by

hyperforin, a novel anticancer drug from St. John's wort that acts by induction of apoptosis. *Oncogene.* 2002; 21: 1242-50.

130) Schmidtke LM, Blackman JW, Clark AC, Grant-Preece P. Wine Metabolomics: Objective Measures of Sensory Properties of Semillon from GC-MS Profiles. *J Agric Food Chem.* 2013; [Epub ahead of print]

131) Schuhmacher R, Krska R, Weckwerth W, Goodacre R. Metabolomics and metabolite profiling. *Anal Bioanal Chem.* 2013; 405: 5003-4.

132) Sharma KV, Davids LM. Hypericin-PDT-induced rapid necrotic death in human squamous cell carcinoma cultures after multiple treatment.*Cell Biol Int.* 2012; 36: 1261-6.

133) Shelp BJ, Mullen RT, Waller J. Compartimentation of GABA metabolism raises intriguing questions. *Trends Plant Sci.* 2012; 17: 57-9.

134) Simmler C, Napolitano JG, McAlpine JB, Chen SN, Pauli GF. Universal quantitative NMR analysis of complex natural samples. *Current Opinion in Biotechnology.* 2014; 25: 51-59.

135) Sivakumar G, Yu KW, Hahn EJ, Paek KY. Optimization of organic nutrients for ginseng hairy roots production in large-scale bioreactors. *Current Sci.* 2005; 89: 641- 649.

136) Sivanandhan G, Arun M, Mayavan S, Rajesh M, Mariashibu TS, Manickavasagam M, Selvaraj N, Ganapathi A. Chitosan enhances withanolides production in adventitious root cultures of Withania somnifera (L.) Dunal. *Industrial Crops and Products.* 2012; 37: 124-9.

137) Smilde AK, Jansen JJ, Hoefsloot HC, Lamers RJAN, Greef Jvd, Timmerman ME: ANOVA-simultaneous component analysis (ASCA): a new tool for analyzing designed metabolomics data. *Bioinformatics.* 2005, 21:3043-3048.

138) Snedden WA, Arazi T, Fromm H, Shelp BJ. Calcium/Calmodulin Activation of Soybean Glutamate Decarboxylase. *Plant Physiol.* 1995; 108: 543-549.

139) Stevens, PF. Clusiaceae-Guttiferae. In: Kubitzki, K. The Families and Genera of Vascular Plants (Vol IX). Springer; Berlin, Germany; 2007 p. 48-66.

140) Sulpice R, Nikoloski Z, Tschoep H, Antonio C, Kleessen S, Larhlimi A, Selbig J, Ishihara H, Gibon Y, Fernie AR, Stitt M. Impact of the carbon and nitrogen supply on relationships and connectivity between metabolism and biomass in a broad panel of Arabidopsis accessions. *Plant Physiol.* 2013; 162: 347-63.

141) Szymańska E, Saccenti E, Smilde AK, Westerhuis JA. Double-check: validation of diagnostic statistics for PLS-DA models in metabolomics studies. *Metabolomics.* 2012; 8: 3-16.

142) Tatsis EC, Boeren S, Exarchou V, Troganis AN, Vervoort J, Gerothanassis IP. Identification of the major constituents of Hypericum perforatum by LC/SPE/NMR and/or LC/MS. *Phytochemistry.* 2007; 68: 383-93.

143) Tocci N, D'Auria FD, Simonetti G, Panella S, Palamara AT, Debrassi A, Rodrigues CA, Filho VC, Sciubba F, Pasqua G. Bioassay-guided fractionation of extracts from *Hypericum perforatum* in vitro roots treated with carboxymethylchitosans and determination of antifungal activity against human fungal pathogens. *Plant Physiol Biochem.* 2013; 70: 342-7.

144) Tocci N, Ferrari F, Santamaria AR, Valletta A, Rovardi I, Pasqua G. Chitosan enhances xanthone production in *Hypericum perforatum* subsp. *angustifolium* cell cultures. *Nat Prod Res.* 2010; 24:286-93.

145) Tocci N, Simonetti G, D'Auria FD, Panella S, Palamara AT, Valletta A, Pasqua G. Root cultures of *Hypericum perforatum* subsp. *angustifolium* elicited with chitosan and production of xanthone-rich extracts with antifungal activity. *Appl Microbiol Biotechnol.* 2011; 91:977-87.

146) Tocci N, D'Auria FD, Simonetti G, Panella S, Palamara AT, Pasqua G. A three-step culture system to increase the xanthone production and antifungal activity of *Hypericum perforatum* subsp. angustifolium in vitro roots. *Plant Physiol Biochem.* 2012; 57:54-8.

147) Toyomasu T, Kagahara T, Okada K, Koga J, Hasegawa M, Mitsuhashi W, Sassa T, Yamane H. Diterpene phytoalexins are biosynthesized in and exuded from the roots of rice seedlings. *Biosci Biotechnol Biochem.* 2008; 72: 562-7.

148) Urdang, G. Pharmacopoeia Londinensis of 1618. Madison: State Historical Society of Wisconsin. 1944.

149) Verpoorte R, Choi YH, Kim HK. NMR-based metabolomics at work in phytochemistry. *Phytochem Rev*. 2007; 6:3–14.

150) Vis DJ, Westerhuis JA, Smilde AK, van der Greef J. Statistical validation of megavariate effects in ASCA. *BMC Bioinformatics*. 2007; 8: 322.

151) Wagner L, Trattner S, Pickova J, Gómez-Requeni P, Moazzami AA. ^{1}H NMR-based metabolomics studies on the effect of sesamin in Atlantic salmon (Salmo salar). *Food Chem.* 2014; 147: 98-105.

152) Walker TS, Pal Bais H, Vivanco JM. Jasmonic acid-induced hypericin production in cell suspension cultures of Hypericum perforatum L. (St. John's wort). *Phytochemistry*. 2002; 60: 289-93.

153) Weckwerth W, Loureiro ME, Wenzel K, Fiehn O. Differential metabolic networks unravel the effects of silent plant phenotypes. *Proc Natl Acad Sci U S A*. 2004; 101: 7809-14.

154) Weckwerth W. Metabolomics in systems biology. *Annu. Rev. Plant Biol.* 2003; 54: 669-89.

155) Wölfle U, Seelinger G, Schempp CM. Topical Application of St. John's Wort (Hypericum perforatum). *Planta Med.* 2013 [Epub ahead of print].

156) Yaeno T Matsuda O, Iba K. Role of chloroplast trienoic fatty acids in plant disease defense responses. *Plant J*. 2004; 40: 931-41.

157) Yamazaki M, Mochida K, Asano T, Nakabayashi R, Chiba M, Udomson N, Yamazaki Y, Goodenowe DB, Sankawa U, Yoshida T, Toyoda A, Totoki Y, Sakaki Y, Góngora-Castillo E, Buell CR, Sakurai T, Saito K.. Coupling deep transcriptome analysis with untargeted metabolic profiling in Ophiorrhiza pumila to further the understanding of the biosynthesis of the anti-cancer alkaloid camptothecin and anthraquinones. *Plant Cell Physiol.* 2013; 54: 686-96.

158) Yang SY, Kim HK, Lefeber AW, Erkelens C, Angelova N, Choi YH, Verpoorte R. Application of two-dimensional nuclear magnetic resonance spectroscopy to quality control of ginseng commercial products. *Planta Med.* 2006; 72: 364-9.

159) Yin H, Fretté XC, Christensen LP, Grevsen K. Chitosan oligosaccharides promote the content of polyphenols in Greek oregano (*Origanum vulgare* ssp. *hirtum*). *J Agric Food Chem.* 2012; 60: 136-43.

160) Zdunić G, Godevac D, Milenković M, Vucićević D, Savikin K, Menković N, Petrović S. Evaluation of Hypericum perforatum oil extracts for an antiinflammatory and gastroprotective activity in rats. *Phytother Res.* 2009; 23: 1559-64.

161) Zdunić G, Godevac D, Milenković M, Vucićević D, Savikin K, Menković N, Petrović S. Evaluation of Hypericum perforatum oil extracts for an antiinflammatory and gastroprotective activity in rats. *Phytother Res.* 2009; 23: 1559-64.

162) Zhang A, Sun H, Wang X. Power of metabolomics in biomarker discovery and mining mechanisms of obesity. *Obes Rev.* 2013; 14: 344-9.

163) Zhang AH, Qiu S, Xu HY, Sun H, Wang XJ. Metabolomics in diabetes. *Clin Chim Acta.* 2013; 429C: 106-110.

164) Zhang DW, Liu X, Xie D, Chen R, Tao XY, Zou JH, Dai J: Two new diterpenoids from cell cultures of Salvia miltiorrhiza. *Chem Pharm Bull.* 2013, 61:576-80.

165) Zhao J, Davis LC, Verpoorte R. Elicitor signal transduction leading to production of plant secondary metabolites. *Biotechnol Adv.* 2005; 23:283-333.

166) Zobayed SMA, Murch SJ, Rupasinghe HPV, Saxena PK. In vitro production and chemical characterization of St. John's wort (Hypericum perforatum L. cv 'New Stems'). *Plant Science.* 2004; 166: 333-340.

167) Zulak KG, Weljie AM, Vogel HJ, Facchini PJ. Quantitative 1H NMR metabolomics reveals extensive metabolic reprogramming of primary and secondary metabolism in elicitor-treated opium poppy cell cultures. *BMC Plant Biol.* 2008; 8:5.